UNIVERSITY OF THE
WITWATERSRAND,
JOHANNESBURG

School of Molecular and Cell Biology

University of the Witwatersrand

Johannesburg

VEGF receptor-stimulated signal transduction in human oesophageal squamous cell carcinoma cells

Claire Ann Tinderholm

533712

Supervisor: Prof. R.B. Veale

A thesis submitted to the Faculty of Science, University of the Witwatersrand, Johannesburg, in fulfilment of the requirements for the degree of Doctor of Philosophy.

Johannesburg, March 2019

Declaration

I declare that this thesis is my own, unaided work. It is being submitted for the Degree of Doctor of Philosophy at the University of the Witwatersrand, Johannesburg. It has not been submitted before for any degree or examination at any other University.

Claire Ann Tinderholm

28 March 2019 at Johannesburg

Abstract

Signal transduction pathways are essential for regulation of many biological processes, the disruption of which underlies the development of cancer. The autocrine signalling mechanism induced by vascular endothelial growth factor (VEGF) has been implicated in carcinogenesis and cancer progression by contributing to increased cell proliferation, apoptosis prevention, metastasis and increased resistance to treatment. VEGF receptor-stimulated signalling may be an important factor contributing to human oesophageal squamous cell carcinoma (HOSCC) progression and metastasis. HOSCC is prevalent worldwide and a primary cause of cancer death among South African Black males. This form of cancer is renowned for its aggressiveness and high rate of metastasis. Current therapies including surgery, radiotherapy and chemotherapy are largely ineffective and the prognosis is generally poor therefore effective HOSCC prevention and treatment is essential. The ability of VEGFR stimulation to aid in HOSCC progression was evaluated by analysing abundance of active signalling intermediates though western blotting in combination with assessment of cellular proliferation via an MTT assay and observation of cellular migration through scratch-wound assays. An autocrine VEGF/VEGFR signalling axis was found to exist in HOSCCs, where autocrine VEGFR-stimulated signal transduction enhances HOSCC proliferation and initiates HOSCC metastasis. Abrogation of VEGFR induced PI3K/PKB and MAPK/ERK signalling pathways at various specific intermediates revealed an intricate balancing, wherein if one pathway is shutdown VEGFR stimulation may initiate the other to compensate for its loss. In this manner VEGFR signalling contributes to proliferation of HOSCC cells via both the PI3K/PKB and MAPK/ERK/RSK signalling pathways. The VEGFR triggered HOSCC metastatic response however, occurs primarily through the PI3K signalling pathway. Combined inhibition of VEGFR and PI3K/PKB signalling was found to synergistically reduce HOSCC proliferation, reduce HOSCC initiation of metastasis and prevent compensation via salvage pathways. Combination therapy targeting both the VEGFR signalling pathway and the PI3K/PKB signalling pathway is thus a promising option in the treatment of human oesophageal squamous cell carcinoma where the therapies would act together to reduce metastasis, curb drug resistance and synergistically decrease HOSCC proliferation.

Research Outputs

List of associated presentations

Poster Presentations

Tinderholm, C., Houston-McMillan, E. and Veale, R. Ros lead to an increase in active PKB via a VEGF dependent pathway in HOSCC cells. Molecular Biosciences Research Thrust Postgraduate Research Day. University of the Witwatersrand, Johannesburg.03 Dec 2015. p70.

Tinderholm, C. A. and Veale, R. B. (2016). VEGF influences signalling intermediates in pathways leading to proliferation and migration in HOSCC. 7th Cross-Faculty Postgraduate Symposium. University of the Witwatersrand, Johannesburg. 01 Mar 2016. p130.

Tinderholm, C. A. and Veale, R. VEGF receptor-stimulated signal transduction in human oesophageal squamous cell carcinoma cells. Molecular Biosciences Research Thrust Postgraduate Research Day. University of the Witwatersrand, Johannesburg.08 Dec 2016. p41.

Tinderholm, C.A. and Veale, R.B. VEGF receptor-stimulated signalling contributes to cell migration of human oesophageal squamous cell carcinoma. Cancer Research Symposium. University of the Witwatersrand, Johannesburg. 09 Feb 2017. p20.

Tinderholm, C.A. and Veale, R. Elucidating the signalling mechanism by which VEGFR contributes to human oesophageal squamous cell carcinoma cell migration. 8th Cross-Faculty Postgraduate Symposium. University of the Witwatersrand, Johannesburg. 26 Oct 2017. p11.

Tinderholm, C.A. and Veale, R. VEGFR-stimulated PI3K signalling induces human oesophageal squamous cell carcinoma metastatic behaviour. Molecular Biosciences Research Thrust Postgraduate Research Day. University of the Witwatersrand, Johannesburg. 29 Nov 2018.

Oral Presentations

Tinderholm, C.A. and Veale, R. VEGFR induced proliferation of human oesophageal squamous cell carcinoma occurs via a MAPK/ERK dependent pathway. Molecular Biosciences Research Thrust Postgraduate Research Day. University of the Witwatersrand, Johannesburg. 30 Nov 2017. p14.

List of associated publications

Submitted to Molecular and Cellular Biochemistry, Pending Review:
Manuscript number: MCBI-D-19-00145
Tinderholm, C.A. and Veale, R. Combined targeting of VEGFR and PI3K synergistically reduces proliferation of human oesophageal squamous cell carcinoma.

Acknowledgements

Foremost, I would like to express my sincere gratitude to my supervisor Prof. Rob Veale for his invaluable support and guidance, both inside the lab and out. Thank you for all your advice, time, effort and kindness, it is most appreciated.

I would also like to thank Mrs Elsabe Scott and Miss Sabeeha Mahomed for training me in the arts of cell biology, for their technical support and endless patience. As well as Sandile Buthelezi for he's cell biology tips, tricks and wisdom.

Many thanks, to my colleagues and friends in the cell biology lab for trouble-shooting sessions, laughs and crazy moments.

To my friends thank you for all the heart-to-hearts and equally ridiculous conversations. In particular Sabeeha; thank you for understanding without explanation – four blinks, for your encouragement, for caring and for sharing.

A special thanks to my mom, dad and brother for their love, support, strength and assurance. Thank you for believing in me even when I didn't.

Finally, with utmost gratitude I would like thank the University of the Witwatersrand and the National Research Foundation for financial support.

Table of Content

Declaration i

Abstract ii

Research Outputs iii

Acknowledgements v

List of Abbreviations xi

List of Figures xii

List of Tables xiii

Chapter 1: General Introduction 1

1.1 Signal transduction in cancer 1

1.2 VEGF receptor-stimulated signal transduction in cancer 1

1.2.1 Protein kinase B 5

1.2.2 Glycogen synthase kinase-3β 7

1.2.3 Focal adhesion kinase 8

1.2.4 Non-canonical mediation of VEGFR signalling 9

1.3 Cancer in South Africa 10

1.3.1 Human Oesophageal Squamous Cell Carcinoma 10

1.4 VEGF receptor-stimulated signal transduction in HOSCC 12

Objective and aims 13

Chapter 2: VEGFR-stimulated signal transduction in HOSCC proliferation 14

2.1 Introduction 14

2.2 Materials and Methods 16

2.2.1 Tissue culture 16

2.2.2 Treatment set to provide insight into VEGFR-stimulated signal transduction in proliferation of HOSCC 16

2.2.3 Protein extraction 17

2.2.4 Protein concentration determination 17

2.2.5 Sodium Dodecyl Sulphate–Polyacrylamide Gel Electrophoresis 18
2.2.6 Western blot 18
2.2.7 Semi-quantitative analysis 20
2.2.8 Cellular proliferation assay 21
2.2.9 Comparisons and statistical analysis 21
2.3 Results 23
2.3.1 Quantification of VEGF protein content in HOSCC 23
2.3.2 Effect of VEGFR stimulation on HOSCC proliferation 25
2.3.3 Abundance of signalling intermediates central to proliferation under standard HOSCC culture conditions 26
2.3.4 Effect of VEGFR signalling on intermediates central to proliferation 27
2.4 Discussion 30
Chapter 3: The role of the VEGFR-induced PI3K/PKB signalling pathway in HOSCC proliferation 35
3.1 Introduction 35
3.2 Materials and Methods 37
3.2.1 Tissue culture 37
3.2.2 Treatment set to provide insight into the VEGFR-induce PI3K/PKB signalling pathway 37
3.2.3 Protein extraction 37
3.2.4 Protein concentration determination 37
3.2.5 Sodium Dodecyl Sulphate–Polyacrylamide Gel Electrophoresis 37
3.2.6 Western blot 38
3.2.7 Semi-quantitative analysis 38
3.2.8 Cellular proliferation assay 38
3.2.9 Comparisons and statistical analysis 38
3.3. Results 39
3.3.1 Effect of PI3K inhibition on HOSCC proliferation 39

3.3.2 Effect of PI3K inhibition on signalling intermediates central to proliferation in HOSCC 40
3.3.3 Effect of PI3K inhibition in combination with VEGFR inhibition on HOSCC proliferation 41
3.3.4 Effect of PI3K inhibition in combination with VEGFR inhibition on signalling intermediates central to proliferation in HOSCC 43
3.4 Discussion 46
Chapter 4: The role of the VEGFR-induced MAPK/ERK/RSK signalling pathway in HOSCC proliferation 49
4.1 Introduction 49
4.2 Materials and Methods 51
4.2.1 Tissue culture 51
4.2.2 Treatment set to provide insight into VEGFR-induce MAPK/ERK/RSK signalling pathway 51
4.2.3 Protein extraction 51
4.2.4 Protein concentration determination 51
4.2.5 Sodium Dodecyl Sulphate–Polyacrylamide Gel Electrophoresis 51
4.2.6 Western blot 52
4.2.7 Semi-quantitative analysis 52
4.2.8 Cellular proliferation assay 52
4.2.9 Comparisons and statistical analysis 52
4.3 Results 53
4.3.1 Effect of RSK inhibition on HOSCC proliferation 53
4.3.2 Effect of RSK inhibition on signalling intermediates central to proliferation in HOSCC 54
4.3.3 Effect of RSK inhibition in combination with VEGFR inhibition on HOSCC proliferation 55
4.3.4 Effect of RSK inhibition in combination with VEGFR inhibition on signalling intermediates central to proliferation in HOSCC 56

4.4 Discussion 59
Chapter 5: VEGFR-stimulated signal transduction in migration of HOSCC 63
5.1 Introduction 63
5.2 Materials and Methods 65
5.2.1 Tissue culture 65
5.2.2 Treatment set to provide insight into VEGFR-stimulated signal transduction in migration of HOSCC 65
5.2.3 Protein extraction 65
5.2.4 Protein concentration determination 65
5.2.5 Sodium Dodecyl Sulphate–Polyacrylamide Gel Electrophoresis 65
5.2.6 Western blot 65
5.2.7 Semi-quantitative analysis 66
5.2.8 Assay of migratory cell morphology 66
5.2.9 Comparisons and statistical analysis 67
5.3 Results 68
5.3.1 VEGFR stimulation affects HOSCC migration 68
5.3.2 HOSCC cell lines contain pPKB, pGSK3βser9 and pFAK signalling intermediates putative in migration 71
5.3.3 VEGFR signalling affects pPKB, pGSK3βser9 and pFAK signalling intermediates putative in HOSCC migration 73
5.4 Discussion 76
Chapter 6: The role of the VEGFR-induced PI3K/PKB signalling pathway in HOSCC migration 79
6.1 Introduction 79
6.2 Materials and Methods 81
6.2.1 Tissue culture 81
6.2.2 Treatment set to provide insight into VEGFR-induce PI3K/PKB signalling pathway 81

6.2.3 Protein extraction 81
6.2.4 Protein concentration determination 81
6.2.5 Sodium Dodecyl Sulphate–Polyacrylamide Gel Electrophoresis 81
6.2.6 Western blot 82
6.2.7 Semi-quantitative analysis 82
6.2.8 Assay of migratory cell morphology 82
6.2.9 Comparisons and statistical analysis 82
6.3 Results 83
6.3.1 PI3K inhibition decreases HOSCC migration 83
6.3.2 Effect of PI3K inhibition on signalling intermediates central to migration in HOSCC 84
6.3.3 Effect of PI3K inhibition in combination with VEGFR inhibition on HOSCC migration 86
6.3.4 Effect of PI3K inhibition in combination with VEGFR inhibition on signalling intermediates central to migration in HOSCC 87
6.4 Discussion 90
Chapter 7: General discussion 92
7.1 Conclusion 95
References 96
Appendix A 109
Appendix B 116
Appendix C 119
Appendix D 121

List of Abbreviations

BSA	Bovine Serum Albumin
dH_2O	Distilled water
DMEM	Dulbecco's Modified Eagle Medium
DMSO	Dimethyl Sulfoxide (DMSO)
ECM	Extracellular matrix
EDTA	Ethylenediamine Tetraacetic Acid
EMT	Epithelial–mesenchymal transition
ERK	extracellular signal-regulated kinase
FAK	Focal Adhesion Kinase
FCS	Fetal Calf Serum
GSK3	Glycogen Synthase Kinase
HOSCC	Human Oesophageal Squamous Cell Carcinoma
MAPK	mitogen-activated protein kinase
MTT	3-(4,5-dimethylthiazol-2-yl)-2,5-diphenyltetrazolium bromide
PAGE	Polyacrylamide Gel Electrophoresis
PBS	Phosphate Buffered Saline
PI3K	Phosphoinositide 3-kinase
PKB	Protein Kinase B
PMSF	Phenylmethylsulfonyl Fluoride
RSK	Ribosomal S6 Kinase
SDS	Sodium Dodecyl Sulphate
TBS	Tris-buffered Saline
TBST	Tris-buffered Saline with Tween®20
VEGF	Vascular Endothelial Growth Factor
VEGFR	Vascular Endothelial Growth Factor Receptor
WHCO	Wits Human Carcinoma of the Oesophagus

List of Figures

Figure 1: VEGFR-stimulated signal transduction pathways 4
Figure 2: VEGF protein content in HOSCC cell lines 24
Figure 3: VEGFR signalling influences the proliferation of HOSCC cell lines 25
Figure 4: pPKB and pGSK3βser9 protein content in HOSCC cell lines 27
Figure 5: VEGFR signalling influences the abundance of pPKB and pGSK3βser9 in HOSCC cell lines 28
Figure 6: PI3K inhibition influences the proliferation of HOSCC cell lines 39
Figure 7: PI3K inhibition influences the abundance of pPKB and pGSK3βser9 in HOSCC cell lines 40
Figure 8: Combined VEGFR and PI3K inhibition influences the proliferation of HOSCC cell lines 42
Figure 9: Combined inhibition of both VEGFR and PI3K signalling synergistically reduces proliferation of HOSCC cell lines 43
Figure 10: Combined VEGFR and PI3K inhibition influences the abundance of pPKB and pGSK3βser9 in HOSCC cell lines 44
Figure 11: Abrogation of VEGFR-induced PI3K signal transduction in HOSCC 50
Figure 12: RSK inhibition influences the proliferation of HOSCC cell lines 53
Figure 13: RSK inhibition influences the abundance of pPKB and pGSK3βser9 in HOSCC cell lines 54
Figure 14: Combined VEGFR and RSK inhibition influences the proliferation of HOSCC cell lines 56
Figure 15: Combined VEGFR and RSK inhibition influences the abundance of pPKB and pGSK3βser9 in HOSCC cell lines 57
Figure 16: Abrogation of VEGFR-induced RSK signal transduction in HOSCC 60
Figure 17: VEGFR-stimulation induces HOSCC cell migratory morphology 69
Figure 18: VEGFR signalling influences the migration of HOSCC cell lines 70
Figure 19: pFAK protein content in HOSCC cell lines 72
Figure 20: VEGFR signalling influences the abundance of pPKB, pGSK3βser9 and pFAK in HOSCC cell lines 74
Figure 21: PI3K inhibition influences the migration of HOSCC cell lines 83

Figure 22: PI3K inhibition influences the abundance of pPKB, pGSK3βser9 and pFAK in HOSCC cell lines 85
Figure 23: Combined VEGFR and PI3K inhibition influences the migration of HOSCC cell lines 87
Figure 24: Combined VEGFR and PI3K inhibition influences the abundance of pPKB, pGSK3βser9 and pFAK in HOSCC cell lines 88
Figure B1: Example of a standard curve for protein concentration determination of cell lysate samples 116
Figure C1: SDS-PAGE resolved whole cell protein extracts 119
Figure C2: Dot blot confirming functionality of the anti-VEGF antibody 120

List of Tables

Table 1: Signalling intermediates in pathways central to cell proliferation, survival and migration 5
Table 2: pPKB, pGSK3βser9, VEGF and β-Actin antibodies for western blotting; dilutions and incubation conditions 20
Table 3: pFAK antibody for western blotting; dilutions and incubation conditions 66
Table B1: Example of densitometry results and normalisation 118

VEGF receptor-stimulated signal transduction in human oesophageal squamous cell carcinoma cells

Chapter 1: General Introduction

1.1 Signal transduction in cancer

The transmission of information into and throughout the cell via signal transduction is crucial to generate the appropriate response in normal cells. The development of cancer involves disruption of these signalling pathways allowing cells to escape homeostatic controls that normally suppress inappropriate proliferation, survival of abnormal cells and migration outside of their normal niche (Sever and Brugge, 2015). Cancer is defined as an uncontrolled division and spread of abnormal cells (Hanahan and Weinberg, 2011) and its characteristics include increased and uncontrolled proliferation, loss of sensitivity to tumour suppressors, apoptosis resistance, self-renewal, induction of angiogenesis, replicative immortality, invasion of surrounding tissue and metastasis (Hanahan and Weinberg, 2011). Cell signalling is essential for regulation of these processes and thus disruption of signal transduction pathways underlies the development of cancer (Sever and Brugge, 2015). An improved knowledge of the molecular abnormalities which distinguishes cancer from healthy cells would greatly aid in the identification of targets for therapy. In recent years there has been a notable increase in the quantity and variety of drugs which specifically target signalling intermediates, giving further evidence to the importance of signal transduction in the disease context (Popov, 2005).

1.2 VEGF receptor-stimulated signal transduction in cancer

Signal transduction is predominantly stimulated by growth factors which through binding to receptors on the cell surface initiate intracellular signalling pathways to control many cellular processes (Hanahan and Weinberg, 2011). One such growth factor, vascular endothelial growth factor (VEGF), is dysregulated in many human tumours and has been implicated in carcinogenesis and cancer progression (Rapisarda and Melillo, 2012). Hypoxia is a major stimulator of VEGF expression, thus VEGF overexpression in tumour cells is generally

regarded to be a result of hypoxic conditions intrinsic to the formation of tumours (Mimeault and Batra, 2013). VEGF is a family of growth factors which comprises of VEGF-A, VEGF-B, VEGF-C, VEGF-D and placental growth factor. Members of the VEGF family vary slightly in terms of their expression pattern, receptor specificity and biological functions (Koch and Claesson-Welsh, 2012). VEGF-A is the most intensely studied and has several isoforms (VEGF-A_{121}, VEGF-A_{145}, VEGF-A_{148}, VEGF-A_{165}, VEGF-A_{183}, VEGF-A_{189} and VEGF-A_{206}; nomenclature refers to amino acid number) due to alternative splicing of a single gene containing eight exons (Houck et al., 1991). Tumour cells most commonly secrete the VEGF-A_{165} and VEGF-A_{121} isoforms (Keyt et al., 1996; Price et al., 2001). VEGF secreted by tumour cells promotes cancer by functioning in a paracrine manner (acting upon nearby cells) to induce angiogenesis and thus promote tumour growth and survival indirectly as well as in an autocrine manner (acting upon the same cells) by directly contributing to enhanced cancer cell proliferation, apoptosis prevention, metastasis and resistance to treatment (Goel and Mercurio, 2013; Rapisarda and Melillo, 2012).

In a paracrine manner VEGF acts to promote angiogenesis, the formation of new blood vessels or sprouting of existing vessels by inducing proliferation and migration of endothelial cells (Karkkainen and Petrova, 2000). Normal angiogenesis occurs during embryonic development after which the vasculature remains largely quiescent except transiently for physiological processes such as wound repair and female reproductive cycling (Hanahan and Folkman, 1996). Angiogenesis is essential for cancer progression and metastasis as extensive vasculature is required to supply the cancer cells with nutrients and oxygen while removing carbon dioxide and metabolic waste (Folkman, 1990; Hanahan and Weinberg, 2011). In the absence of angiogenesis tumours are not able to grow larger than 1-2 mm in diameter due to the limits of diffusion (Folkman, 1990). Increased abundance of blood vessels surrounding the tumour also offers a route through which cancer cells can escape and metastasise to other areas of the body (Bergers and Benjamin, 2003). In addition to inducing angiogenesis, VEGF also promotes lymphangiogenesis and vascular hyperpermeability in a paracrine manner (Senger, 2010).

In contrast to the paracrine function of VEGF which has been extensively studied, the autocrine pathway by which VEGF promotes cancer progression is not fully understood. During angiogenesis VEGF induces proliferation and migration of endothelial cells for the development of new blood vessels (Karkkainen and Petrova, 2000). Autocrine VEGF stimulated signalling may influence tumour cells in a similar manner to promote tumour cell

proliferation and migration. Autocrine VEGF induced signalling has been reported to promote proliferation, survival, migration and invasion of cancer cells (Bachelder et al., 2001, 2002; Goel and Mercurio, 2013; Price et al., 2001; Samuel et al., 2011; Spannuth et al., 2009; Su et al., 2006; Takahashi et al., 1995). Understanding disruption of the autocrine signalling mechanism induced by VEGF may therefore provide insight into carcinogenesis and cancer progression.

The theory that VEGF contributes to tumour cell function requires that tumour cells express VEGF receptors and can thus respond to VEGF stimulus (Goel and Mercurio, 2013). VEGF receptors were originally believed to be confined to endothelial cells (for their function in angiogenesis) but many cancer types are now known to express VEGF receptors (Goel and Mercurio, 2013). The level of VEGF receptor expression has also been shown to associate with disease stage, progression, poor prognosis, metastasis and recurrence (Goel and Mercurio, 2013). The classical VEGF receptors (VEGFRs) are receptor tyrosine kinases namely VEGFR1 (/FLT1), VEGFR2 (/FLK1/KDR) and VEGFR3 (/FLT4) (Koch and Claesson-Welsh, 2012; Kowanetz, 2006). VEGFR2 is the dominant receptor facilitating VEGF-A signalling in endothelial cells for angiogenesis (Kowanetz, 2006). VEGFR1 may function as a decoy receptor to regulate VEGFR2 signalling by sequestering VEGF-A as VEGFR1 binds to VEGF-A with a higher affinity but generates a weaker response than VEGFR2 (Karkkainen and Petrova, 2000; Koch and Claesson-Welsh, 2012). VEGFR3 does not associate with VEGF-A but rather VEGF-C or VEGF-D to induce lymphangiogenesis (Karkkainen and Petrova, 2000; Koch and Claesson-Welsh, 2012). In addition neuropilins may contribute to VEGFR signalling by functioning as co-receptors for VEGF (Prud'homme and Glinka, 2012; Soker et al., 1998). The neuropilins lack catalytic activity of their cytoplasmic domain and therefore lack intrinsic signalling capability (Geretti et al., 2008; Prud'homme and Glinka, 2012). Neuropilins however, play a role in regulation of growth factor receptors as well as integrin signalling and may contribute to cancer progression in this manner (Goel and Mercurio, 2013; Goel et al., 2013).

The first step in VEGFR-stimulated signal transduction is the binding of VEGF to its tyrosine kinase receptor (Ji et al., 2014; Koch and Claesson-Welsh, 2012). Ligand binding causes a conformational change in the receptor which induces receptor dimerization. The juxtapositioned kinase domains of the receptor on the cytoplasmic face of the membrane then activate one another by trans-phosphorylation (Koch and Claesson-Welsh, 2012). Activated VEGFRs then activate a variety of targets such as those discussed below which promote cell

proliferation, survival and metastasis (Koch and Claesson-Welsh, 2012). The myriad of signal transduction networks involved in carcinogenesis and cancer progression are extremely complex and interwoven. This study will therefore focus on three signalling intermediates; protein kinase B (PKB), glycogen synthase kinase-3β (GSK3β) and focal adhesion kinase (FAK) which are suspected to be key mediators of VEGFR-stimulated signal transduction for cancer cell proliferation, survival and migration (refer to Figure 1 and Table 1).

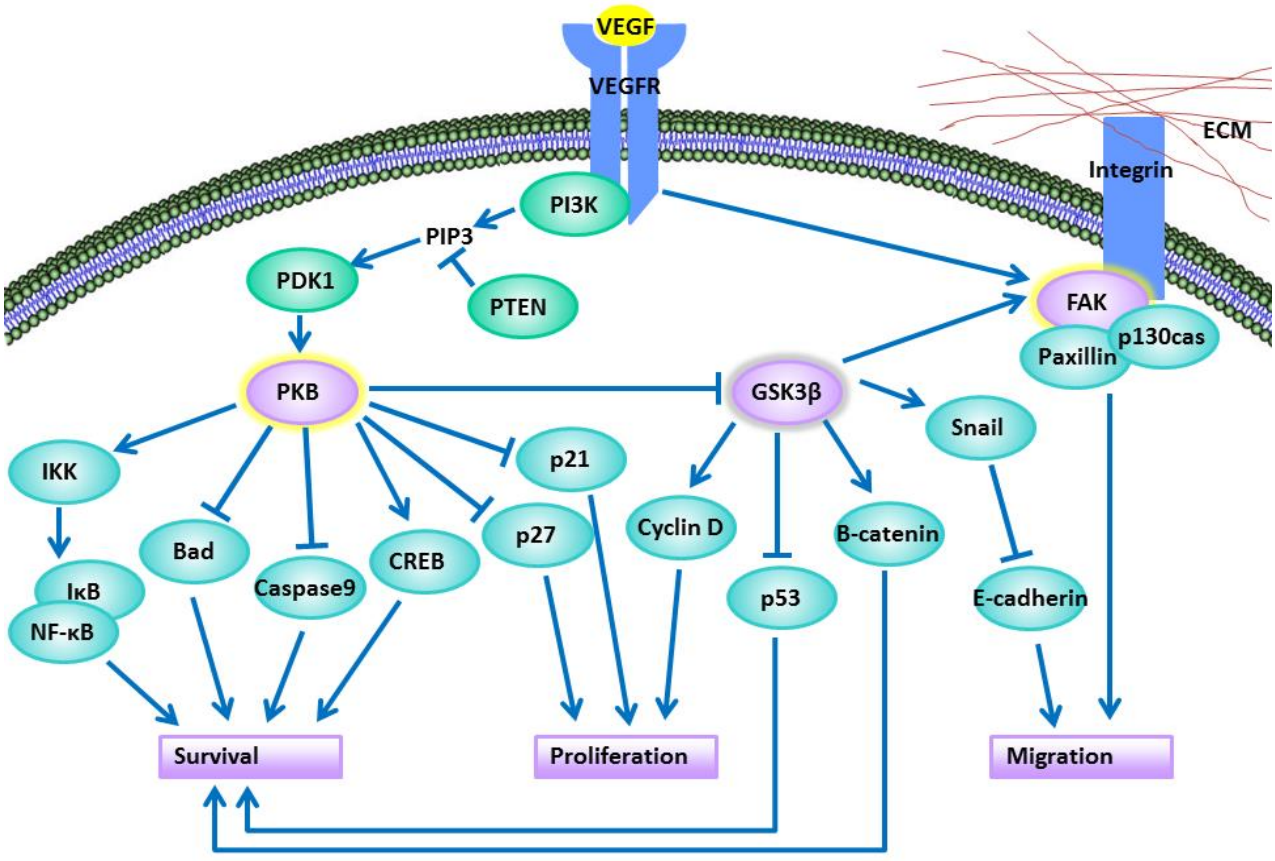

Figure 1: VEGFR-stimulated signal transduction pathways

VEGF binding to VEGFR initiates PKB, GSK3β and FAK mediated pathways for cell survival, proliferation and migration. VEGFR-stimulated signalling results in the activation (yellow glow) of PKB and FAK, where active PKB contributes to cell survival, proliferation and growth while active FAK effects migration, adhesion and cell shape. In contrast, VEGFR-stimulated signalling results in the inactivation (grey glow) of GSK3β, hindering its tumour suppressor activity and thus resulting in increased survival, proliferation and migration. [Figure generated by author]

Table 1: Signalling intermediates in pathways central to cell proliferation, survival and migration

Signalling intermediate	Phosphorylation state	Active/Inactive	Function
PKB	pPKBser473	Active	Cell growth, proliferation, survival
GSK3β	pGSK3βtyr216	Active	Tumour suppressor, apoptosis
	pGSK3βser9	Inactive	Survival, proliferation, chemo-resistance, migration
FAK	pFAKtyr397	Active	Migration, adhesion, cell shape

1.2.1 Protein kinase B

The ability of cancer cells to sustain proliferative signalling is possibly the most fundamental characteristic of cancer. In contrast to normal cells which carefully regulate signals for cell growth and division, cancer cells deregulate these signals and thus exhibit increased and uncontrolled proliferation (Hanahan and Weinberg, 2011). A study by Lichtenberger et al. (2010) found VEGFR signalling to induce cell proliferation in an autocrine manner independent of angiogenesis. Autocrine VEGFR-stimulated signal transduction is suspected to invoke cancer progression via the phosphoinositide 3-kinase/protein kinase B (PI3K/PKB) pathway important for cell survival and proliferation (Lee et al., 2012; Zeng et al., 2001).

PKB, also commonly referred to as Akt, is a key component of the PI3K pathway where it plays a pivotal role in the regulation of cellular processes associated with the cancer phenotype, including cell growth, proliferation and survival (Vara et al., 2004). The PI3K/PKB signalling pathway is frequently altered in many human cancers, and is thus an attractive therapeutic target (Vara et al., 2004). Increased PKB protein expression and activity has been found in gastric, breast, prostate, ovarian and brain cancers (Bellacosa et al., 1995; Cheng et al., 1996; Staal, 1987; Sun et al., 2001) while the PI3K gene (*PIK3C*) is amplified in ovarian and cervical cancers (Ma et al., 2000; Shayesteh et al., 1999). A gain-of-function mutation resulting in constitutively active PKB has been identified in human breast, colorectal and ovarian cancer (Carpten et al., 2007). Over expression or permanent activation of surface receptors in cancer cells also results in enhanced and/or constitutive activity of the PI3K/PKB pathway thereby increasing proliferation and survival, for example human epidermal growth factor receptor 2/Neu receptor overexpression in breast carcinoma (Harari

and Yarden, 2000; Vara et al., 2004). In addition, mutation of phosphatase and tension homologue leads to permanent PI3K/PKB activation in the advanced stages of several tumours including glioblastoma, endometrial and prostate cancer (Simpson and Parsons, 2001).

Upon activation of growth factor receptor tyrosine kinases such as VEGFR, PI3K is recruited to the membrane where it synthesises phosphatidylinositol-3,4,5-trisphosphate (PIP3) which in turn recruits PKB to the membrane where it is activated by phosphoinositide-dependent protein kinase-1 (Chin and Toker, 2009; Vara et al., 2004). The PKB serine/ threonine kinase is then translocated to the nucleus where many of its substrates are localised (Meier and Hemmings, 1999). PKB promotes proliferation and cell growth by regulating the activity of a variety of substrates such as glycogen synthase kinase-3 (GSK3) (Cross et al., 1995; Jope et al., 2007), phosphodisterase-3B, mammalian target of rapamycin (Inoki et al., 2002), insulin receptor substrate-1, the forkhead family member FKHR, and the cyclin-dependent kinase inhibitors $p21^{CIP1/WAF1}$ (Zhou et al., 2001) and $p27^{KIP1}$ (Shin et al., 2002) involved in protein synthesis, glycogen metabolism and cell cycle regulation (Blume-Jensen and Hunter, 2001; Vara et al., 2004). PKB also enhances apoptosis resistance and survival through inactivating by phosphorylation proapoptotic proteins such as Bad, procaspase-9 and Forkhead transcription factors which induce expression of proapoptotic genes (Kandasamy and Srivastava, 2002; Vara et al., 2004). Conversely the antiapoptotic IκB kinase protein and cyclic adenosine monophosphate response element-binding protein transcription factor are activated by PKB induced phosphorylation resulting in increased transcription of survival genes (Vara et al., 2004).

PKB was previously thought to only be involved in cancer cell survival and proliferation however early studies have found PKB may play a significant role in cell mobility and invasion. For example PKB enhances fibroblast lamellapodia via girdin (Enomoto et al., 2005), mouse mammary epithelial invasion via matrix metalloproteinase-2 (Park et al., 2001), fibrosarcoma mobility via nuclear factor-κB (Kim et al., 2001), invasion of human pancreatic cancer cells via insulin-like growth factor 1 receptor up-regulation (Tanno et al., 2001) and epithelial to mesenchyme transition (EMT) resulting in reduced intercellular adhesion and increased motility in squamous carcinoma cells (Grille et al., 2003). It is thus evident that PKB functions in pathways leading to migration and invasion besides its conventional role in proliferation and survival.

1.2.2 Glycogen synthase kinase-3β

Glycogen synthase kinase-3 (GSK3) has emerged as an important signalling intermediate regulating the response to insulin or growth factor stimulation such as VEGFR (Grimes and Jope, 2001). GSK3 contributes to cancer progression because of its crucial role in the regulation of many cellular functions such as cell division, migration, gene expression, apoptosis and inflammation (Jope et al., 2007). Although formerly thought to be restricted to glycogen metabolism GSK3 is now recognised to act as a serine/threonine kinase on numerous substrates (over 50) to carry out its many functions (Cohen and Frame, 2001; Jope et al., 2007). The functions of GSK3 are tightly regulated by the subcellular localisation of GSK3, the formation of GSK3 containing protein complexes, the phosphorylation of GSK3 itself, and the phosphorylation state of its substrates (Jope and Johnson, 2004). Inhibition of GSK3 has been suggested as a major target of oncogenic processes in order to enhance proliferative and invasive signalling while impeding apoptotic signalling (Jope et al., 2007).

Two isoforms of GSK3: exist GSK3α and GSK3β, although their functions overlap and are thus redundant in most cases, research has focused on the GSK3β isoform (Force and Woodgett, 2009). The activity of GSK3β is commonly inhibited in cancer cells by phosphorylation of the regulatory serine-9 (Jope and Johnson, 2004) predominantly mediated via two major signalling systems often deregulated in cancer; the PI3K/PKB and Wnt/β-catenin signalling pathways (Jope et al., 2007). Activation of Wnt signalling in cancer results in GSK3β inhibition, GSK3β is therefore unable to phosphorylate β-catenin which targets it for degradation (Polakis, 1999). The accumulated β-catenin then acts to enhance cell growth and survival by initiation of gene expression, including oncogenes such as cyclin D1, Myc and c-jun (Polakis, 1999). The activity of GSK3β is also inhibited via the PI3K/PKB signalling pathway as PKB directly phosphorylates GSK3β on the inhibitory serine residue (Cross et al., 1995; Grimes and Jope, 2001; Jope et al., 2007). In addition, GSK3β regulates apoptosis by promoting the actions of key tumour suppressor proteins such as p53 (Watcharasit et al., 2003). Inhibition of GSK3β has been shown to impede apoptotic signalling pathways and hence enhances resistance to chemotherapy as shown in hepatoma cell lines (Beurel et al., 2004, 2005). Furthermore, GSK3β phosphorylates numerous oncogenic elements such as c-Myc, β-catenin, Snail and B-cell lymphoma 3-encoded protein which targets them for degradation (Polakis, 1999; Viatour et al., 2004; Zhou et al., 2004)

and prevents protein synthesis by phosphorylation of the eukaryotic translation initiation factor 2B (Welsh and Proud, 1993). GSK3β therefore acts as a tumour suppressor, where its common inhibition in cancer is associated with cancer progression and survival (Jope et al., 2007). In accordance, GSK3β has been found to be constitutively inhibited in human hepatocellular carcinoma (Ban et al., 2003) and its expression down-regulated in squamous cell carcinoma of the tongue (Goto et al., 2002) and advanced prostate cancer (Mulholland et al., 2006). A study by Samuel et al. (2010) found loss of VEGFR signalling resulted in increased spontaneous apoptosis and chemo-sensitivity, thus it is possible that VEGFR signalling may act to inhibit GSK3β thereby impeding apoptotic signalling pathways while enhancing resistance to chemotherapy.

Besides its role in cancer progression, GSK3β has been implicated in metastasis. Since active GSK3β marks the Snail transcription factor for degradation, inhibition of GSK3β in cancer cells causes accumulation of Snail which suppresses the expression of the E-cadherin adhesion protein thus promoting cancer cell invasion and metastasis (Zhou et al., 2004). Inhibited GSK3β also promotes migration as in this form it is unable to phosphorylate adenomatous polyposis coli protein, which then associates with the plus-ends of microtubules and controls the direction of cell extension (Etienne-Manneville and Hall, 2003). In addition, active GSK3β reduces the activity of FAK therefore GSK3β inhibition would result in more active FAK which aids in cell spreading and migration (Bianchi et al., 2005). GSK3β inhibition therefore plays an integral role in cancer by contributing to increased proliferation, survival and migration (Jope et al., 2007).

1.2.3 Focal adhesion kinase

Samuel et al. (2010) found VEGFR-stimulated signalling to be associated with increased cell motility and invasion. Migration of cancer cells requires dynamic interplay between the extracellular matrix (ECM) and the actin cytoskeleton at focal adhesion sites (Brakebusch and Fässler, 2003; Wolf and Friedl, 2006). Focal adhesion kinase (FAK) is a non-receptor tyrosine kinase which functions to promote cell migration by bridging signals between integrins and growth factor receptors (Mitra et al., 2005; Sieg et al., 2000). Upon integrin or growth factor stimulation FAK is activated by Tyr-397 phosphorylation, which provides a binding site for Src family kinases (Schaller et al., 1994), PI3K (Chen and Guan, 1994) and phospholipase C (Zhang et al., 1999). Binding of Src to FAK, results in further phosphorylation of FAK at Tyr-576/577 essential for full FAK activation. The activated

FAK-Src complex is then able to mediate phosphorylation of numerous adhesion components such as p130Cas and paxillin involved in the dynamic regulation of cell attachment and migration (Chodniewicz and Klemke, 2004; Turner, 2000). FAK activity has been associated with the disassembly of focal contacts where its loss results in defects in focal contact turnover (Webb et al., 2004). FAK also functions in the regulation of actin and microtubule structures as well as the formation and disassembly of cell-cell contacts through FAK-mediated regulation of Rho-family GTPases (Palazzo et al., 2004).

Expression of FAK is heightened in metastatic cancers of the breast, prostate, colon and brain (Cance et al., 2000; Gabarra-Niecko et al., 2003; Lark et al., 2005; Owens et al., 1995) where it contributes to changes in cell shape and the formation of invadopodia for migration and invasion (Chan et al., 2009; Hauck et al., 2002; Hsia et al., 2003; Mitra et al., 2005). Studies have shown disruption of FAK blocks the response to cell motility cues (Schlaepfer et al., 2004), blocks mammary carcinoma metastases to the lungs (van Nimwegen et al., 2005) and prevents carcinoma formation in a mouse transgenic cancer model (Lahlou et al., 2007). VEGFR-stimulated signalling has been inferred to induce FAK activation essential for regulation of focal adhesions and migration (Rousseau et al., 2000).

1.2.4 Non-canonical mediation of VEGFR signalling

In addition to the above described pathways VEGFR signalling is involved in epithelial-mesenchymal transition (EMT), a conversion leading to an undifferentiated state and increased aggressiveness. EMT can be induced in normal epithelial cells and differentiated carcinoma cells by stimulation with VEGF resulting in reduced cell–cell interactions and increased motility (Mak et al., 2010). Conversely VEGF expression increased in response to EMT in colorectal carcinoma cell cultures and VEGFR-stimulated signalling was therefore suspected to have an essential role in the ability of cancer cells to migrate and survive in the absence of any cell-cell contacts (Bates et al., 2003). VEGFRs were also shown to increase upon EMT and inhibition of VEGFR1 was shown to cause considerable apoptosis in cells that underwent EMT. VEGF/VEGFR autocrine signalling was therefore concluded to be crucial for EMT and the survival of colorectal carcinoma cells (Bates et al., 2003).

Furthermore autocrine VEGFR-stimulated signalling has been implicated to have a fundamental role in carcinogenesis and the function of cancer stem cells (Goel and Mercurio, 2013). Many tumours contain a small amount of cancer stem cells which have the capacity to self-renew and initiate the growth of new tumours (Driessens et al., 2012). Several studies of

early stage squamous carcinoma indicate the involvement of VEGFR-stimulated signalling in the function of cancer stem cells (Beck et al., 2011). Inhibition of VEGFR2 was found to reduce the amount of cancer stem cells present in a tumour and weaken their self-renewal potential (Beck et al., 2011). In established tumours deletion of VEGFA was shown to result in tumour regression by reducing proliferation and renewal of cancer stem cells (Beck et al., 2011).

Autocrine VEGFR-stimulated signalling in tumour cells may therefore be an important factor contributing the cancerous state. Indeed autocrine VEGFR-stimulated signalling has been shown to be characteristic of highly aggressive cancers and poorly differentiated carcinomas (Cao et al., 2012).

1.3 Cancer in South Africa

Cancer is a major cause of death worldwide with an estimated 8.2 million cancer deaths occurring in 2012 alone (Ferlay et al., 2013). Aside from the suffering imposed on the individual diagnosed, their friends and family; cancer has a huge economic burden (Stewart and Wild, 2014). It has been estimated that the global financial cost of cancer resulting from premature death and disability, discounting direct medical expenses was $895 billion in 2008 (American Cancer Society, 2010). The number of new cancer cases is projected to increase from approximately 14.1 million in 2012 to 19.3 million in the year 2025 (Ferlay et al., 2013). The rising cancer toll places great strain on health-care systems especially in developing countries which are ill-equipped to deal with the increasing number of cancer patients (Stewart and Wild, 2014). The plight of cancer in South Africa is no exception from worldwide trends; indeed it may be worse as South Africa faces heightened prevalence of some particularly aggressive cancer forms such as human oesophageal squamous cell carcinoma.

1.3.1 Human Oesophageal Squamous Cell Carcinoma

Oesophageal cancer is the eighth most common cancer worldwide and the primary cause of cancer death among South African Black males (Blot, 1994; Ferlay et al., 2013). This form of cancer is renowned for its aggressiveness and high rate of metastasis (Klimstra, 1994). Oesophageal cancer is detected late in the majority of patients as advanced metastatic disease.

Patients have a poor prognosis with 88 % mortality of incidences due to late diagnosis and the rapid spread of cancer cells (Ferlay et al., 2013; Stoner and Gupta, 2001).

There are two main forms of oesophageal cancer, namely human oesophageal squamous cell carcinoma (HOSCC) and oesophageal adenocarcinoma. The most predominant is HOSCC, which accounts for more than 90 % of oesophageal cancer cases worldwide (Stoner and Gupta, 2001). HOSCC affects the oesophageal epithelium and is characterised by fungating, ulcerating or infiltrating lesions (Stoner and Gupta, 2001). HOSCC is often associated with lymph node metastases and cancer recurrence (Aurello et al., 2006). Current therapies including surgery, radiotherapy and chemotherapy are largely ineffective and the prognosis is generally poor (Stoner and Gupta, 2001).

There is more than a 20-fold difference in incidence of oesophageal cancer between the different regions of the world with approximately 80 % of the cases occurring in less developed regions (Ferlay et al., 2013). HOSCC has a varied geographical distribution with increased incidences in certain parts of China, Iran, South Africa, Uruguay, France and Italy (Schottenfeld, 1984; Sons, 1987). HOSCC is particularly prevalent among the Black population in the Transkei region of South Africa (Du Plessis et al., 1999). The varied geographical distribution lead researchers to suspect that particular environmental factors contribute significantly to the aetiology of HOSCC (Stoner and Gupta, 2001).

Like most cancers, the aetiology of HOSCC is multifactorial and involves several environmental and/or genetic factors (Stoner and Gupta, 2001). Excessive tobacco use is suspected to be the principal risk factor for HOSCC as several of its constituents have been implicated in oesophageal carcinoma pathogenesis (Stoner and Gupta, 2001). Alcohol consumption further exacerbates the risk of tobacco smokers to develop HOSCC (Stoner and Gupta, 2001). Salt-pickled, salt-cured and mouldy food consumption may also play a role in the development of oesophageal carcinoma due to frequent contamination with N-nitrosamine carcinogens and fungal toxins (Stoner and Gupta, 2001). In addition other factors such as vitamin and trace mineral deficiencies, consumption of hot beverages and fungal invasion of oesophageal tissues are associated with an increased risk of HOSCC (Stoner and Gupta, 2001). Certain genetic abnormalities have also been found to be consistently associated with HOSCC (Mandard et al., 2000; Stoner and Gupta, 2001). Much research is still required to pinpoint the exact factors involved in HOSCC development and thereby design an effective strategy for its prevention. In the meantime the high prevalence of

HOSCC in South Africa requires research into the mechanisms of HOSCC progression and metastasis.

1.4 VEGF receptor-stimulated signal transduction in HOSCC

Signal transduction pathways are essential for regulation of many biological processes and thus disruption of these signal transduction pathways are involved in many cancers (Vara et al., 2004). The signal transduction pathway stimulated by the VEGF receptor is disrupted in many human tumours where it contributes to increased cell proliferation, apoptosis prevention, angiogenesis promotion, metastasis and increased resistance to treatment. Since autocrine VEGFR-stimulated signalling has been implicated in proliferation and metastasis of other highly aggressive cancers (Cao et al., 2012), it may be an important factor contributing to HOSCC progression and metastasis. The study by Inoue et al. (1997) determined that HOSCC cells produce VEGFs, specifically VEGF-A_{165} and VEGF-A_{121} isoforms. Furthermore they found high levels of VEGF to be associated with well differentiated tumours, deeper invasion, increased blood vessels, greater incidences of distant metastases and poorer prognosis (Inoue et al., 1997). In addition a more recent study by Liu et al (2011) found the mRNA levels of VEGF-C, VEGFR2 and VEGFR3 to be significantly increased in HOSCC in comparison to adjacent normal oesophageal tissues. VEGF protein expression was reported to be significantly higher in deeply infiltrating HOSCC tissue in comparison to superficially infiltrating tissue and higher in HOSCC tissue with lymph node metastases in comparison to tissues without lymph node metastases (Zhao et al., 2015). It was therefore concluded that VEGFR-stimulated signalling is associated with tumour progression and increased malignancy of HOSCC. Although paracrine induction of angiogenesis accounts for many malignant characteristics of VEGFR-stimulated signalling, autocrine VEGFR-stimulated signalling is suspected to contribute via an as yet unclear mechanism (Inoue et al., 1997; Zhao et al., 2015). An improved understanding of VEGFR dependant autocrine signalling may therefore provide insight into the aberrant signalling pathways by which HOSCC progresses, invades and metastasises. In addition the knowledge derived from this study may be useful for the identification of signalling pathways and intermediates which could potentially be targeted to hinder HOSCC progression.

Objective and aims

The objective of this research is to determine the influence of VEGFR-stimulated signal transduction in HOSCC and thereby elucidate the mechanism by which autocrine VEGFR signalling aids in HOSCC proliferation and metastasis.

The specific aims include:

- To establish the existence of an autocrine VEGF/VEGFR signalling axis in HOSCC
- To investigate the influence of VEGFR-stimulated signal transduction on HOSCC proliferation and migration
- To investigate the influence of VEGFR-stimulated signal transduction on HOSCC signalling intermediates central to proliferation and migration
- To discern the pathways through which autocrine VEGFR-stimulation acts to influence proliferation and migration
- To investigate the interdependence of signalling intermediates activated as a result of VEGFR-stimulated signal transduction in HOSCC
- To investigate the behavioural function of VEGFR-stimulation induced signalling intermediates in HOSCC

Chapter 2: VEGFR-stimulated signal transduction in HOSCC proliferation

2.1 Introduction

VEGFR stimulated signal transduction was previous thought to be limited to endothelial cells for the process of angiogenesis. More recent evidence however, suggests a role for autocrine VEGFR signalling in tumour cells (Goel and Mercurio, 2013). Many tumour types are now known to have disrupted autocrine VEGFR stimulated signalling which contributes to their enhanced proliferation. Indeed increased VEGF expression in many human tumours is often associated with worsening clinical parameters. Specifically VEGF expression has been correlated with poor survival or outcome in breast (Ghosh et al., 2008; Goel et al., 2013; de Jong et al., 1998; Mylona et al., 2007), colon (Takahashi et al., 1995; Wei, 2005), gastric (Ozdemir et al., 2006), oral squamous (Kyzas, 2005; Riedel et al., 2000), lung (Carrillo de Santa Pau et al., 2009; Decaussin et al., 1999; Lantuéjoul et al., 2003; Seto et al., 2006) and mesothelioma (Strizzi et al., 2001) cancer. The ability of cancer cells to produce VEGFR and thus have the potential to respond to VEGFR stimulus further supports the theory of an autocrine VEGFR signalling mechanism within cancer cells. VEGFR2 receptor expression has been correlated with disease stage and progression in bladder (Xia et al., 2006) and colon (Giatromanolaki et al., 2007; Takahashi et al., 1995) cancers. Furthermore VEGFR2 expression has been correlated with poor survival or outcome in breast (Ghosh et al., 2008; de Jong et al., 1998; Nakopoulou et al., 2002) endometrial (Giatromanolaki et al., 2006), hepatocellular (Huang et al., 2011) and lung cancer (Carrillo de Santa Pau et al., 2009; Decaussin et al., 1999; Seto et al., 2006; Yang et al., 2011). We believe the autocrine VEGF/VEGFR signalling axis may be similarly disrupted in HOSCC where enhanced VEGF/VEGFR signalling may lead to deregulation of HOSCC proliferation.

The precise mechanism by which disrupted autocrine VEGFR signalling contributes to these cancer promoting behaviours has however not yet been pin pointed. PKB mediated signalling has long been known as a major player in cancer cell proliferation (Vara et al., 2004). In addition, prior studies show HOSCCs possess high levels of active PKB which increase upon EGFR stimulation (Shaw, 2011). We thus postulate PKB is a mediator of autocrine VEGFR induced proliferation. Furthermore as a downstream target of both the PI3K/PKB and mitogen-activated protein kinase/extracellular signal-regulated kinase (MAPK/ERK)

signalling pathways important in proliferation, GSK3β has been implicated in the development and progression of many cancers (Jope et al., 2007). GSK3β is also crucial in the regulation of diverse cellular functions such as cell division, gene expression, and apoptosis (Jope et al., 2007). We therefore suspect GSK3β may have a role in mediating VEGFR-induced cancer promoting behaviours of HOSCC such as enhanced proliferation and survival.

In order to determine whether an autocrine VEGFR signalling axis exists in HOSCC, the production of VEGF by HOSCC was assessed in conjunction with the response of HOSCC to VEGFR stimulus. Autocrine VEGFR-stimulated signalling in HOSCC may act to increase HOSCC proliferation and thus the effect on proliferation was investigated. In addition, the influence of VEGFR signalling on intermediates (PKB and GSK3β) suspected to be integral to autocrine VEGFR-stimulated signal transduction was also investigated. Taken together these inquiries would shed light on VEGFR signal transduction pathways in HOSCC proliferation.

2.2 Materials and Methods

2.2.1 Tissue culture

Five moderately differentiated human oesophageal squamous cell carcinoma cell lines of South African origin Wits Human Carcinoma of the Oesophagus (WHCO, where WH is omitted in figures due to space constraints) WHCO1, WHCO3, WHCO5, WHCO6 and human oesophageal carcinoma SNO were obtained from the Cell Biology Laboratory, School of Molecular and Cell Biology, University of the Witwatersrand (Bey et al., 1976; Takahashi et al., 1990; Veale and Thornley, 1989). In addition the well characterised human breast adenocarcinoma cell line MCF7 and human non-small cell lung carcinoma cell line H1299 were obtained for use as controls. The MCF7 cell line was used as a positive control because they are known to secrete VEGF and are able to respond to VEGF stimulus (Cascio et al., 2010). The H1299 cell line was used as a positive control for VEGF, pPKB, pGSK3βser9 and pFAK expression as it is known to express these proteins at detectable levels, through routine use in the Cell Biology Laboratory, School of Molecular and Cell Biology, University of the Witwatersrand. All cell lines were cultured under conditions found to be optimal and thus standard for HOSCC culture (Bey et al., 1976; Takahashi et al., 1990; Veale and Thornley, 1989). Cells were cultured in DMEM : Hams F12 (3:1) (Appendix A.1) media supplemented with 10 % fetal calf serum (FCS) (Highveld Biologicals) on 10 cm Corning tissue culture dishes at 37 °C, 5 % atmospheric carbon dioxide. Upon reaching approximately 80 % confluency the cells were passaged as follows. Cells were rinsed twice with pre-warmed sterile phosphate buffered saline (PBS) (Appendix A.2) before being detached from the culture dish by treatment with trypsin (Gibco BRL): ethylenediamine tetraacetic acid (EDTA) (BDH Laboratory Reagents) (Appendix A.3) for 5 min. The detached cells were then transferred to a new culture dish and resuspended in fresh culture media.

Three biological replicates of each experiment were performed. For each experimental set replicates took place on three separate occasions on cell cultures of different passage (passage range 20-120).

2.2.2 Treatment set to provide insight into VEGFR-stimulated signal transduction in proliferation of HOSCC

Cells cultured to approximately 70 % confluency in 6 cm tissue culture dishes were rinsed twice with sterile pre-warmed PBS and fresh media was provided. Cultures were then treated

with VEGF (Sigma-Aldrich®, V7259) for 10 minutes at final concentration of 50 µg/ml in fresh media or with Axitinib (a VEGFR inhibitor) (Abcam®, ab141985) in dimethyl sulfoxide (DMSO) at final concentration of 10 µmol/L in fresh media for an hour, 10 minutes prior to completion of the treatment VEGF was added to a final concentration of 50 µg/ml. Control experiments were carried out simultaneously in the exact same manner with corresponding DMSO concentrations lacking the treatment.

2.2.3 Protein extraction

Total cellular protein was extracted from the above mentioned cell lines. The tissue culture medium was aspirated and cultures were washed twice in sterile PBS. A small amount of PBS containing the serine protease inhibitor phenylmethylsulfonyl fluoride (PMSF) (1 mM) (Appendix A.4) and phosphatase inhibitors Na_3VO_4 (10 mM) (Appendix A.5) and NaF (5 mM) (Appendix A.6) was added. The cells were then scraped from the culture dish into the liquid and transferred into a sterile eppendorf tube. The suspension was centrifuged for 60 seconds in a TOMY HF-120 centrifuge (1 145 xg). The supernatant was discarded and the pellet resuspended in double Laemmli lysis buffer (Appendix A.7) then boiled for 5 minutes. The resultant cell lysate was centrifuged at 12 000 x g for 15 minutes at 4 °C in a PRISM™ Refrigerated Microcentrifuge and stored at -20 °C.

2.2.4 Protein concentration determination

The protein concentration of cell lysate samples was determined following the methodology of Bramhall et al. (1969). The high SDS concentration (4 %) contained in Laemmli double lysis buffer used for protein extraction is known to cause interference with several protein quantification assays. The method describe by Bramhall et al. (1969) minimises inference due to SDS as SDS present in samples is washed off samples after fixation to a membrane, therefore increasing the accuracy of protein concentration determination. Highly accurate protein concentration determination is of particular importance since VEGF and the phosphorylated proteins studied here are present in very low concentrations in cell lysate samples.

Whatman® filter paper was rinsed in distilled water for 20 minutes and dehydrated by rinsing in 95 % ethanol, 100 % ethanol and 100 % actetone for 5 minutes each before being air dried. A standard curve of known protein amount was constructed by spotting 1, 3, 6, 12, 16 and 20 µg of Bovine Serum Albumin (BSA) dissolved in Laemmli double lysis buffer (1 µg/µl) onto

the dried filter paper, as well as 2 µl cell lysate of unknown protein concentration. The filter paper was air dried again and the proteins fixed to the filter paper with 7.5 % trichloracetic acid (Appendix A.8) for 45 minutes. The filter paper was stained with coomassie blue (Appendix A.9) for an hour and then destained (Appendix A.10.) for an hour. After drying each of the stained protein spots were cut out and eluted in 5 ml of elution solution (Appendix A.11) overnight in the dark. The absorbance readings of the BSA protein standards and the cell lysate samples were read using an Abbota SV1100 Spectrophotometer at a wavelength of 595 nm, blanked with elution solution. A standard curve of absorbance versus protein amount was constructed and used to determine the protein amount (per 2 µl spotted) and subsequently protein concentration of the cell lysate samples (Appendix B.1).

2.2.5 Sodium Dodecyl Sulphate–Polyacrylamide Gel Electrophoresis

Equivalent amounts of total protein were resolved by reducing Sodium Dodecyl Sulphate–Polyacrylamide Gel Electrophoresis (SDS-PAGE). A separating gel (10 % acrylamide) (Appendix A.13) was cast between two glass plates using the Mighty Small™ SE245 Dual Gel Caster and allowed to polymerise under a thin layer of 0.2 % SDS (Appendix A.12) to exclude air which hinders polymerisation. The SDS layer was then removed and a stacking gel (5 % acrylamide) (Appendix A.14) was laid above the separating gel. A comb was inserted into the stacking gel to form wells in which to load the samples. Upon polymerisation the gel and supporting glass plates were transferred into the Mighty Small™ SE250 Electrophoresis Unit and the reservoirs appropriately filled with electrophoresis running buffer (pH 8.3) (Appendix A.16). The comb was removed and cell lysate samples of equivalent total protein amounts (40 µg unless stated otherwise) were loaded into the wells alongside a small amount of PageRuler™ Prestained Protein Ladder (Fermentas Life Science). The gel was electrophoresed at constant current of 21 mA per gel. The resolved protein samples were visualised by staining the gel in coomassie blue (Appendix A.9) for an hour and then destaining for an hour (Appendix A.15).

2.2.6 Western blot

Cell lysate samples were resolved by 10 % SDS-PAGE as described above and the polyacrylamide gel cropped to appropriate size based on the expected molecular weight of the protein of interest using the molecular weight marker as a guide. The resolved proteins were then transferred onto Hybond™-C nitrocellulose membrane (Sartorius) using a Bio-Rad

Criterion™ Blotter containing chilled transfer buffer (pH 8.3) (Appendix A.17) at 400 mA for 2-3 hours. Thereafter the nitrocellulose membrane was washed once in tris-buffered saline (TBS) (Appendix A.18) and placed in a blocking solution of 5 % milk powder in TBS with Tween®20 (TBST) (Appendix A.19) for 1 hour. The membrane was then washed twice in TBST for 5 minutes each and incubated in primary antibody solution (refer to Table 2 below). Residual antibody was removed by washing the membrane thrice in TBST (5 min each) before incubation in secondary antibody solution (refer to Table 2 below). Secondary antibody incubation and all following steps were carried out in the dark as much as possible to prevent photochemical bleaching of the light sensitive secondary antibody. Residual antibody was again removed by washing the membrane thrice in TBST (5 min each) and once in TBS. The membrane was then incubated in SuperSignal™ West Pico Chemiluminescent Substrate (Appendix A.21) for 5 minutes after which it was removed, sealed in cling film and exposed to CL-XPosure™ X-ray Film (Thermo Fisher Scientific) in the dark. The film was then developed by rinsing in developer solution (Appendix A.22), followed by water, fixer solution (Appendix A.23) and lastly water. To control for protein loading, each cell lysate sample was also probed with an anti-β-actin antibody.

The VEGF western blot protocol was optimised as follows. A dot blot was performed in order to assess the functionality of the anti-VEGF antibody (Appendix C.2). Whilst the antibody's functionality was confirmed much optimisation of the VEGF western blot protocol was required including adjustments of both primary (1:100 – 1:5000) and secondary antibody concentration (1:2000 – 1:50 000), dilution buffer (0-5 % milk vs BSA in PBS) for each antibody as well as adjustment of primary antibody incubation time (1 hour – overnight). Many intervals and combination were attempted and, while not ideal, the best conditions were found to be primary anti-VEGF antibody diluted 1: 200 in PBS incubated 3 hours at room temperature followed by secondary antibody diluted 1:10 000 in PBS for an hour.

Table 2: pPKB, pGSK3βser9, VEGF and β-Actin antibodies for western blotting; dilutions and incubation conditions

Protein of interest	pPKB	pGSK3βser9	VEGF	β-Actin
Primary antibody	Phospho-Akt (Ser473) Antibody (Cell Signalling Technology®, #9271)	Phospho-GSK-3β (Ser9) Antibody (Cell Signalling Technology®, #9336)	Rabbit anti-VEGF (Invitrogen™, 18-0254)	Anti-Actin (Sigma-Aldrich®, A2066)
Transfer time (hr)	2	2	1	2
Dilution (antibody : buffer)	1: 1 000	1: 1 000	1: 200	1: 2 500
Buffer	5 % BSA in TBST	2.5 % BSA in TBST	PBS	2.5 % milk powder in PBS
Incubation conditions	Overnight at 4 °C	Overnight at 4 °C	3 hours at room temperature	Overnight at 4 °C
Secondary antibody	Anti-Rabbit IgG Peroxidase Conjugate (Sigma-Aldrich®, A6154)	Anti-Rabbit IgG Peroxidase Conjugate (Sigma-Aldrich®, A6154)	Anti-Rabbit IgG Peroxidase Conjugate (Sigma-Aldrich®, A6154)	Anti-Rabbit IgG Peroxidase Conjugate (Sigma-Aldrich®, A6154)
Dilution (antibody: buffer)	1: 2 000	1: 3 000	1: 10 000	1: 20 000
Buffer	5 % milk powder in TBST	2.5 % milk powder in Blocking Buffer (Appendix A.20.)	PBS	PBS
Incubation conditions	1 hour at 30 °C in the dark	1 hour at room temperature in the dark	1 hour at room temperature in the dark	1 hour at 30 °C in the dark

2.2.7 Semi-quantitative analysis

Western blot X-ray film images were digitised with the use of a Hewlett Packard ScanJet G3110 desktop scanner. Densitometric analysis was then performed using Image Studio™ Lite 5.2 software to determine relative protein expression levels and thus allow semi-quantitative comparisons.

Since densitometry is a semi-quantitative method which measures a protein's abundance relative to that of other samples and only a limited number of samples can be subjected to western blotting simultaneously due to limited wells of an SDS-PAGE (10 in this case), the effect of changes in exposure and development between blots was controlled for by always measuring the protein's abundance relative to the positive control untreated H1299 cell lysate (set at 100). The abundance of a particular protein is assumed to be unchanging across untreated H1299 cell lysate samples, thus allowing comparison of the relative expression levels of a particular protein across multiple blots.

In addition, the ratio of exposure between samples also fluctuates between blots and was controlled for by adjusting the ratio of an untreated WHCO6 internal control to the H1299 positive control to match the corresponding ratio under standard HOSCC culture conditions (Appendix B.2). This normalisation gave a more reliable estimate of the relative protein abundance of control and treatment samples allowing for more accurate statistical comparison without altering the change due to treatment as these samples were always run together on the same blot and thus multiplied by the same factor.

2.2.8 Cellular proliferation assay

Cellular proliferation was detected through a MTT (3-(4,5-dimethylthiazol-2-yl)-2,5-diphenyltetrazolium bromide) tetrazolium reduction assay. HOSCC and control cell cultures were seeded equally into 3 cm dishes. Cultures were treated as described in Chapter 2, Section 2.2.2 and the cells allowed to incubate for 24 hr. The MTT substrate solution (Appendix A.24) was then added to the cells in culture at a final concentration of 6 mM and incubated at 37 °C for 2 hours followed by 2 hours of incubation in isopropanol to dissolve the formazan crystals. The quantity of formazan produced (reflective of the number of viable cells) per sample was then determined by measuring the absorbance at 570 nm.

2.2.9 Comparisons and statistical analysis

The percentage change (Δ %) between treated and control samples was calculated as described in equation 1 below.

Equation 1: $$\Delta\,\% = \frac{\%_{treated} - \%_{control}}{\%_{control}} \times 100$$

where a positive % Δ indicates an increase due to treatment
and a negative % Δ indicates a decrease due to treatment

Each experiment was performed in triplicate and the mean percentage change between the treated and control samples was determined for each cell line and represented on a graph. The standard error of each experiment was calculated as describe in equation 2 and represented with error bars on the graph.

Equation 2: $SE = \frac{s}{\sqrt{n}}$

where s is the sample standard deviation
and n is the size of the sample i.e. 3

A student's T-test was performed on Microsoft® Excel® to determine whether the difference between the means of the treated and control samples was significant at a 95 % confidence level ($p < 0.05$).

2.3 Results

In order to assess the effect of VEGFR-stimulated signal transduction in HOSCC, the change in abundance of the activation state of signalling intermediates central in processes contributing to cancer progression was assessed. In contrast to total protein present in substantial amounts in the cell, phosphorylated protein forms are present in very small quantities (Sefton, 1998). High quality protein extraction and accurate protein concentration determination is therefore essential in order to allow accurate comparison between samples, of particular importance due to the sensitivity of the western blot technique. Protein determination standard curves were of consistently high precision ($R^2 \geq 0.98$) assuring accurate protein concentration determination (Appendix B.1) of particular importance since even small errors could having significant effects on relative abundance of phosphorylated protein due to their very low concentrations in the cell lysate samples. Protein extraction was confirmed to be of high quality as SDS-PAGE resolved protein extracts to display a distinct banding pattern of intact protein, uncontaminated by DNA and cellular debris (Appendix C.1). Furthermore, the equal staining of each lane indicated the same amount of total protein was loaded in each lane as a result of accurate protein concentration determination (Appendix C.1). Consistency in amount of protein loaded for western blotting was further examined by analysis of the amount of β-actin present, which was consistent across cell lines and treatments for each blot (Figure 2a, Figure 4a and Figure 19a). Confidence in the accuracy of protein concentration and loading meant that the determined relative abundance of a protein is a true reflection of that present in the cell culture sample.

2.3.1 Quantification of VEGF protein content in HOSCC

In order for VEGFR signalling to play a role in HOSCC carcinogenesis and progression, HOSCC cells need to both produce VEGF and respond to its stimulus. VEGF is expressed and functional at exceedingly low concentrations (1-50 pg/ml for biological activity) necessitating the loading of very large quantities of total cellular protein (120 μg) onto an SDS-PAGE gel for detection via western blotting (Cascio et al., 2010; Weigand et al., 2005). In addition very high primary antibody concentrations (1: 200) were required for VEGFR detection (see Chapter 2, Section 2.2.6). The VEGF protein content of HOSCC was thus assessed via semi-quantitative western blot analysis under these conditions (Figure 2).

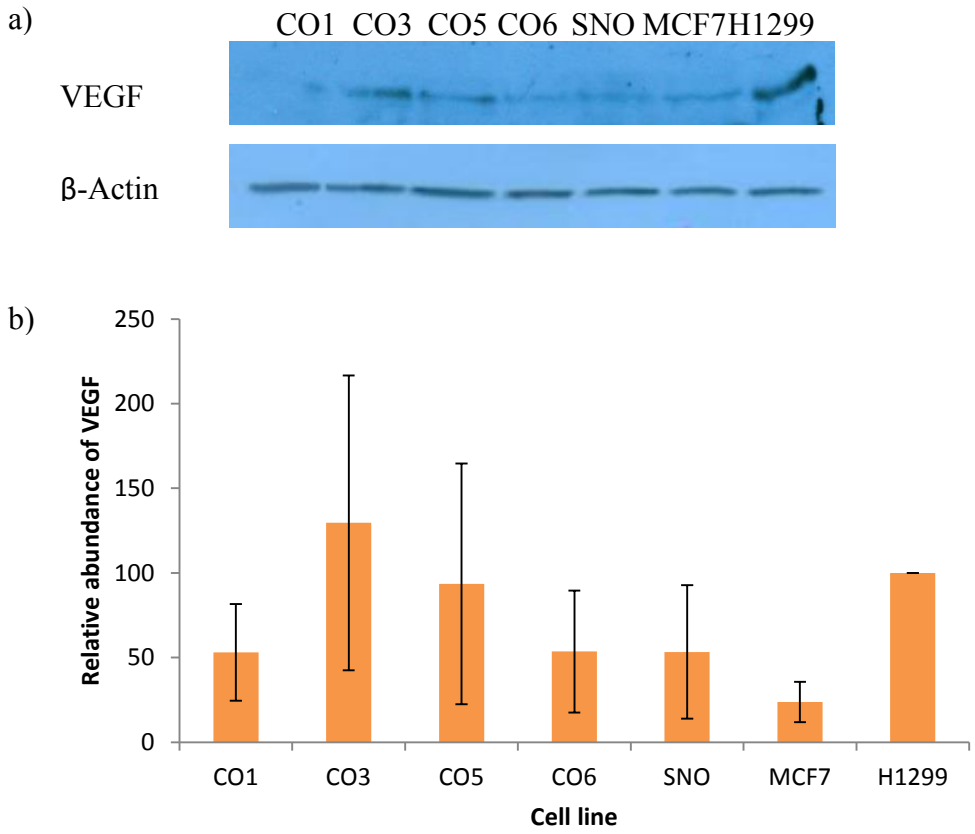

Figure 2: VEGF protein content in HOSCC cell lines

a) The HOSCC cell lines, MCF7 and H1299 control cell lines contain VEGF protein. Western blotting detected the VEGF monomer at 21 kDa and β-Actin served as the loading control. b) The mean abundance of VEGF (n ≥ 3) in each HOSCC cell line was determined via densitometric analysis, relative to the H1299 external control set at 100. Standard error denoted as error bars.

It is evident that like many other cancer types HOSCCs have acquired the ability to aberrantly produce VEGF (Figure 2). The human breast adenocarcinoma cell line MCF7 was used as a positive control because it is known to both produce and respond to VEGF (Cascio et al., 2010). While all HOSCC cell lines did in fact produce VEGF the level at which they did so varied. The WHCO1, WHCO6 and SNO cell lines produce more than double the quantity of VEGF as the MCF7 positive control cell line while the WHCO5 and H1299 cell lines produced approximate four times as much as the MCF7 positive control and the WHCO3 cell line produced the most VEGF, roughly five and a half time the quantity of VEGF produced by MCF7s (Figure 2). HOSCC cells are therefore confirmed to produce VEGF (as indicated above) almost certainly a precursor to its secretion. Moreover this study postulates VEGF may be able to stimulate the same HOSCC cells from which it originated in an autocrine manner to further HOSCC progression.

The abundance of VEGF protein content in the HOSCC cell lines was measured relative to the positive control untreated H1299 cell lysate (set at 100). Through routine use in the Cell Biology Laboratory, School of Molecular and Cell Biology, University of the Witwatersrand where this study was based, the H1299 cell line is known to produce high levels of the signalling intermediates (pPKB, pGSK3β and pFAK) investigated here. High levels VEGF protein in the H1299 cell line further supports its usefulness as a positive control for the expression of the proteins investigated in this study and thus as robust standard to which the abundance of expressed protein may be set (see Chapter 2, Section 2.2.7).

2.3.2 Effect of VEGFR stimulation on HOSCC proliferation

Elevated abundance of VEGF in HOSCCs suggests a potential for autocrine VEGFR-stimulated signalling which may influence proliferation and survival of HOSCC. In order to confirm the role of VEGFR signalling in proliferation the effect of VEGFR stimulation and inhibition on cellular proliferation was observed though an MTT assay (Figure 3).

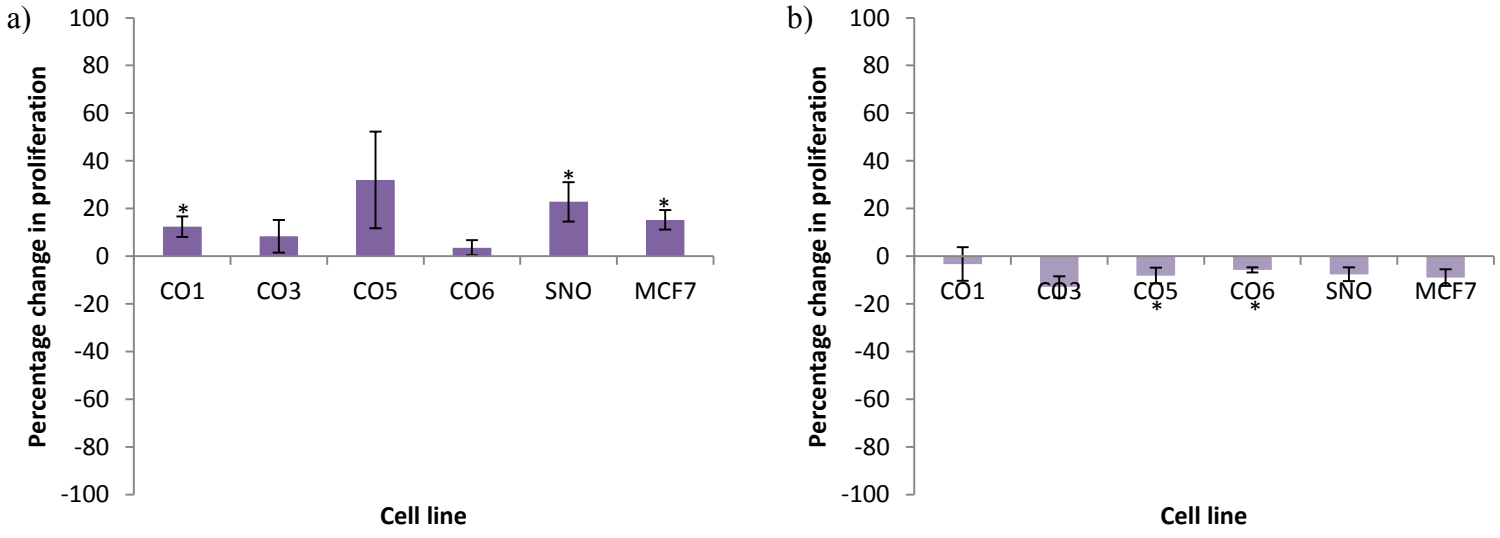

Figure 3: VEGFR signalling influences the proliferation of HOSCC cell lines

a) VEGFR stimulation increases proliferation of HOSCC cell lines (VEGFR stimulated vs control) while b) VEGFR inhibition decreases HOSCC proliferation (VEGFR inhibited vs control). HOSCC cell lines and the MCF7 control cell line were treated for 24 hours, after which an MTT proliferation assay was performed ($n \geq 3$). The mean difference was represented as percentage change and standard error denoted as error bars. Significant difference at a 95 % confidence level ($p <= 0.05$) between the means of control and treated samples is indicated by an *.

HOSCC cell lines stimulated with VEGF displayed an increase in proliferation, owing to more cells being present in VEGFR-stimulated cultures 24 hours after equivalent seeding (Figure 3a). Conversely, VEGFR inhibition leads to a decrease in proliferation of HOSCC cell lines (Figure 3b). The effect of VEGFR stimulation and inhibition on proliferation was confirmed in the MCF7 control cell line (Figure 3) known to respond to VEGFR-signal transduction (Cascio et al., 2010). The data presented here therefore indicates VEGFR-stimulated signal transduction influences the proliferation of HOSCC cell lines.

2.3.3 Abundance of signalling intermediates central to proliferation under standard HOSCC culture conditions

Intermediates central to proliferation were of keen interest because of the suspected role of VEGFR signalling to further cancer progression via these pathways. In order to allow comparison across cell lines levels of pPKB and pGSK3βser9 (Table 1) were determined under standard HOSCC culture conditions (refer to Chapter 2, Section 2.2.2 Tissue Culture) (Figure 4).

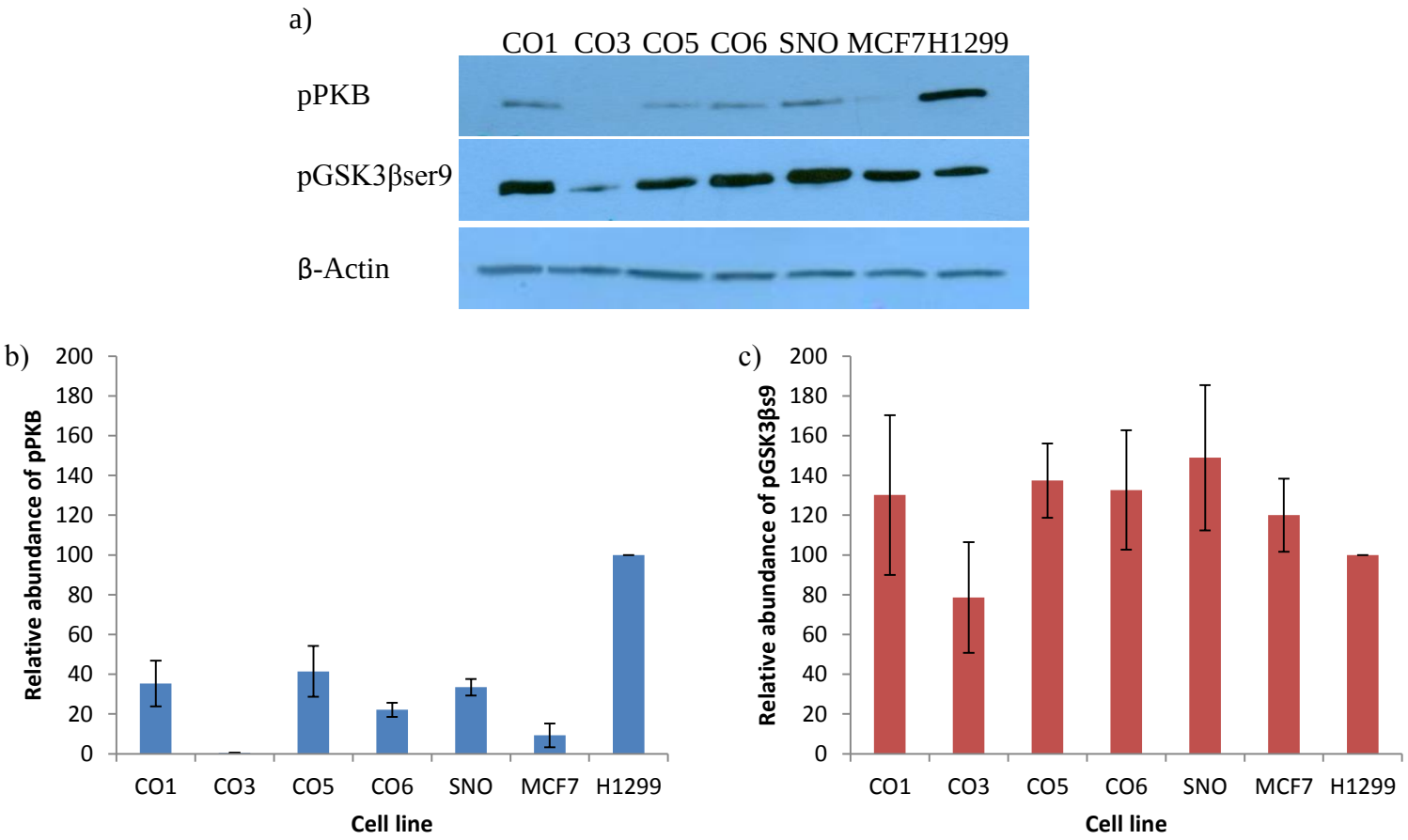

Figure 4: pPKB and pGSK3βser9 protein content in HOSCC cell lines

a) The HOSCC cell lines, MCF7 and H1299 control cell lines contain pPKB and pGSK3βser9 protein. Western blotting detected pPKB at 56 kDa and pGSK3βser9 at 48 kDa. β-Actin served as the loading control. b) The mean abundance of pPKB and pGSK3βser9 ($n \geq 3$) in each HOSCC cell line was determined via densitometric analysis, relative to the H1299 external control set at 100. Standard error denoted as error bars.

Measurable quantities of pPKB (active PKB) and pGSK3βser9 (inactive GSK3β) are present in HOSCC cell lines under standard culture conditions, with the exception of pPKB in the WHCO3 cell line (Figure 4). In these forms pPKB and pGSK3βser9 aid in cancer progression, see Table 1. A change in these protein levels upon VEGFR stimulation relative to a control would indicate affected pathways and these changes can be compared across cell lines.

2.3.4 Effect of VEGFR signalling on intermediates central to proliferation

The ability of VEGFR stimulation to influence cancer progression was evaluated by monitoring the change in abundance of phosphorylated signalling intermediates; pPKB - active PKB a key contributor to proliferation and pGSK3βser9 - inactive GSK3β a tumour

suppressor in its active form. The change in abundance of these key intermediates due to VEGFR stimulation and VEGFR inhibition was determined for all HOSCC cell lines and the control MCF7 cell line (Figure 5).

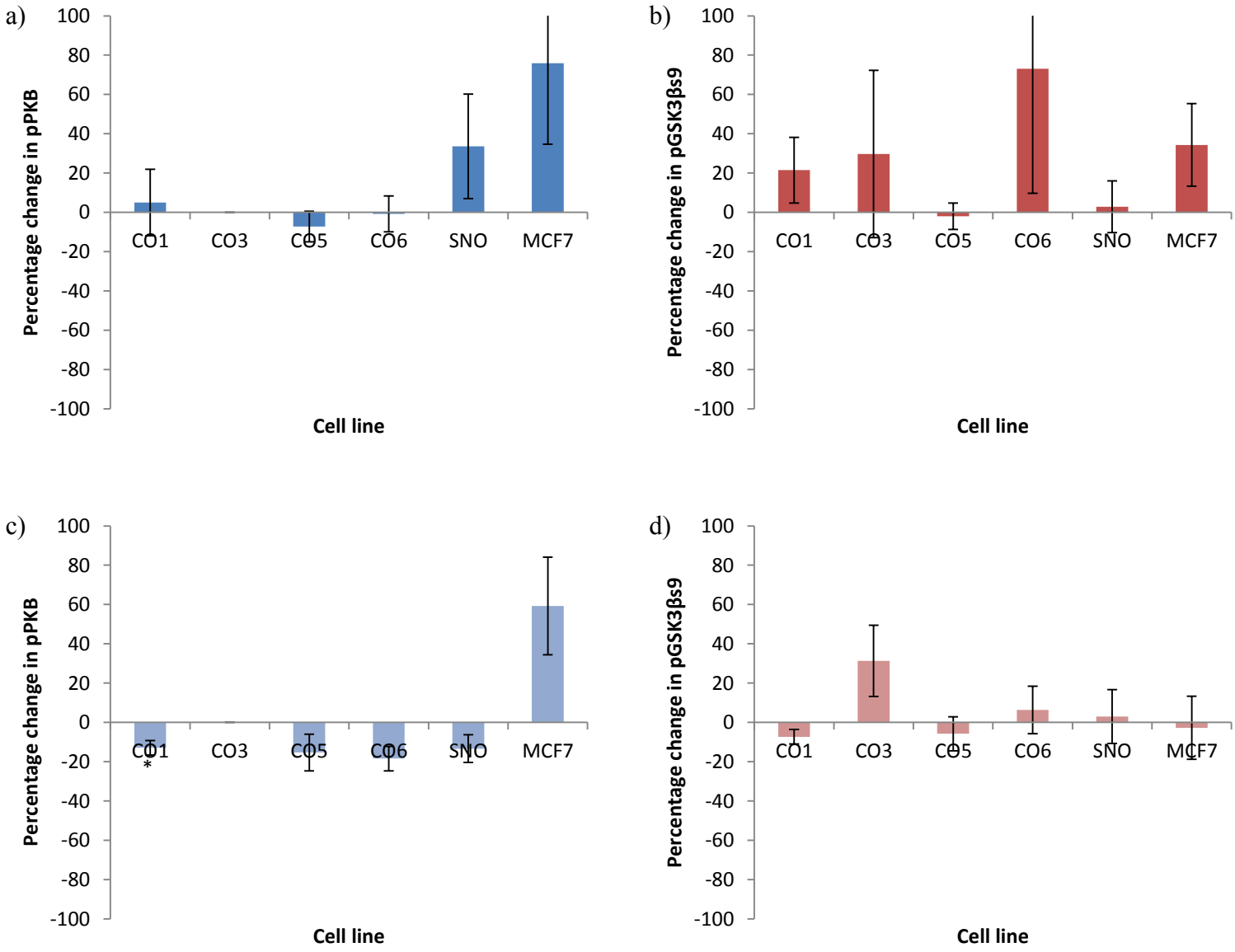

Figure 5: VEGFR signalling influences the abundance of pPKB and pGSK3βser9 in HOSCC cell lines

a) In the majority of HOSCC cell lines VEGFR stimulation (VEGFR stimulated vs control) has negligible effect on pPKB abundance but b) increases pGSK3βser9 abundance while c) VEGFR inhibition (VEGFR inhibited vs control) decreases pPKB abundance but d) has negligible effect on pGSK3βser9 abundance. Abundance of pPKB and pGSK3βser9 were determined via western blotting followed by densitometric analysis, relative to the H1299 external control set at 100. The mean difference ($n \geq 3$) was represented as percentage change and standard error denoted as error bars. Significant difference at a 95 % confidence level ($p <= 0.05$) between the means of control and treated samples is indicated by an *.

VEGFR stimulation influences signalling pathways critical for cell proliferation, indicated via an increase in pPKB (active PKB) or an increase in pGSK3βser9 (inactive GSK3β) abundance in the HOSCC cell lines (Figure 5a and b, refer to Table 1). Inhibition of VEGFR signalling results in deactivated PKB mediated proliferation pathways but had negligible effect on the GSK3β tumour suppressor pathway, indicated via a decrease in pPKB (active PKB) abundance and a negligible change in pGSK3βser9 (inactive GSK3β) in the majority of HOSCC cell lines (Figure 5c and d, refer to Table 1). The fact that inhibition of VEGFR signalling affects downstream intermediates (Figure 5) as well as proliferation (Figure 3) further confirms the function of an autocrine VEGFR-stimulated signalling pathway in HOSCC. Despite at least 3 experimental replicates ($n \geq 3$), the behavioural nature of the experiments results in some non-statistically significant data (a discussion in this regard follows, see Section 2.4).

2.4 Discussion

The high-prevalence of HOSCC in South Africa combined with its aggressiveness and high rate of metastasis necessitated research into aberrant signalling pathways of HOSCC and intermediates which could potentially be targeted (Ferlay et al., 2013; Stoner and Gupta, 2001). The effects of VEGFR-stimulated signal transduction was thus assessed in HOSCC as a model. In order for autocrine VEGFR-stimulated signalling to play a role in HOSCC carcinogenesis and progression, HOSCC cells need to produce VEGF - not usually present in adult oesophageal cells outside of early development - and be able to respond to its stimulus (Hanahan and Folkman, 1996). Detection and quantification of secreted protein in tissue culture media is difficult to achieve due to the high abundance of serum proteins interfering with and masking the presence of inherently low concentrations of secreted proteins (1-50 pg/ml of VEGF for biological activity) (Hathout, 2007; Weigand et al., 2005). The level of total cellular VEGF was therefore measured instead as VEGF protein expression is assumed to be a precursor to its secretion where any VEGF present in cells is likely present in secretory bodies and will eventually be secreted. The five South African HOSCC cell lines studied here were found to contain VEGF protein (Figure 2). This result is in accordance with those of prior studies which found expression of VEGF mRNA in HOSCC of Japanese origin (Inoue et al., 1997) and heightened levels of VEGF protein in HOSCC of Chinese origin (Zhao et al., 2015). Cascio et al. (2010) determined untreated MCF7 cells secrete approximately 193 pg/ml of VEGF from 4 x 10^5 cells, assuming the MCF7s studied here are producing VEGF at the same rate by extrapolation HOSCC cell lines produce approximately 8-20 times the maximum amount required for biological activity (Weigand et al., 2005). The ability of HOSCC cell lines to produce VEGF may play an important role in the paracrine induction of angiogenesis vital for bringing sustaining blood vessels towards the tumour and thus allowing tumour progression, metastasis and increase in size beyond the limitations diffusion (Folkman, 1990; Karkkainen and Petrova, 2000).

VEGF protein produced by HOSCCs may also act in an autocrine signalling manner upon the same HOSCC cells to increase cell proliferation, growth, survival, apoptosis resistance, migration and invasion as indicated in other cancer types (Goel and Mercurio, 2013; Rapisarda and Melillo, 2012). VEGFR-stimulated signal transduction was thus suspected to play a role in HOSCC proliferation. This was confirmed in a behavioural context wherein VEGFR-stimulated signal transduction induced the enhanced proliferation of all HOSCC cells lines (Figure 3a). The extent to which exogenous VEGFR-stimulation enhances HOSCC

proliferation is however varied, ranging from a rather slight increase (3.6 %) in the WHCO6 cell line to a marked increase (32 %) in the WHCO5 cell line with a significant increase in proliferation observed in both the WHCO1 and SNO cell lines. On the other hand, abrogation of VEGFR signalling lead to a slight but consistent reduction of HOSCC proliferation (Figure 3b); where the reduction in proliferation was significant in the WHCO5 and WHCO6 cell lines.

The VEGFR-stimulated autocrine signalling mechanism in HOSCC proliferation was investigated by monitoring phosphorylated signalling intermediates (pPKB and pGSK3βser9) central in processes contributing to cancer progression. The phosphorylated form rather than the total abundance of these intermediates were studied as it is the phosphorylation status which regulates the activity of these signalling intermediates rather than purely their presence in the cell (Jope and Johnson, 2004; Sefton, 1998; Vara et al., 2004). The phosphorylated forms of such proteins however only accounts for a very small portion of the total forms of that protein and thus is present in exceedingly small concentrations making detection much more difficult (Sefton, 1998). In addition the low concentrations necessitate the use of high quality protein extracts and accurate concentration determination as the slightest inaccuracy could have drastic effects on the detected abundance of phosphorylated protein due to the required sensitivity of the detection technique. Protein extraction was shown to be of high quality, uncontaminated by DNA and cellular debris (SDS-PAGE: Appendix C.1) and high precision protein determination standard curves resulted in accurate protein concentration determination (Appendix B.1) confirmed by equal staining of SDS-PAGE lanes (Appendix C.1) and consistent β-actin content across cell lines and treatments for each blot (Figure 2a, Figure 4a and Figure 19a). The detected relative abundance of signalling intermediates in their phosphorylated forms was therefore considered to be a true reflection of that present in the sample from cultured cells.

In its phosphorylated form PKB is active and a key intermediate in pathways leading to proliferation and migration respectively. In contrast the serine 9 phosphorylation of GSK3β is inhibitory reducing the tumour suppressor activity of this signalling intermediate (refer to Table 1). HOSCC cell lines were verified to contain pPKB and pGSK3βser9 in measurable quantities under standard HOSCC culture conditions; with the exception of very low pPKB quantities in the WHCO3 cell line, a well-established mutation (Figure 4). The presence of these intermediates in such forms indicates that under standard HOSCC culture conditions HOSCCs have activated signalling of proliferative pathways (presence of active PKB) and

inactivation of tumour suppressive pathways (presence of inactive GSK3β). VEGF produced by HOSCCs may be acting in autocrine manner upon the same cells contributing to these signal transduction pathways associated with the cancerous state along with the convergence of other transforming mutations of HOSCC such as EGFR overexpression, p53 mutation, etc. (Stoner and Gupta, 2001).

VEGFR-stimulated signal transduction was confirmed to occur in HOSCC as VEGF supplementation was shown to affect the phosphorylation state of proposed signalling intermediates (Figure 5). Given the behavioural nature of the data analysed in this study, increasing the number of experimental replicates (above $n \geq 3$) would only marginally increase the statistical significance of the results while massively increasing the project length and cost. While statistically significant effects would strengthen our results, the behavioural nature of our approach means that it is not so much the exact extent of the change that is important but rather the trend. For instance, if a treatment always increases proliferation, be it a 10 %, 20 % or 30 % increase in proliferation, each time proliferation is increased and thus this trend is considered a veritable response. The reliability of such trends as a basis for data interpretation is further supported by the fact that the interpretation of the results in this thesis would remain unchanged if only significant responses were taken into account. The WHCO1 cell line had the most frequent statistically significant responses, if only this cell line were considered the major finding of this thesis would persist: VEGFR stimulation significantly increases proliferation in the WHCO1 cell line accompanied by an increasing trend in all the HOSCC cell lines, VEGFR inhibition significantly decreases pPKB in the WHCO1 cell line accompanied by a decreasing trend in all the HOSCC cell lines and so on. We are therefore of the opinion that significant effects may be generalised to the other cell lines and that an increasing or decreasing trend is a substantive result in its self.

Extracellar VEGF is therefore able to bind and stimulate its receptors to initiate signal transduction in HOSCC. Although the fact that HOSCC are able to respond to VEGF confirms the presence of its receptors it would be enlightening to determine precisely which VEGFRs are present and in what quantities. The existence of a VEGF/VEGFR autocrine signalling axis in HOSCC was confirmed as HOSCC cells are able to both produce and respond to VEGF stimulus.

Exogenous VEGFR-stimulation enhanced proliferation and survival signalling by augmenting PKB mediated proliferation signalling (increased active PKB) or enhancing

inhibition of the tumour suppressive functioning of GSK3β (increased inactive GSK3β) (Figure 5a and b, Table 1). Interestingly, while exogenous VEGFR stimulation was associated with both enhanced PKB mediated proliferation signalling (increased active PKB) and a greater inhibition of the tumour suppressive functioning of GSK3β (increased inactive GSK3β), each of the HOSCC cell lines displayed an association with either one or the other afore mentioned pathways while the other remained unchanged (Figure 5a and b). For example, upon exogenous VEGFR-stimulation the SNO HOSCC cell line displayed a marked increase in PKB mediated proliferation signalling (increased active PKB) but displayed no associated change in the inhibition of the tumour suppressive functioning of GSK3β. Conversely, the WHCO6 HOSCC cell line displayed no change in PKB mediated proliferation signalling associated with enhanced VEGFR signalling but displayed a marked increase in the inhibition of the tumour suppressive functioning of GSK3β (increased inactive GSK3β) associated with enhanced VEGFR signalling. VEGFR signalling may thus act through either a PKB mediated or GSK3β mediated pathway to enhance HOSCC cellular proliferation. Nevertheless the control MCF7 breast adenocarcinoma cell line known to respond to VEGF (Cascio et al., 2010) showed a marked increase in both PKB mediated proliferative signalling and enhanced inhibition of the tumour suppressive functioning of GSK3β. It should however be noted that in cases where no change in abundance of signalling intermediate appears to be associated with VEGFR stimulation this may not be a true representation as HOSCC cell lines were found to produce VEGF and thus the unstimulated control cell lines are likely already displaying enhanced VEGFR-stimulated signalling though either or both the PKB or GSK3β mediated pathways. Cultures of abrogated VEGFR signalling were thus assessed to allow a clearer-cut comparison. In addition since VEGFR-stimulated signal transduction enhances proliferative and survival pathways in HOSCC cell lines, abrogation of VEGFR-stimulated signal transduction could be of therapeutic benefit. Abrogation of VEGFR-stimulated signalling was shown to diminish PKB mediated proliferative signalling across all HOSCC cell lines (Figure 5c). In this instance abrogation of VEGFR signalling resulted in a distinct and consistent decrease in the abundance of active PKB ranging from a significant decrease of -13 % in the WHCO1 cell line to -18.4 % in the WHCO6 cell line. The effect of abrogated VEGFR signalling on GSK3β tumour suppressive signalling was more ambiguous with negligible change in abundance of inactive GSK3β upon VEGFR abrogation across the HOSCC cell lines (Figure 5d). Interestingly, abrogation of VEGFR stimulated signalling in the control MCF7 breast adenocarcinoma cell line resulted in increased PKB mediated signalling but no change in GSK3β mediated signalling

(Figure 5c and d). Perhaps this finding may be linked to the poor response and resistance of breast carcinoma to anti-VEGFR therapy (Kristensen et al., 2014).

Since PKB is a prominent player in cellular proliferation pathways, decreased PKB mediated signal transduction as a result of abrogation of the VEGFR pathway is expected to reduce HOSCC proliferation. This was confirmed from a behavioural perspective where VEGFR abrogation was shown to reduce proliferation of HOSCC cell lines (Figure 3b). These results complement previous studies which found that blockade of VEGFR-signalling functions via a PKB mediated pathway to induce anti-tumour effects and enhance cell death of human astrocytoma and fibrosarcoma cell lines (Lee et al., 2012). Taken in conjunction, the results presented above affirm our suspicions that abrogation of VEGFR signalling decreases proliferation of HOSCC (Figure 3b) through a decrease in proliferative signalling (Figure 5c). Targeting VEGFR may thus have potential as a therapeutic, reducing HOSCC proliferation.

Chapter 3: The role of the VEGFR-induced PI3K/PKB signalling pathway in HOSCC proliferation

3.1 Introduction

The current investigation found VEGFR signalling to enhance proliferation of HOSCC cell lines though elevated PKB mediated signalling or enhanced inhibition of GSK3β tumour suppressor activity. On the other hand, abrogation of VEGFR signalling diminished PKB mediated proliferative signalling and thus reduced proliferation across all HOSCC cell lines, see above. It would thus be reasonable to postulate that anti-VEGFR therapy would effectively reduce HOSCC proliferation.

VEGFR targeted therapies have been developed for the treatment of human cancers and proven beneficial in the treatment of some advanced stage malignancies (Ellis and Hicklin, 2008a). The response to anti-VEGFR therapy is varied benefiting some patient in the form of progression free survival while a significant portion of patients fail to respond to VEGFR targeted therapy even transiently (Batchelor et al., 2007; Burris and Rocha-Lima, 2008; Shojaei and Ferrara, 2008). Even in cases where VEGFR therapy stabilises disease and halts progression many tumours eventually become resistant to VEGFR therapy and patients relapse (Bergers and Hanahan, 2008; Ellis and Hicklin, 2008b; Shojaei and Ferrara, 2008). Both acquired and intrinsic resistance is likely due to the extreme complexity and redundancy of signalling interactions within cells. Redundancy and cross-talk between signalling pathways is essential and generally of benefit to the cell or organism as a single or few aberrations in the signalling pathways are compensated for via cross talk in the signal transduction network initiating a salvage pathway with a similar function and thus homeostasis is maintained (Gong and Zhang, 2005; Sun and Bernards, 2014). However in terms of drug therapy aimed at targeting a single signalling intermediate, pathway cross talk may well initiate a salvage pathway allowing cells to recover from therapy (Logue and Morrison, 2012; Sun and Bernards, 2014).

In addition, a number of toxic side effects have been observed in patients on anti-VEGFR therapy, emphasising poor understanding of the VEGFR mechanism of action and development of resistance (Jain et al., 2006). Toxic side effects of anti-VEGFR therapy could potentially be reduced by lowered drug doses in the case where combination targeting of VEGFR and another step in the pathway enhance efficacy and specificity.

The variability of anti-VEGFR therapy efficacy may thus be attributed to initiation of a salvage pathway through which cancer cells can continue to proliferate and migrate. The PI3K/PKB pathway has long been acclaimed as a prominent pathway in cancer cell proliferation (Vara et al., 2004). The PI3K/PKB signalling pathway was thus proposed to have a vital role in VEGFR-induced HOSCC proliferation. Furthermore, as it appears integral to VEGFR induced HOSCC proliferation, the manner in which VEGFR-stimulated PI3K/PKB signalling contributes to HOSCC proliferation was investigated by manipulation of this pathway at various points.

3.2 Materials and Methods

3.2.1 Tissue culture

Tissue culture of the five HOSCC cell lines as well as the H1299 control cell line was performed as described in Chapter 2, Section 2.2.1.

3.2.2 Treatment set to provide insight into the VEGFR-induce PI3K/PKB signalling pathway

Cells cultured to approximately 70 % confluency in 6 cm tissue culture dishes were rinsed twice with sterile pre-warmed PBS and fresh media was provided. Cultures were then treated with each combination of the following: VEGF (Sigma-Aldrich®, V7259, at a final concentration of 50 μg/ml for 10 minutes), a VEGFR inhibitor (Axitinib) (Abcam®, ab141985, at a final concentration of 10 umol/L for an hour) and an inhibitor of PI3K (Sigma-Aldrich®, LY294002, at a final concentration of 20 μM for 1 hour). Control experiments were carried out simultaneously in the exact same manner with corresponding DMSO concentrations lacking the treatment.

3.2.3 Protein extraction

Total cellular protein was extracted from control, VEGFR stimulated, PI3K inhibited, combination VEGFR stimulated-PI3K inhibited, VEGFR inhibited and combination VEGFR inhibited-PI3K inhibited cultures according to the procedure detailed in Chapter 2, Section 2.2.3.

3.2.4 Protein concentration determination

The protein concentration of control, VEGFR stimulated, PI3K inhibited, combination VEGFR stimulated-PI3K inhibited, VEGFR inhibited and combination VEGFR inhibited-PI3K inhibited samples was determined according to the procedure detailed in Chapter 2, Section 2.2.4.

3.2.5 Sodium Dodecyl Sulphate–Polyacrylamide Gel Electrophoresis

The control, VEGFR stimulated, PI3K inhibited, combination VEGFR stimulated-PI3K inhibited, VEGFR inhibited and combination VEGFR inhibited-PI3K inhibited cell lysate samples were electrophoresed following the methodology laid out in Chapter 2, Section 2.2.5.

3.2.6 Western blot

Control, VEGFR stimulated, PI3K inhibited, combination VEGFR stimulated-PI3K inhibited, VEGFR inhibited and combination VEGFR inhibited-PI3K inhibited cell lysate samples resolved by SDS-PAGE were immunoblotted with anti-pPKB antibody, anti-pGSK3β antibody and anti-β-actin antibody as described in Chapter 2, Section 2.2.6.

3.2.7 Semi-quantitative analysis

Semi-quantitative analysis was carried out as described in Chapter 2, Section 2.2.7.

3.2.8 Cellular proliferation assay

Cellular proliferation was detected through a MTT reduction assay as described in Chapter 2, Section 2.2.8.

3.2.9 Comparisons and statistical analysis

The percentage change, standard error and probability of significance between treated and control samples were calculated as described in Chapter 2, Section 2.2.9.

3.3. Results

3.3.1 Effect of PI3K inhibition on HOSCC proliferation

Since the PI3K/PKB signalling pathway is suspected to be key in VEGFR-stimulation induced proliferation of HOSCCs, the effect of PI3K inhibition on HOSCC cellular proliferation was determined both in the presence and absence of VEGFR stimulation (Figure 6).

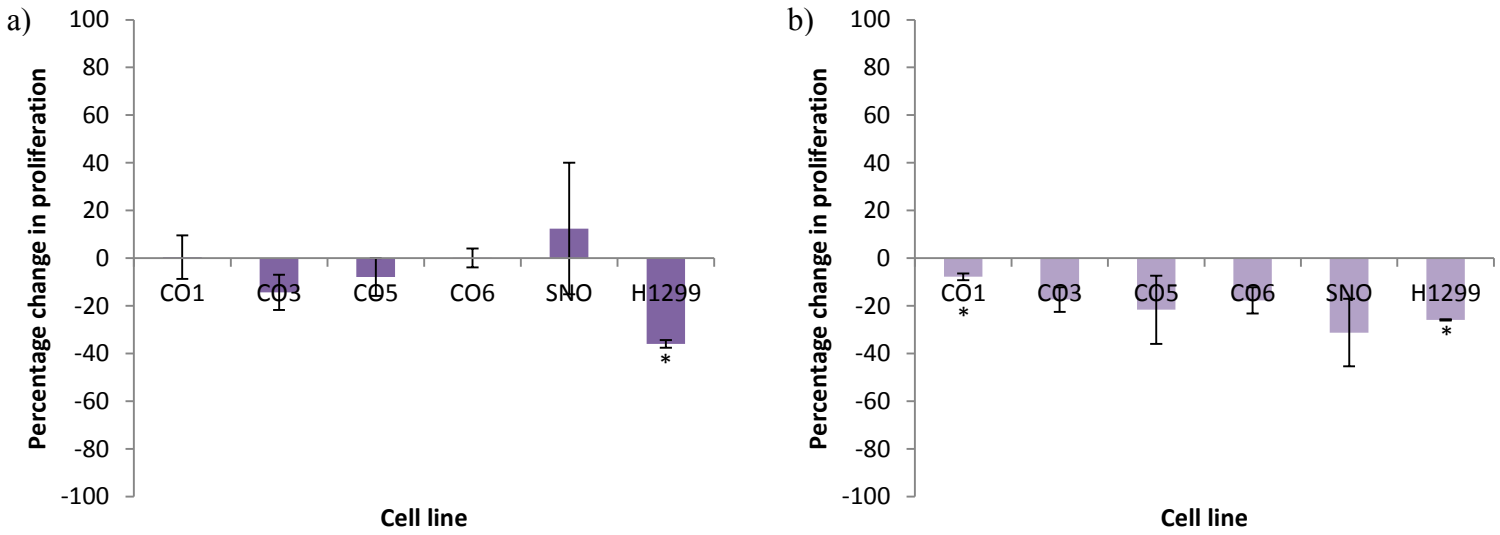

Figure 6: PI3K inhibition influences the proliferation of HOSCC cell lines

a) In the majority of HOSCC cell lines PI3K inhibition has a negligible effect on proliferation (PI3K inhibited vs control) while b) in the presence of VEGFR stimulation PI3K inhibition decreased HOSCC proliferation (VEGFR stimulated-PI3K inhibited vs VEGFR stimulated). HOSCC cell lines and the H1299 control cell line were treated for 24 hours, after which an MTT proliferation assay was performed ($n \geq 3$). The mean difference was represented as percentage change and standard error denoted as error bars. Significant difference at a 95 % confidence level ($p <= 0.05$) between the means of control and treated samples is indicated by an *.

Under standard tissue culture conditions PI3K inhibition had negligible effect on proliferation in the majority of HOSCC cell lines (Figure 6a). However, during VEGFR stimulation PI3K inhibition causes a slight decrease in proliferation of all HOSCC cell lines (Figure 6b). The H1299 cell line was used as a control for PI3K inhibition because it is known to have a functional PI3K/PKB pathway (Choi et al., 2009; Hsieh et al., 2013), confirmed by high levels of active PKB (pPKB) found here (Figure 4b). The effect of PI3K inhibition on the control H1299 cell line is as expected, where PI3K inhibition both alone and during VEGFR stimulation was confirmed to decrease proliferation (Figure 6).

3.3.2 Effect of PI3K inhibition on signalling intermediates central to proliferation in HOSCC

In light of the above evidence that PI3K inhibition reduces HOSCC proliferation during VEGFR stimulation (Figure 6), the corresponding effect on signalling intermediates was investigated in order to assess whether the proliferative effect occurs via such signalling pathways (Figure 7).

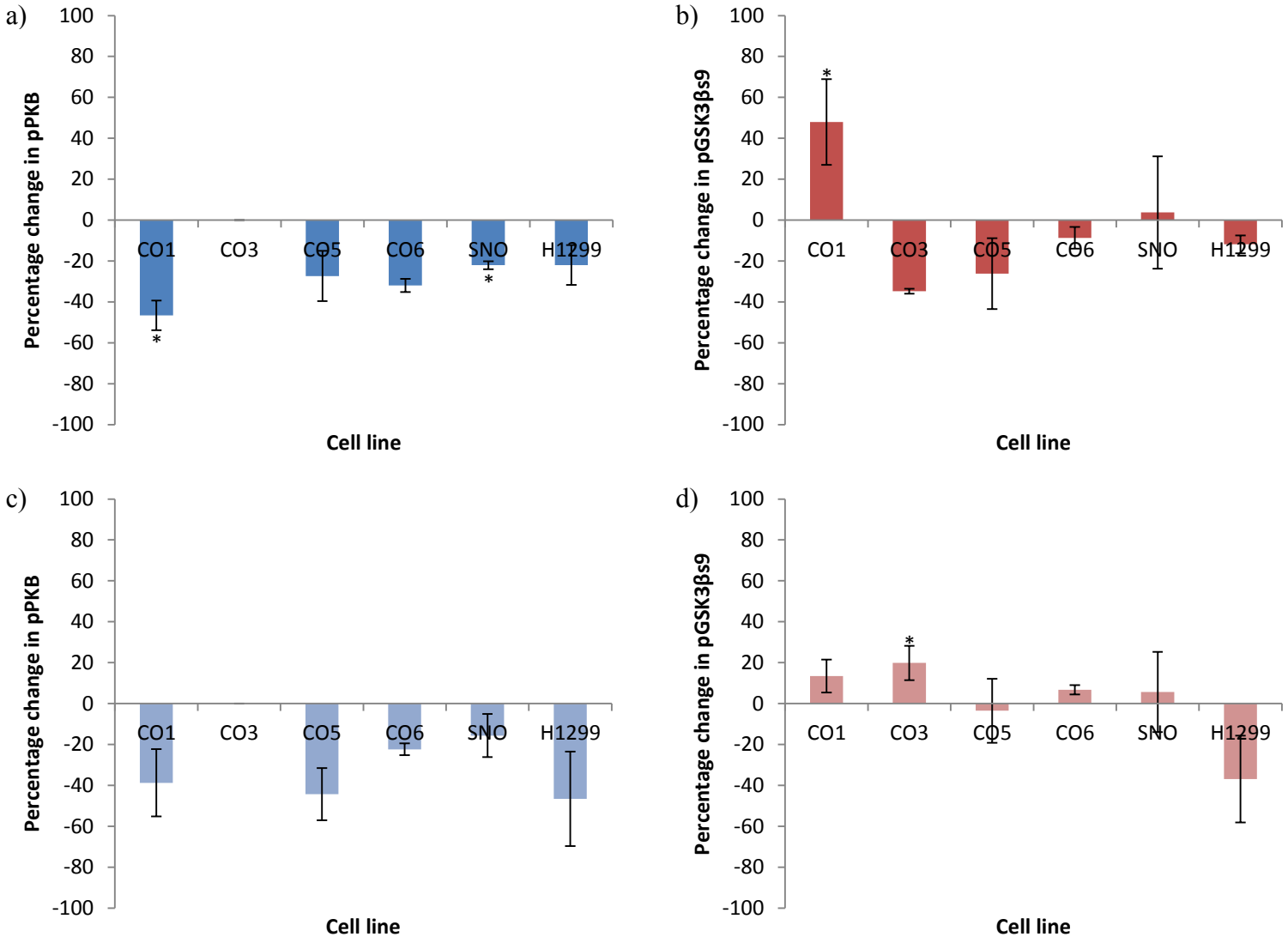

Figure 7: PI3K inhibition influences the abundance of pPKB and pGSK3βser9 in HOSCC cell lines

a) PI3K inhibition (PI3K inhibited vs control) decreases pPKB abundance of HOSCC cell lines but b) has a varied effect on pGSK3βser9 abundance while c) in the presence of VEGFR stimulation PI3K inhibition (VEGFR stimulated-PI3K inhibited vs VEGFR stimulated) decreases pPKB abundance and d) has an enhancing or negligible effect on pGSK3βser9 abundance in the majority of HOSCC cell lines. Abundance of pPKB and pGSK3βser9 were determined via western blotting followed by densitometric analysis, relative to the H1299 external control set at 100. The mean difference ($n \geq 3$) was represented as percentage change and standard error denoted as error bars. Significant difference at a 95 % confidence level ($p <= 0.05$) between the means of control and treated samples is indicated by an *.

Inhibition of PI3K signalling results in deactivated PKB mediated proliferation pathways as expected, indicated via a decrease in pPKB (active PKB) abundance across all HOSCC cell lines and the H1299 control cell line (Figure 7a, refer to Table 1). In addition, PI3K inhibition resulted in decreased or negligible effect on pGSK3βser9 in the majority of HOSCC cell lines as well as the H1299 control (Figure 7b).

Abrogation of PI3K signalling during VEGFR stimulation continued to decrease pPKB across all the HOSCC cell lines and the H1299 control as expected (Figure 7c). In contrast, abrogation of PI3K signalling during VEGFR stimulation either increased pGSK3βser9 or had very little effect on pGSK3βser9 (Figure 7d). The opposing effect of pGSK3βser9 during inhibition of VEGFR-induced PI3K signalling could potentially be neutralised by combined inhibition.

3.3.3 Effect of PI3K inhibition in combination with VEGFR inhibition on HOSCC proliferation

Abrogation of VEGFR-stimulated signal transduction and abrogation of PI3K signal transduction have both been found to independently reduce HOSCC cellular proliferation, refer to Figure 3b and Figure 6 above. The effect of PI3K inhibition in combination with VEGFR inhibition on HOSCC proliferation was therefore investigated (Figure 8).

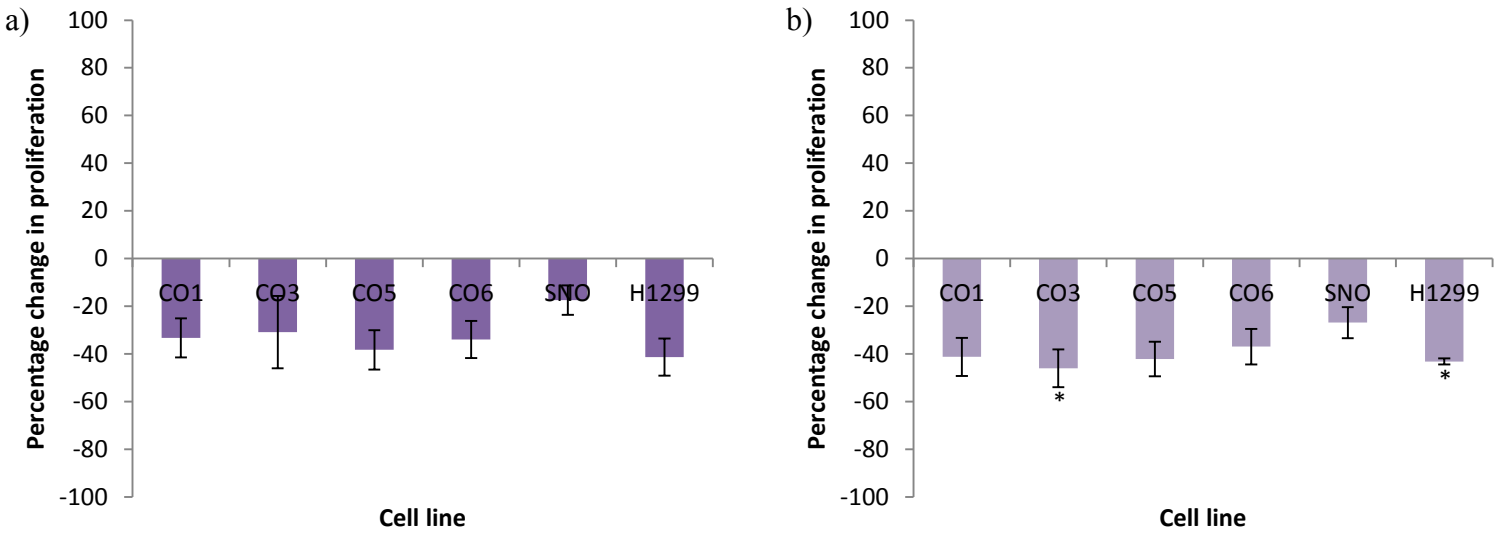

Figure 8: Combined VEGFR and PI3K inhibition influences the proliferation of HOSCC cell lines

a) Combined VEGFR-PI3K inhibition decreases proliferation of HOSCC cell lines vs VEGFR inhibition alone and b) vs control cultures. HOSCC cell lines and the H1299 control cell line were treated for 24 hours, after which an MTT proliferation assay was performed ($n \geq 3$). The mean difference was represented as percentage change and standard error denoted as error bars. Significant difference at a 95 % confidence level ($p <= 0.05$) between the means of control and treated samples is indicated by an *.

Combined VEGFR and PI3K inhibition causes a marked decrease in the proliferation of VEGFR inhibited HOSCC as compared to cultures in which VEGFR alone was inhibited (Figure 8a). In addition, combined VEGFR and PI3K inhibition also reduces proliferation as compared to control cultures (Figure 8b). The effect of combined VEGFR-PI3K inhibition in HOSCC is consistent with the effect on the H1299 control cell line (Figure 8).

The effect of combined VEGFR and PI3K inhibition on HOSCC proliferation was then compared to the additive effect of each inhibition treatment alone (Figure 9).

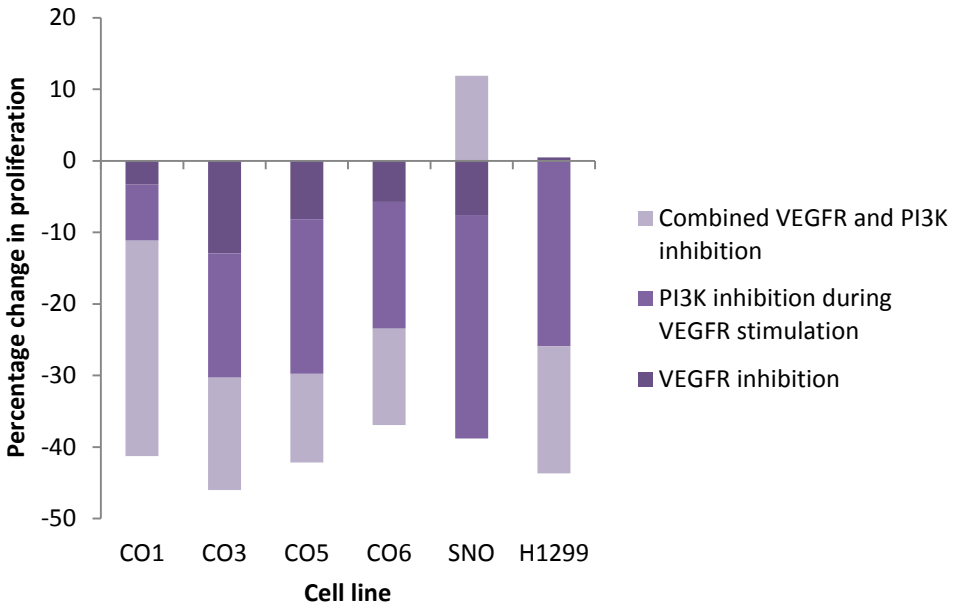

Figure 9: Combined inhibition of both VEGFR and PI3K signalling synergistically reduces proliferation of HOSCC cell lines

The decrease in proliferation due to combined inhibition of both VEGFR stimulation and PI3K signalling is greater than the sum of the decrease in proliferation due to VEGFR inhibition and PI3K inhibition. HOSCC cell lines and the MCF7 control cell line were treated for 24 hours, after which an MTT proliferation assay was performed ($n \geq 3$). The mean difference was represented as percentage change.

With the exception of the SNO cell line, the decrease in HOSCC cellular proliferation due to combined VEGFR inhibition and PI3K inhibition is greater than the sum of the decrease due to either treatment alone (Figure 9), suggesting a synergistic effect is at play.

3.3.4 Effect of PI3K inhibition in combination with VEGFR inhibition on signalling intermediates central to proliferation in HOSCC

As this study found combined VEGFR and PI3K inhibition markedly reduces HOSCC proliferation (Figure 8), the effect of PI3K inhibition in combination with VEGFR inhibition on signalling intermediates central to proliferation was investigated (Figure 10).

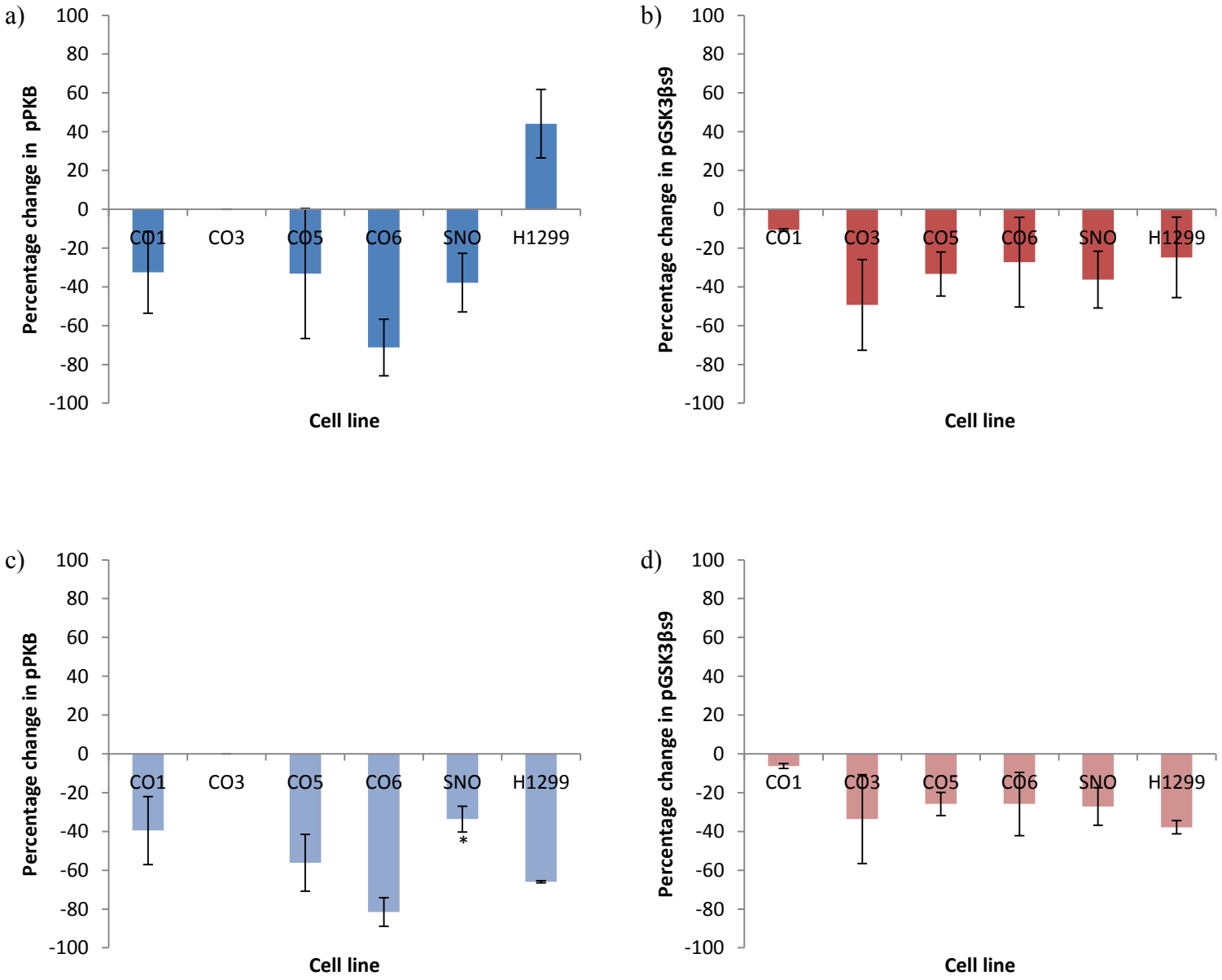

Figure 10: Combined VEGFR and PI3K inhibition influences the abundance of pPKB and pGSK3βser9 in HOSCC cell lines

a) Combined VEGFR-PI3K inhibition decreases pPKB abundance and b) pGSK3βser9 abundance of HOSCC cell lines vs VEGFR inhibition alone and c) decreases pPKB abundance and d) pGSK3βser9 abundance vs control cultures. Abundance of pPKB and pGSK3βser9 were determined via western blotting followed by densitometric analysis, relative to the H1299 external control set at 100. The mean difference ($n \geq 3$) was represented as percentage change and standard error denoted as error bars. Significant difference at a 95 % confidence level ($p <= 0.05$) between the means of control and treated samples is indicated by an *.

Combined VEGFR and PI3K inhibition both deactivates PKB mediated pathways and activates GSK3β tumour suppressor pathways as expected. Indicated via a decrease in pPKB (active PKB) abundance and a decrease in pGSK3βser9 (inactive GSK3β) across all HOSCC cell lines, as compared to cultures in which VEGFR alone was inhibited (Figure 10a and b, refer to Table 1).

Likewise, combined VEGFR and PI3K inhibition also both reduced pPKB (decreased active PKB) and reduced pGSK3βser9 (decreased inactive GSK3β) signalling across all HOSCC cell lines and the H1299 control cell line as compared to control cultures (Figure 10c and d).

3.4 Discussion

The role of the VEGFR-induced PI3K/PKB signalling pathway in HOSCC proliferation was investigated because we found abrogation of VEGFR signalling to be associated with reduced proliferation and decreased PKB mediated signalling of HOSCCs, refer to Chapter 2. Abrogation of the PI3K signalling pathway was predicted to greatly influence the abundance of active downstream signalling intermediates such as PKB and GSK3β involved in proliferation and thereby decrease HOSCC proliferation.

Cellular proliferation was expected to decrease due to abrogation of the PI3K/PKB signalling pathway. This was confirmed in the H1299 non-small cell lung carcinoma cell line (Figure 6) known to have a functional PI3K/PKB signalling pathway (Choi et al., 2009; Hsieh et al., 2013). Abrogation of the PI3K signalling pathway however, had a negligible effect on HOSCC cellular proliferation, resulting in no change in proliferation in the majority of HOSCC cell lines (Figure 6a). Therefore under standard tissue culture conditions the PI3K/PKB signalling pathway is likely not essential for proliferation of the majority of HOSCC cell lines.

During stimulation of VEGFR signal transduction, abrogation of the PI3K/PKB signalling pathway lead to a slight but distinct decrease in cellular proliferation across all HOSCC cell lines when compared to VEGFR stimulation only (Figure 6b). Indicating that although the PI3K/PKB signalling pathway is not essential for HOSCC proliferation under standard conditions, VEGFR induced PI3K/PKB mediated signalling is at least partially responsible for enhanced HOSCC cellular proliferation due to VEGFR stimulation. The data presented here complements that of a recent study by Bhattacharya (2016) which found that VEGFR-signalling functions via a PKB mediated pathway to enhance cell survival and reduce chemo-sensitivity of colorectal cancer cell lines.

The involvement of VEGFR-induced PI3K/PKB signalling in proliferation was also investigated in a signalling context. Our study found abrogation of PI3K signalling lead to a pronounced reduction in PKB mediated proliferative signalling across all the HOSCC cell lines as well as the H1299 non-small cell lung carcinoma cell line (Figure 7a). Indicating PKB activity is dependent on PI3K activity as expected, and confirming the existence of a PI3K/PKB signalling axis in HOSCCs. Even in the presence of exogenous VEGFR stimulation abrogation of PI3K signalling still caused a marked decrease in PKB mediated signalling across HOSCC cell lines (Figure 7c). VEGFR signalling is thus not able to cause

the recovery of PKB signalling during PI3K inhibition meaning the induction of PKB signalling by VEGFR is solely dependent on PI3K.

Since PKB is known to directly inhibit GSK3β activity it follows that in the control H1299 cell line reduced PKB activity as a result of PI3K abrogation lead to reduced inhibition of GSK3β as expected (Figure 7b). Abrogation of PI3K signalling and thus decreased PKB signalling also reduced GSK3β inhibition as expected in the WHCO3 and WHCO5 cell lines (Figure 7b). Conversely, abrogation of PI3K signalling and the subsequent decreased in PKB signalling had no effect on GSK3β inhibition in the WHCO6 and SNO cell lines and lead to a significant increase in WHCO1 GSK3β inhibition (Figure 7b). An alternative pathway must therefore also be able to contribute towards GSK3β inhibition.

Moreover, VEGFR-stimulated signalling further enhances the ability of HOSCC cells to compensate for the loss of PI3K by initiating salvage pathways involving GSK3β. Although PKB is known to directly inhibit GSK3β, in the presence of exogenous VEGFR stimulation abrogation of PI3K signalling (and thus reduced PKB signalling) did not reduce GSK3β inhibition as expected but rather heightened inhibition of GSK3β tumour suppressive signalling (increased inactive GSK3β) in WHCO1 and WHCO3 cell lines while having less effect on GSK3β inhibition in the WHCO5, WHCO6 and SNO cell lines (Figure 7d). In contrast, inhibition of VEGFR-induced PI3K signalling continued to markedly reduce GSK3β inhibition in the H1299 control cell line (Figure 7d). VEGFR signalling (which causes an increase in GSK3β inhibition compared to control) is therefore still able to cause an increase in GSK3β inhibition during PI3K inhibition. So although PI3K is usually upstream of GSK3β, PI3K is not essential for GSK3β mediated inhibition stimulated by VEGFR. VEGFR signalling activates PKB solely through the PI3K pathway whereas the effect of VEGFR-stimulation to inhibit of GSK3β tumour suppressive signalling is not mediated by PI3K. It is therefore possible that VEGFR-signalling also functions via an unidentified PKB independent GSK3β mediated pathway to aid in HOSCC proliferation and survival.

Indeed, cell lines wherein GSK3β inhibition is enhanced during VEGFR stimulation to compensate for the loss of PI3K/PKB signalling (WHCO1 and WHCO3) displayed the least reduction in proliferation due to abrogation of PI3K signalling as compared to the other HOSCC cell lines where inhibition of GSK3β signalling is maintained but not heightened (Figure 6b and 7d). Initiation of a VEGFR induced GSK3β mediated salvage pathway thus at least partially negates the anti-proliferative effects of PI3K abrogation. The efficacy of

blocking members of the PI3K/PKB pathway with the aim of reducing HOSCC tumour cell proliferation would therefore likely be marginalised by autocrine VEGFR stimulated signalling in HOSCCs. VEGF present in high quantities in HOSCC is able to act in an autocrine manner upon the same HOSCC cells from which it was produced to compensate for PI3K targeted therapies by initiating salvage pathways and thus negating the anti-proliferative effects of anti-PI3K therapies.

Combined inhibition of VEGFR and PI3K was therefore investigated as a means to prevent pathway compensation and potentially further reduce HOSCC proliferation. Combined targeting of VEGFR and PI3K lead to a distinct decrease in HOSCC proliferation (Figure 8) through a marked reduction in PKB mediated proliferative signalling (Figure 10a and c). In fact in the majority of HOSCC cell lines, combined inhibition of VEGFR and PI3K reduced proliferation more than the sum of the decrease due to either treatment alone (Figure 9). It is hoped that the synergistic effect of anti-VEGFR anti-PI3K therapy to reduce proliferation *in vitro* translates *in vivo* to reduce HOSCC tumour cell proliferation and hence stabilize or reduce tumour size. Such combination therapy also acts to prevent the initiation of alternative salvage pathways involving GSK3β, indicated by consistently decreased inhibition of GSK3β tumour suppressor signalling (Figure 10b and d) and thus is expected to prevent resistance to VEGFR targeted therapy. Combination therapy aimed at both the VEGFR signalling pathway and the PI3K/PKB signalling pathway may therefore be effective in the treatment of HOSCC where the therapies would act synergistically to reduce proliferation and combat drug resistance.

Chapter 4: The role of the VEGFR-induced MAPK/ERK/RSK signalling pathway in HOSCC proliferation

4.1 Introduction

The ability of VEGFR stimulated signal transduction to initiate a salvage pathway allowing HOSCC cell lines to recover from, and continue proliferation during, PI3K inhibition is of significance to therapeutic development. Abrogation of the PI3K signalling pathway may be of therapeutic benefit in combating proliferation of cancers such as non-small cell lung carcinoma, inferred from H1299 cell line where it was found that VEGFR stimulation does not appear to have the potential to initiate a salvage pathway involving GSK3β and hence does not allow for sustained proliferation. In contrast the results of this study indicate anti-PI3K strategies may be destined to fail in the treatment of oesophageal squamous cell carcinomas and potentially other highly aggressive carcinoma. VEGF present in high quantity in HOSCCs not only brings about angiogenesis but is able to act directly upon the same HOSCC tumour cells from which it was produced. Autocrine VEGFR stimulation of HOSCCs was found to compensate for PI3K/PKB targeted therapies by initiating salvage pathways such as that involving GSK3β and thus negated the anti-proliferative effects of anti-PI3K/PKB therapies, refer to Chapter 3 and see Figure 11.

An alternative pathway must be responsible for VEGFR induced GSK3β inhibition and enhanced proliferation. Since inhibition of VEGFR-induced PI3K signalling either increased or had no effect on VEGFR-induced GSK3β signalling, it is likely GSK3β signalling which allows VEGFR to enhance proliferation largely undeterred by PI3K inhibition. The MAPK/ERK/ribosomal S6 kinase (RSK) pathway is suspected to be the alternate pathway induced by VEGFR which is responsible for uninterrupted VEGFR induced GSK3β inhibition and proliferation during PI3K inhibition (Figure 11). The MAPK/ERK pathway is a likely candidate as it is known to be stimulated by related growth factors, leads to GSK3β inhibition and a negative feedback loop is present where active PKB inhibits RAF. Therefore during PI3K inhibition where levels of active PKB are reduced, less RAF would be inhibited and consequentially MAPK/ERK signalling would be enhanced to compensate for the lack of PI3K signalling (Figure 11). The involvement of the MAPK/ERK signalling pathway in autocrine VEGFR induced proliferation of HOSCC was therefore investigated.

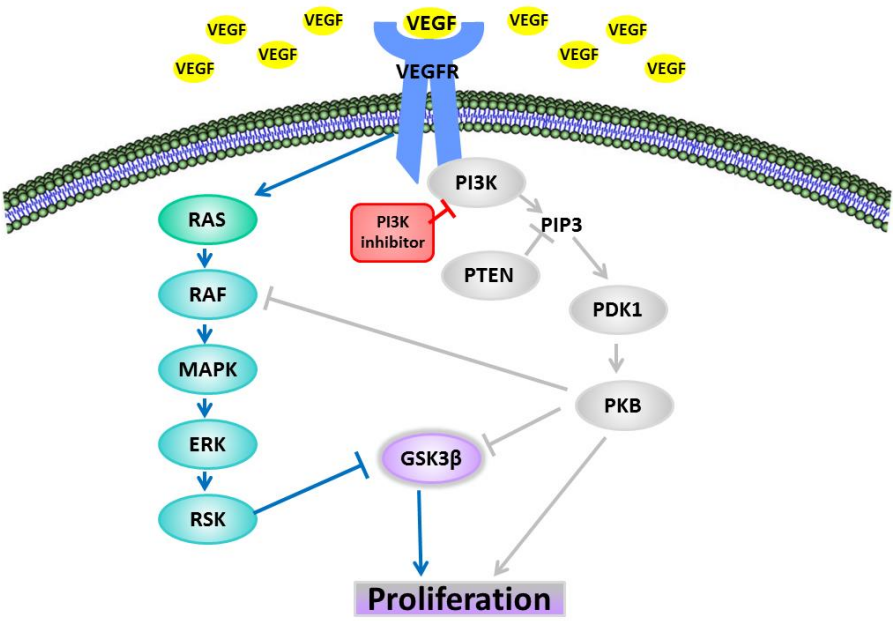

Figure 11: Abrogation of VEGFR-induced PI3K signal transduction in HOSCC

Upon PI3K inhibition, VEGFR-stimulation is unable to activate the PI3K/PKB signalling pathway (greyed out) in HOSCCs. Abrogation of VEGFR-induced PI3K/PKB signalling results in reduced HOSCC proliferation (partially greyed out). VEGFR-induced HOSCC proliferation is thus at least partially dependent on the PI3K/PKB signalling pathway. Reduced PKB activation during PI3K inhibition, however releases the damper on the MAPK/ERK/RSK signalling pathway, where lower levels of active PKB results in less RAF inhibition. VEGFR-stimulation may thus heighten MAPK/ERK/RSK signalling, unrestricted by PKB/RAF negative feedback and thus maintain or even enhance GSK3β inactivation and consequently proliferation. [Figure generated by author]

4.2 Materials and Methods

4.2.1 Tissue culture

Tissue culture of the five HOSCC cell lines as well as the H1299 control cell line was performed as described in Chapter 2, Section 2.2.1.

4.2.2 Treatment set to provide insight into VEGFR-induce MAPK/ERK/RSK signalling pathway

Cells cultured to approximately 70 % confluency in 6 cm tissue culture dishes were rinsed twice with sterile pre-warmed PBS and fresh media was provided. Cultures were then treated with each combination of the following: VEGF (Sigma-Aldrich®, V7259, 50 μg/ml final concentration for 10 minutes), a VEGFR inhibitor (Axitinib) (Abcam®, ab141985, 10 umol/L final concentration of for an hour) and an inhibitor of RSK (BioVision, BI-D1870, at a final concentration of 2.5 μM for 30 minutes). Control experiments were carried out simultaneously in the exact same manner with corresponding DMSO concentrations lacking the treatment.

4.2.3 Protein extraction

Total cellular protein was extracted from control, VEGFR stimulated, RSK inhibited, combination VEGFR stimulated-RSK inhibited, VEGFR inhibited and combination VEGFR inhibited-RSK inhibited cultures according to the procedure detailed in Chapter 2, Section 2.2.3.

4.2.4 Protein concentration determination

The protein concentration of control, VEGFR stimulated, RSK inhibited, combination VEGFR stimulated-RSK inhibited, VEGFR inhibited and combination VEGFR inhibited-RSK inhibited samples was determined according to the procedure detailed in Chapter 2, Section 2.2.4.

4.2.5 Sodium Dodecyl Sulphate–Polyacrylamide Gel Electrophoresis

The control, VEGFR stimulated, RSK inhibited, combination VEGFR stimulated-RSK inhibited, VEGFR inhibited and combination VEGFR inhibited-RSK inhibited cell lysate samples were electrophoresed following the methodology laid out in Chapter 2, Section 2.2.5.

4.2.6 Western blot

Control, VEGFR stimulated, RSK inhibited, combination VEGFR stimulated-RSK inhibited, VEGFR inhibited and combination VEGFR inhibited-RSK inhibited cell lysate samples resolved by SDS-PAGE were immunoblotted with anti-pPKB antibody, anti-pGSK3β antibody and anti-β-actin antibody as described in Chapter 2, Section 2.2.6.

4.2.7 Semi-quantitative analysis

Semi-quantitative analysis was carried out as described in Chapter 2, Section 2.2.7.

4.2.8 Cellular proliferation assay

Cellular proliferation was detected through a MTT reduction assay as described in Chapter 2, Section 2.2.8.

4.2.9 Comparisons and statistical analysis

The percentage change, standard error and probability of significance between treated and control samples were calculated as described in Chapter 2, Section 2.2.9.

4.3 Results

4.3.1 Effect of RSK inhibition on HOSCC proliferation

The MAPK/ERK/RSK signalling pathway is suspected to play a role in VEGFR-stimulation induced proliferation of HOSCCs, the effect of RSK inhibition on HOSCC cellular proliferation was therefore determined both in the presence and absence of VEGFR stimulation (Figure 12).

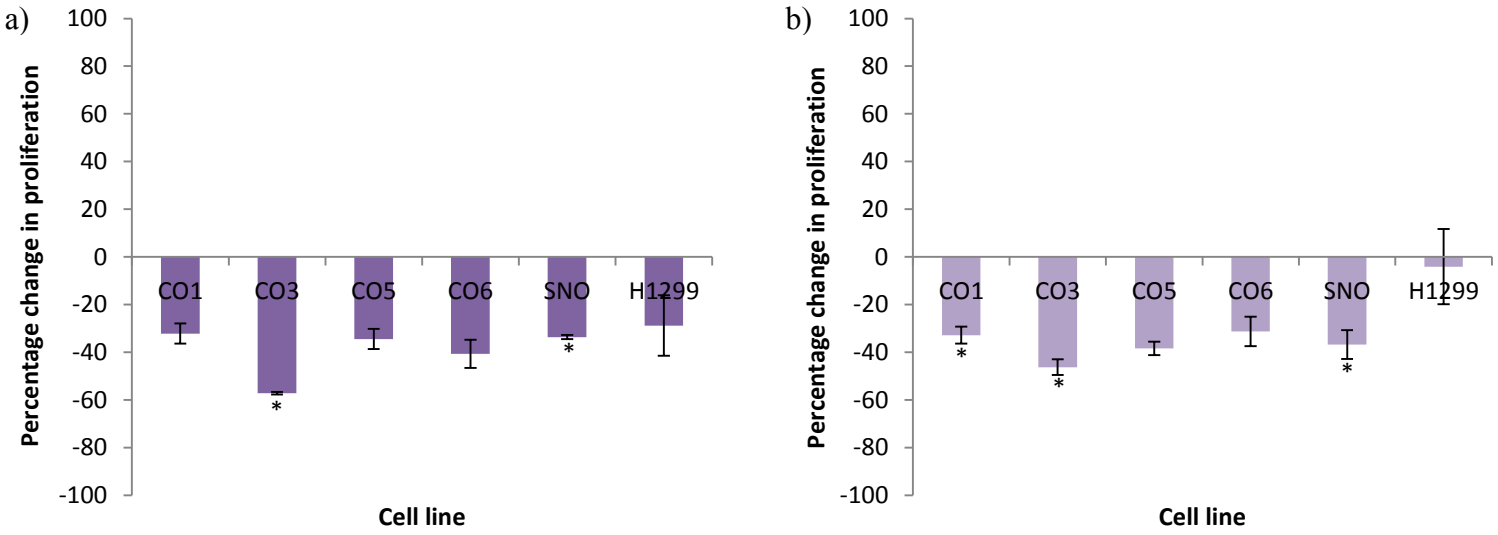

Figure 12: RSK inhibition influences the proliferation of HOSCC cell lines

a) RSK inhibition decreases the proliferation of HOSCC cell lines (RSK inhibited vs control) and b) in the presence of VEGFR stimulation RSK inhibition continues to decrease HOSCC proliferation (VEGFR stimulated-RSK inhibited vs VEGFR stimulated). HOSCC cell lines and the H1299 control cell line were treated for 24 hours, after which an MTT proliferation assay was performed ($n \geq 3$). The mean difference was represented as percentage change and standard error denoted as error bars. Significant difference at a 95 % confidence level ($p <= 0.05$) between the means of control and treated samples is indicated by an *.

RSK inhibition both alone and during VEGFR stimulation resulted in a marked decrease in cellular proliferation across all HOSCC cell lines, as expected (Figure 12a and b). In contrast while RSK inhibition decreased proliferation of the H1299 control cell line under standard tissue culture conditions as expected, during VEGFR stimulation RSK inhibition had negligible effect of H1299 proliferation but continued to decrease HOSCC proliferation (Figure 12a and b).

4.3.2 Effect of RSK inhibition on signalling intermediates central to proliferation in HOSCC

As RSK inhibition reduces HOSCC proliferation both independently and during VEGFR stimulation, the involvement of the RSK signalling pathway in VEGFR induced proliferative signalling was assessed (Figure 13).

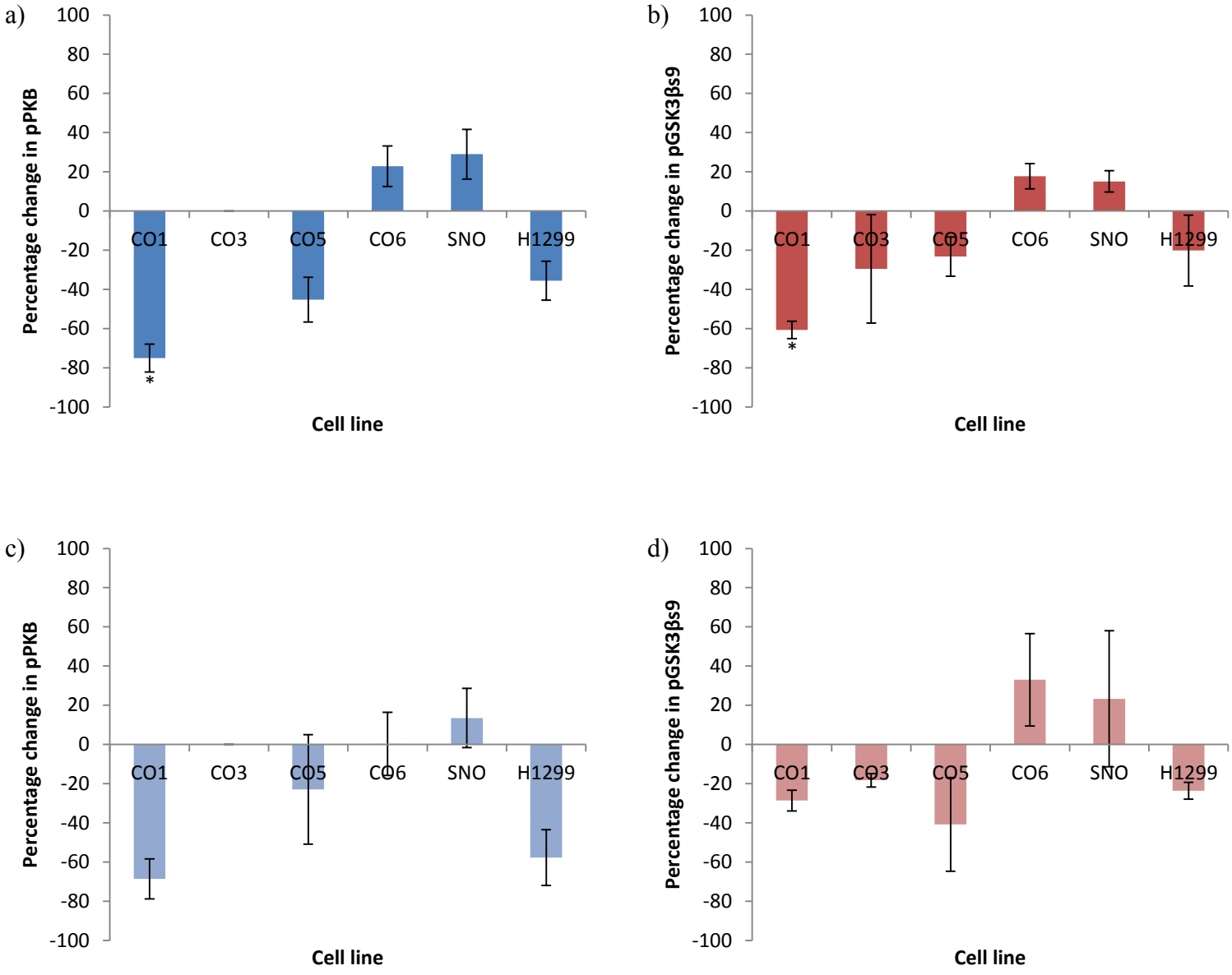

Figure 13: RSK inhibition influences the abundance of pPKB and pGSK3βser9 in HOSCC cell lines

a) RSK inhibition (RSK inhibited vs control) decreases pPKB abundance in some HOSCC cell lines and increases it in others; in the majority of HOSCC cell lines b) RSK inhibition decrease pGSK3βser9 abundance while c) in the presence of VEGFR stimulation RSK inhibition (VEGFR stimulated-RSK inhibited vs VEGFR stimulated) has negligible effect on pPKB abundance but d) either decreases or has negligible effect on pGSK3βser9 abundance. Abundance of pPKB and pGSK3βser9 were determined via western blotting followed by densitometric analysis, relative to the H1299 external control set at 100. The mean difference ($n \geq 3$) was represented as percentage change and standard error denoted as error bars. Significant difference at a 95 % confidence level ($p <= 0.05$) between the means of control and treated samples is indicated by an *.

Inhibition of RSK signalling results in activated GSK3β tumour suppressor pathways as expected, indicated via a decrease in pGSK3βser9 (inactive GSK3β) across the majority of HOSCC cell lines and the H1299 control cell line (Figure 13b, refer to Table 1). Abrogation of RSK signalling during VEGFR stimulation continued to decrease in pGSK3βser9 (inactive GSK3β) in the WHCO1, WHCO3, WHCO5 and H1299 cell lines; but increased pGSK3βser9 (inactive GSK3β) in the WHCO6 and SNO cell lines (Figure 13d).

On the other hand, inhibition of RSK signalling had a varied effect on pPKB (active PKB) abundance across the HOSCC cell lines. RSK inhibition alone decreased pPKB in the WHCO1, WHCO5 and H1299 cell lines while increasing pPKB abundance in the WHCO6 and SNO cell lines (Figure 13a). Abrogation of RSK signalling during VEGFR stimulation decreased pPKB abundance in the WHCO1 and H1299 cell lines while having negligible effect on pPKB in the remaining HOSCC cell lines (Figure 13c). Maintained or even enhanced proliferative signalling during inhibition of VEGFR-induced RSK signalling could potentially be neutralised by combined inhibition with VEGFR.

4.3.3 Effect of RSK inhibition in combination with VEGFR inhibition on HOSCC proliferation

Abrogation of VEGFR-stimulated signal transduction (Figure 3b) and abrogation of RSK signal transduction (Figure 12) have both been confirmed to reduce HOSCC cellular proliferation independently. The effect of RSK inhibition in combination with VEGFR inhibition on HOSCC proliferation was therefore investigated (Figure 14).

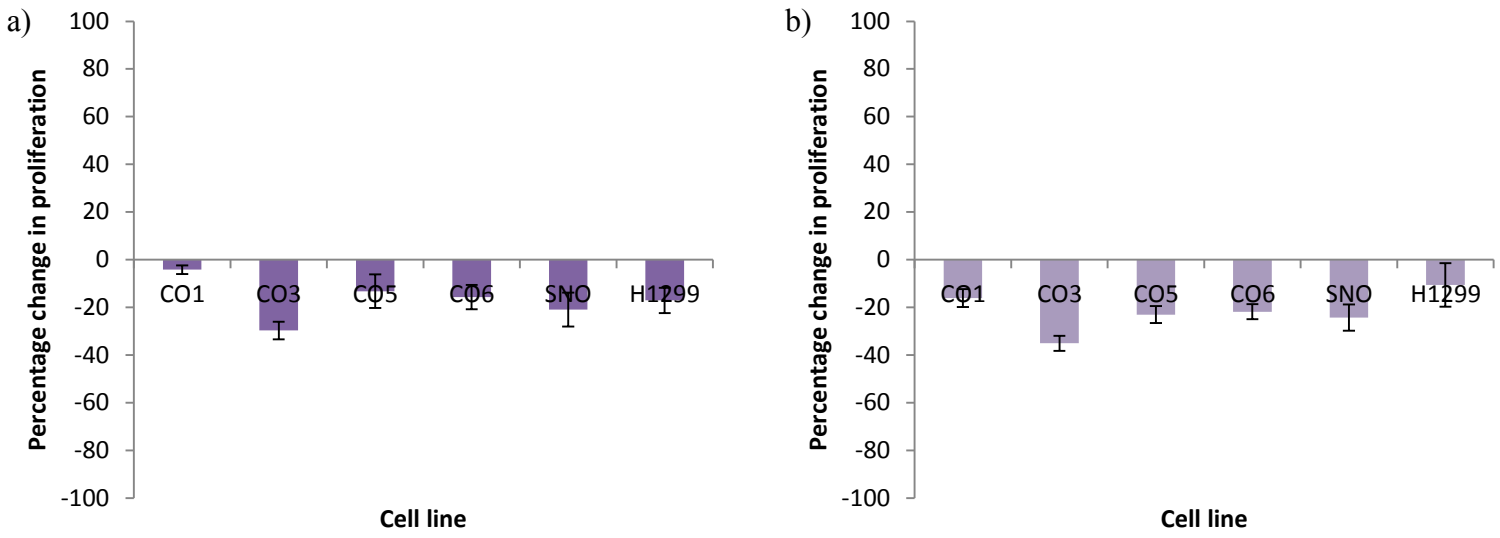

Figure 14: Combined VEGFR and RSK inhibition influences the proliferation of HOSCC cell lines

a) Combined VEGFR-RSK inhibition decreases proliferation of HOSCC cell lines vs VEGFR inhibition alone and b) vs control cultures. HOSCC cell lines and the H1299 control cell line were treated for 24 hours, after which an MTT proliferation assay was performed (n ≥ 3). The mean difference was represented as percentage change and standard error denoted as error bars. Significant difference at a 95 % confidence level ($p <= 0.05$) between the means of control and treated samples is indicated by an *.

Combined VEGFR and RSK inhibition causes a noticeable decrease in the proliferation of HOSCC cell lines and the H1299 control both as compared to control cultures (Figure 14b) and as compared to cultures in which VEGFR alone was inhibited (Figure 14a). However, combined VEGFR and RSK inhibition did not reduce HOSCC proliferation more than the additive effect of the each inhibition alone.

4.3.4 Effect of RSK inhibition in combination with VEGFR inhibition on signalling intermediates central to proliferation in HOSCC

Since it has already been shown above that combined VEGFR and RSK inhibition markedly reduced HOSCC proliferation (Figure 14), the effect of RSK inhibition in combination with VEGFR inhibition was investigated on signalling intermediates central to proliferation (Figure 15).

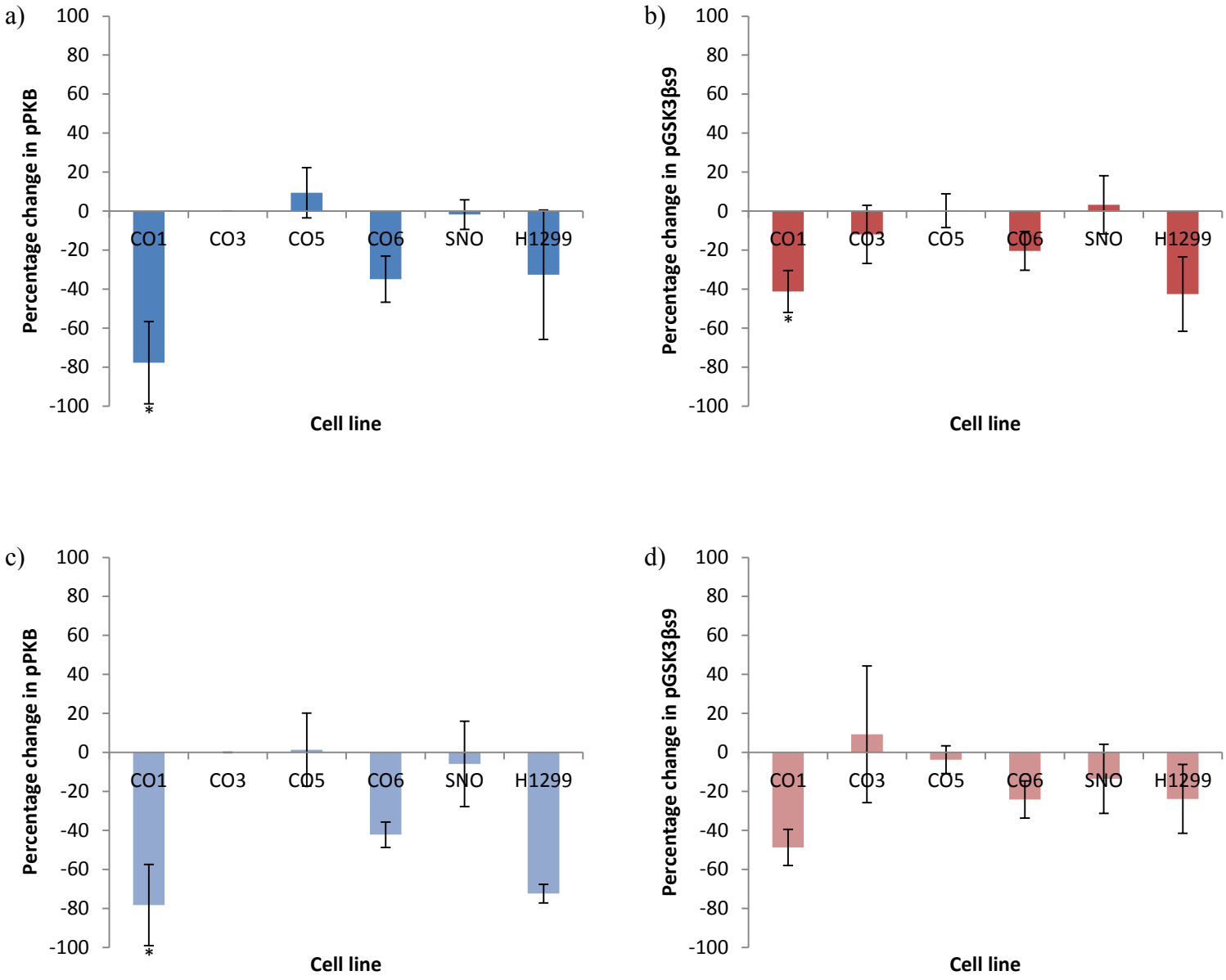

Figure 15: Combined VEGFR and RSK inhibition influences the abundance of pPKB and pGSK3βser9 in HOSCC cell lines

a) Combined VEGFR-RSK inhibition decreased or had negligible effect on pPKB abundance and b) pGSK3βser9 abundance of HOSCC cell lines vs VEGFR inhibition alone and again c) decreased or had negligible effect on pPKB abundance and d) pGSK3βser9 abundance vs control cultures. Abundance of pPKB and pGSK3βser9 were determined via western blotting followed by densitometric analysis, relative to the H1299 external control set at 100. The mean difference ($n \geq 3$) was represented as percentage change and standard error denoted as error bars. Significant difference at a 95 % confidence level ($p <= 0.05$) between the means of control and treated samples is indicated by an *.

Combined VEGFR and RSK inhibition had a varied effect on proliferative signalling intermediates. In the WHCO1 and WHCO6 cell lines and the H1299 control cell line, combined inhibition of VEGFR and RSK caused a decrease in both deactivated PKB mediated pathways and activated GSK3β tumour suppressor pathways as expected. This was indicated via a decrease in pPKB (active PKB) abundance and a decrease in pGSK3βser9 (inactive GSK3β), both as compared to cultures in which VEGFR alone was inhibited (Figure 15a and b, refer to Table 1) and as compared to control cultures (Figure 15c and d, refer to Table 1).

In contrast, combined VEGFR and PI3K inhibition had negligible effect on both active PKB (pPKB) and inactive GSK3β (pGSK3βser9) signalling in the WHCO3, WHCO5 and SNO cell lines, both as compared to cultures in which VEGFR alone was inhibited (Figure 15a and b) and as compared to control cultures (Figure 15c and d).

4.4 Discussion

In order to substantiate that the MAPK/ERK signalling is responsible for VEGFR induced GSK3β inhibition and enhanced proliferation; the pathway was inhibited at RSK. The role of VEGFR-induced MAPK/ERK/RSK signalling in HOSCC proliferation was confirmed in a behavioural context through reduced proliferation during concurrent VEGFR stimulation and RSK inhibition as compared to VEGFR stimulation only (Figure 12b). Indeed abrogation of RSK signalling both in the presence and absence of VEGFR stimulation was confirmed to reduce proliferation across all HOSCC cell lines (Figure 12a and b). The MAPK/ERK/RSK signalling pathway is thus a major contributor towards HOSCC cellular proliferation.

Nevertheless, the effects of abrogated MAPK/ERK/RSK signalling on VEGFR induced signalling intermediates are varied. Abrogation of RSK signalling was confirmed to impede inhibition of GSK3β tumour suppressive signalling (decreased inactive GSK3β) in the majority of HOSCC cell lines as expected because inhibited RSK is unable to inhibit GSK3β (Figure 13b). Furthermore inhibition of RSK during VEGFR stimulation resulted in a marked decrease in GSK3β inhibition in the H1299 control cell line as well as the HOSCC WHCO1, WHCO3 and WHCO5 cell lines (Figure 13d), and so these cell lines are unable to compensate for the loss of RSK through a VEGFR induced GSK3β mediated pathway. In contrast, the WHCO6 and SNO cell line compensated for the loss of RSK signalling by maintaining or enhancing PKB activation and GSK3β inactivation during VEGFR stimulation (Figure 13c and d). These HOSCC cell lines are thus able to compensate for the loss of MAPK/ERK/RSK signalling by enhanced levels of active PKB. It is theorised that this compensation occurs via an mTORC1 mediated mechanism, wherein inhibited RSK is unable to inhibit TSC2 resulting in more active TSC2, which then inhibits mTORC1 functionality. Lower levels of active mTORC1 subsequently result in less PI3K inhibition. More active PI3K is then able to activate PKB mediated signalling which also inhibits GSK3β, refer to Figure 16 below.

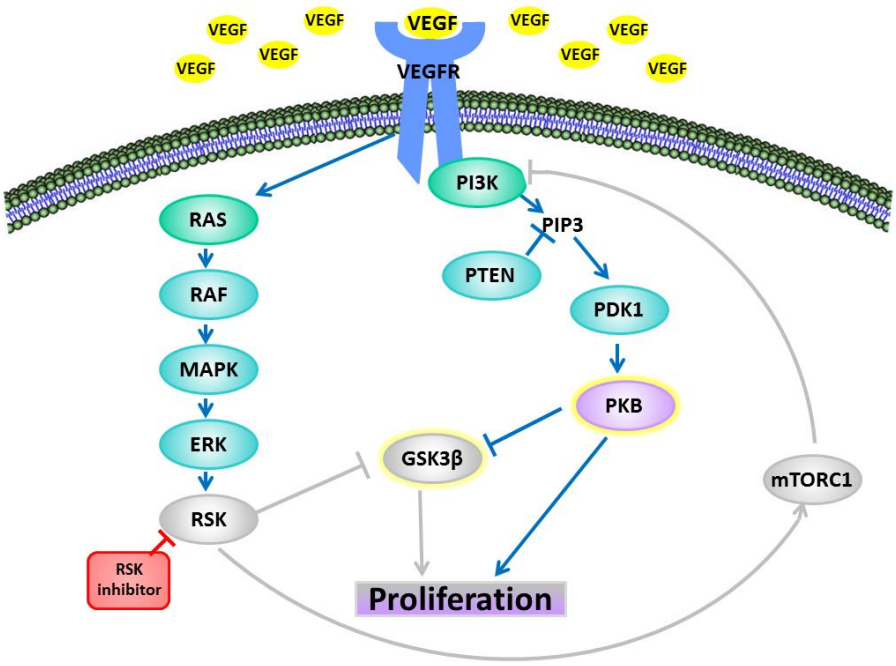

Figure 16: Abrogation of VEGFR-induced RSK signal transduction in HOSCC

Upon RSK inhibition, VEGFR-stimulation is unable to activate the RSK signalling pathway (greyed out) in HOSCCs. Abrogation of VEGFR-induced RSK signalling results in reduced HOSCC proliferation (partially greyed out). VEGFR-induced HOSCC proliferation is thus at least partially dependent on the MAPK/ERK/RSK signalling pathway. RSK inhibition, however releases the damper on the PI3K/PKB signalling pathway, where lower levels of active RSK results in less PI3K inhibition via mTORC1. VEGFR-stimulation may thus heighten PI3K signalling, unrestricted by RSK/PI3K negative feedback and thus maintain PKB activation and GSK3β inactivation. [Figure generated by author]

Although the WHCO6 and SNO cell lines compensate for the loss of RSK signalling (Figure 13), they did not exhibit a less substantial decrease in proliferation due to abrogation of VEGFR induced MAPK/ERK/RSK signalling than other HOSCC cell lines (Figure 12). Initiation of VEGFR induced salvage pathways to compensate for the loss of RSK therefore does not negate the anti-proliferative effect of anti-RSK targeted therapies. VEGFR induce compensation for the loss of RSK may however still have a behavioural influence on HOSCC cell lines. For example; as GSK3β inhibition is known for its role in cell survival, autocrine VEGFR signalling may allow HOSCC cells to compensate for the loss of RSK signalling through a GSK3β mediated pathway and thus potentially maintain or enhance HOSCC cell survival. Combined VEGFR and RSK inhibition was therefore investigated as a means to prevent pathway compensation.

Combined inhibition of VEGFR and RSK continued to reduce HOSCC proliferation (Figure 14) but not more than either treatment alone. In addition, although initiation of salvage

pathways culminating in PKB or GSK3β appear to be reduced, PKB and GSK3β mediated signalling is maintained in some cell lines during combined VEGFR and RSK inhibition (Figure 15). Combined targeting of VEGFR and RSK as a HOSCC treatment option would therefore not be as effective as combined targeting of VEGFR and PI3K, as the therapies do not act synergistically to considerably reduce proliferation nor do they completely curtail signalling pathway compensation.

Abrogation of VEGFR induced PI3K/PKB and MAPK/ERK signalling pathways revealed the different HOSCC cell lines appear to rely on signalling pathways to varying extents. The WHCO6 and SNO cell lines appear to rely more heavily on the PI3K/PKB signalling pathway and are able to use this pathway to compensate for abrogation of MAPK/ERK/RSK signalling. Deduced due to the fact that abrogation of RSK signalling causes an increase in active PKB and inactive GSK3βser9 in the WHCO6 and SNO cell lines (Figure 13) and thus these HOSCC cell lines are able to compensate for the loss of MAPK/ERK/RSK signalling by enhanced PKB mediated signalling. In contrast the WHCO1, WHCO3 and WHCO5 cell lines appear to be more reliant on the MAPK/ERK/RSK signalling pathway. In the WHCO1 and WHCO5 cell lines abrogation of the MAPK/ERK/RSK signalling pathway causes a decrease in levels of active PKB, VEGFR-stimulation is thus unable to increase PKB signalling to compensate for lack of MAPK/ERK/RSK signalling. The WHCO3 cell line, on the other hand, does not possess discernable levels of active PKB under all conditions tested and thus is likely unable to compensate for RSK abrogation via the PI3K/PKB pathway. In addition abrogation of the PI3K/PKB signalling pathway increases the inhibition of GSK3β in the WHCO1 cell line thus this cell line may use the MAPK/ERK/RSK signalling pathway to compensate for the loss of PI3K/PKB signalling.

The differences in regulation of these major signalling pathways in HOSCC may be attributed to the fact that although all of the HOSCC cell lines where characterised as being moderately differentiated each case of cancer arises through a unique combination of aberrations; disrupting cell regulation and hence homeostasis. The results of this study give clear evidence that tumours classified to be of the same malignant grade are indeed different and would respond differently to therapeutics. Although these cancer cell lines were procured and graded many years ago, this system of grading cancers purely based phenotypic traits is still widely used. Clearly a more advanced approach to grading tumours needs to be established taking into account unique aberrations in signalling pathways to allow for more effectively targeted therapy. For example it is expected that a HOSCC patient whose tumour

appears to be more reliant on the PI3K/PKB pathway and able to withstand the loss of MAPK/ERK/RSK signalling would respond poorly to MAPK/ERK/RSK targeted therapy but is anticipated to respond favourably to PI3K/PKB targeted therapy.

Chapter 5: VEGFR-stimulated signal transduction in migration of HOSCC

5.1 Introduction

The findings presented in this study (Chapter 2) definitively validates the existence of an autocrine VEGFR-stimulated signalling pathway in HOSCCs. Moreover as detailed above (Chapters 3 and 4) autocrine VEGFR signalling was found to initiate both MAPK/ERK/RSK and PI3K/PKB signalling pathways for enhance proliferation. Enhanced proliferation is one of the fundamental characteristics of cancer, another of which is metastasis and invasion. HOSCC is a highly metastatic cancer, frequently metastasising to the lymph nodes (Ferlay et al., 2013; Klimstra, 1994; Stoner and Gupta, 2001). It is this ability of cancer cells to invade local tissue and spread to distant sites – a phenomenon known as metastasis which makes cancer such a treacherous disease, as it is often impossible to successfully eradicate all metastases and thus the disease progresses (Ganguly et al., 2013; Sever and Brugge, 2015). As such metastasis and invasion are critical steps in the physiological development of cancer, the prevention of which would be revolutionary.

The process of invasion and metastasis occurs through a series of steps. First the cancer cells invade the local tissue, they then enter nearby blood and lymphatic vessels (intravasation), the cells are then transported through the vascular system to distant tissues, here the cancer cells exit the vascular system (extravasation), form small cancerous nodules known as micrometastases and eventually grow into macroscopic tumours (Fidler, 2003; Hanahan and Weinberg, 2011; Talmadge and Fidler, 2010). Cellular migration is however the crucial initial step in the metastatic process. HOSCC cell migration was therefore the factor assessed in this study because cellular migration is considered a strong indicator of metastasis initiation (Friedl and Wolf, 2003; Gupta and Massagué, 2006; Lauffenburger and Horwitz, 1996; Wolf and Friedl, 2006; Yamaguchi et al., 2005; van Zijl et al., 2011).

Migration requires altered adhesion of cells to each other and to the ECM allowing the cell to move forward (Brakebusch and Fässler, 2003; Wolf and Friedl, 2006). Such a complexed physiological task requires complicated signalling input. As autocrine VEGFR signalling has been implicated in HOSCC proliferative signalling, as detailed above (Chapters 2-4) we were interested to determine whether VEGFR signalling translates to a behavioural/more physiological role in HOSCC migration and invasion.

During angiogenesis VEGFR signalling induces migration of endothelial cells for the development of new blood vessels (Karkkainen and Petrova, 2000). Autocrine VEGFR stimulated signalling may influence tumour cells in a similar manner to promote tumour cell migration. Indeed autocrine VEGFR signalling has been associated with increased metastasis and invasion of many human tumours (Bachelder et al., 2002; Goel and Mercurio, 2013; Price et al., 2001; Spannuth et al., 2009; Su et al., 2006; Takahashi et al., 1995). For example, the VEGFR2 receptor is aberrantly expressed in thyroid and colon cancers where increased expression is associated with increased incidences of metastasis (Giatromanolaki et al., 2007; Rodríguez-Antona et al., 2010; Takahashi et al., 1995). More specifically elevated VEGF expression in HOSCC has been linked with deeper invasion and increased metastasis frequency (Inoue et al., 1997; Zhao et al., 2015). There is however a lack of knowledge in the current literature with regards to the precise role of autocrine VEGFR signalling pathways in cancer cell metastasis and invasion.

Through the course of this investigation autocrine VEGFR-stimulated signalling in HOSCCs was found to function via PKB and GSK3β mediated signalling pathways (Chapters 2-4). The question was thus posed as to whether VEGFR-stimulation induced PKB and GSK3β mediated signalling may also act to enhance HOSCC metastasis and invasion. Aside from their prominent role in proliferation, both PKB and GSK3β have been implicated in migratory signalling. PKB signals for metastasis and invasion via matrix metalloproteinase-2 (Park et al., 2001) and girdin (Enomoto et al., 2005) to name a few; while GSK3β regulates E-cadherin (Zhou et al., 2004) and microtubule extension (Etienne-Manneville and Hall, 2003). In addition, FAK is an important regulator of signals between integrins and growth factor receptors at the cell-ECM attachment interface (Mitra et al., 2005; Sieg et al., 2000). FAK was therefore also included as a proposed mediator of autocrine VEGFR induced migration. Refer to Chapter 1 for a more detailed review of PKB, GSK3β and FAK in metastasis.

In order to elucidate the association of autocrine VEGFR-stimulated signalling with HOSCC invasion and metastasis, the impact of VEGFR-stimulated signalling on HOSCC migration was investigated as well as role of FAK, PKB and GSK3β in mediating HOSCC metastasis. The identification of the pathway through which VEGFR signalling contributes to HOSCC invasion and metastasis may greatly aid in the development of therapeutic strategies for the prevention of HOSCC metastasis.

5.2 Materials and Methods

5.2.1 Tissue culture

Tissue culture of the five HOSCC cell lines as well as the MCF7 and H1299 cell lines was performed as described in Chapter 2, Section 2.2.1.

5.2.2 Treatment set to provide insight into VEGFR-stimulated signal transduction in migration of HOSCC

Cells cultured to approximately 70 % confluency in 6 cm tissue culture dishes were rinsed twice with sterile pre-warmed PBS and fresh media was provided. Cultures were then treated with VEGF (Sigma-Aldrich®, V7259) for 10 minutes at final concentration of 50 μg/ml in fresh media or with Axitinib (a VEGFR inhibitor) (Abcam®, ab141985) in dimethyl sulfoxide (DMSO) at final concentration of 10 μmol/L in fresh media for an hour, 10 minutes prior to completion of the treatment VEGF was added to a final concentration of 50 μg/ml. Control experiments were carried out simultaneously in the exact same manner with corresponding DMSO concentrations lacking the treatment.

5.2.3 Protein extraction

Total cellular protein was extracted from control, VEGFR stimulated and VEGFR inhibited cultures according to the procedure detailed in Chapter 2, Section 2.2.3.

5.2.4 Protein concentration determination

The protein concentration of control, VEGFR stimulated and VEGFR inhibited samples was determined according to the procedure detailed in Chapter 2, Section 2.2.4.

5.2.5 Sodium Dodecyl Sulphate–Polyacrylamide Gel Electrophoresis

The control, VEGFR stimulated and VEGFR inhibited cell lysate samples were electrophoresed following the methodology laid out in Chapter 2, Section 2.2.5.

5.2.6 Western blot

Control, VEGFR stimulated and VEGFR inhibited cell lysate samples resolved by SDS-PAGE were immunoblotted with anti-pPKB antibody, anti-pGSK3β antibody and anti-β-

actin antibody as described in Chapter 2, Section 2.2.6. In addition, samples were also immunoblotted with anti-FAK antibody (Table 3).

Table 3: pFAK antibody for western blotting; dilutions and incubation conditions

Protein of interest	pFAK
Primary antibody	Phospho-FAK (Tyr397) Antibody (Cell Signalling Technology®, #3283)
Transfer time (hr)	3
Dilution (antibody:buffer)	1: 1 000
Buffer	1 % BSA in TBST
Incubation conditions	Overnight at 4 °C
Secondary antibody	Anti-Rabbit IgG Peroxidase Conjugate (Sigma-Aldrich®, A6154)
Dilution (antibody:buffer)	1: 2 000
Buffer	5 % milk powder in TBST
Incubation conditions	1 hour at room temperature in the dark

5.2.7 Semi-quantitative analysis

Semi-quantitative analysis was carried out as described in Chapter 2, Section 2.2.7.

5.2.8 Assay of migratory cell morphology

Migratory cell morphology was detected through scratch-wound assays as described by Karihaloo (2005) and Liang (2007). HOSCC and control cell cultures grown to 70 % confluency were aspirated and rinsed once with sterile pre-warmed PBS. The cultures were then scratch-wounded (2 parallel wounds 2 cm apart) with a sterile 20 µl pipette tip. Following which cultures were washed once more in sterile PBS to remove lifted cells. Fresh media was supplied and cultures were treated as described in Chapter 5, Section 5.2.2. The cells were then incubated for 24 hr. Subsequently the cultures were gently rinsed in PBS and fixed in 4 % paraformaldehyde solution (Appendix A.25) for 15 minutes at room temperature. The cultures were then rinsed again in PBS, stained for 2 minutes in 0.25 % coomassie blue solution and rinsed once more in PBS.

A Leitz Waltzlar Inverted Light Microscope was used to observe cells and images were captured through a DCE-2 Digital Camera Eyepiece (Gentaur) with the aid of ScopePhoto 3.0

software. For each plate the percentage of cells displaying migratory morphologies such as filopodia and lamellipodia as a portion of total cells was determined along the sides of the scratch-wound for 10 fields of view (at 135x magnification). Images at 280x magnification were also captured for display purposes.

5.2.9 Comparisons and statistical analysis

The percentage change, standard error and probability of significance between treated and control samples were calculated as described in Chapter 2, Section 2.2.9.

5.3 Results

5.3.1 VEGFR stimulation affects HOSCC migration

HOSCCs have been found to produce VEGF (Figure 2) which may act upon the same HOSCCs cells in an autocrine manner to induce HOSCC metastasis and invasion. The universally recognised scratch wound healing technique provides a practical solution through which to assess cellular migration in the cell culture environment (Liang et al., 2007). As the initial step in metastasis and invasion, cellular migration is a good indicator pertaining to the initiation of metastasis and invasion (Friedl and Wolf, 2003; Gupta and Massagué, 2006; Lauffenburger and Horwitz, 1996; Wolf and Friedl, 2006; Yamaguchi et al., 2005; van Zijl et al., 2011). The effect of VEGFR stimulation on cellular migration was thus assessed through observation of migratory cell morphology along scratch wounds as demonstrated in Figure 17.

	Control	VEGFR-stimulated
CO1	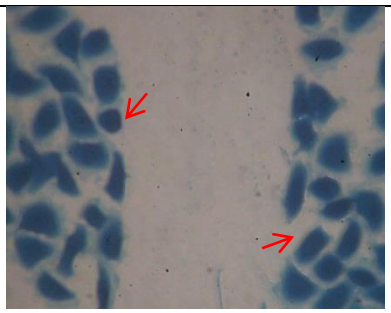	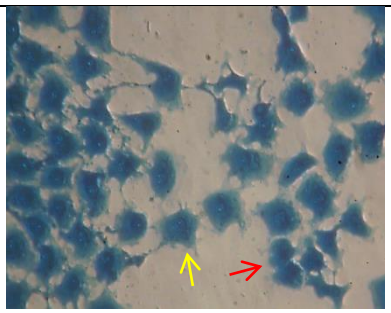
CO3	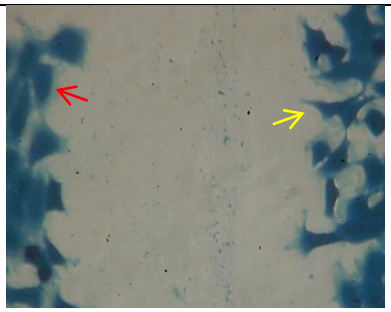	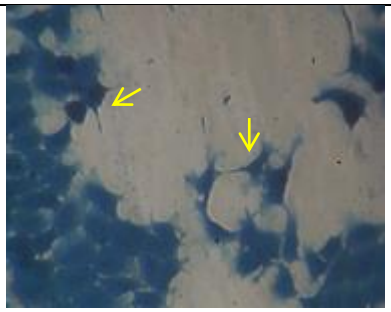

CO5	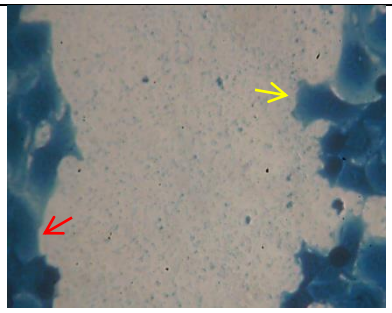	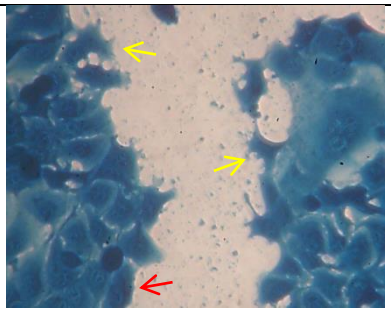
CO6	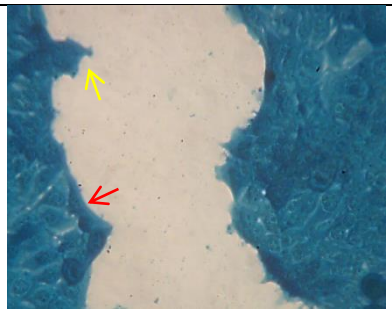	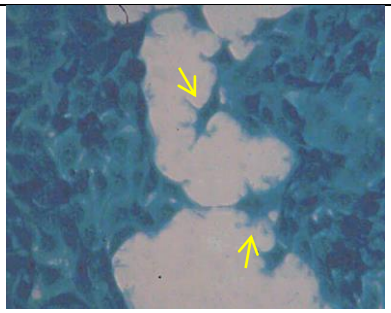
SNO	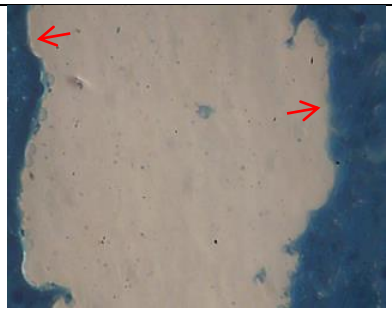	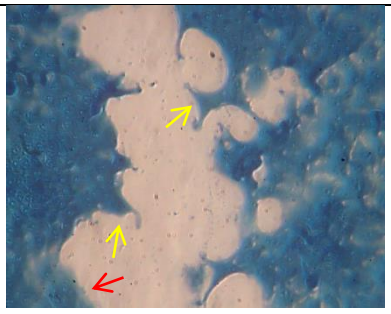
MCF7	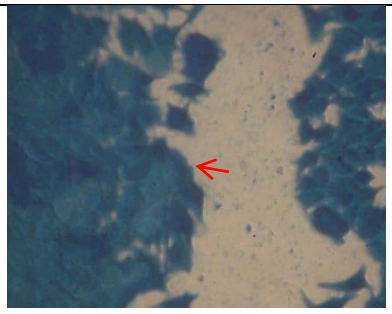	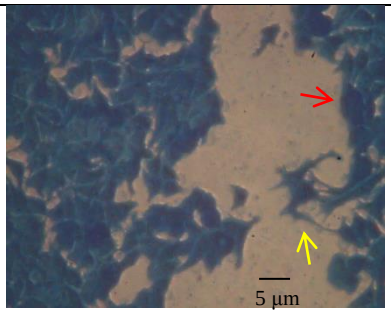

Figure 17: VEGFR-stimulation induces HOSCC cell migratory morphology

VEGFR stimulated HOSCC cell lines have higher incidences of cell migratory morphologies compared to control cultures. HOSCC cell lines and the MCF7 control cell line were scratch-wounded and treated for 24 hours, after which cells were fixed, stained and imaged at 280x magnification. Cells displaying migratory morphology are indicated with yellow arrows, while lack of migratory morphology is indicated with red arrows.

From the images of control and VEGFR stimulated cultures it is clear that cells stimulated with VEGF have more incidences of migratory morphologies than control cultures (Figure 17). For the purposes of this study migratory morphology encompasses filopodial and lamellipodial protrusions as well as sheet-like membrane extensions and long cellular extensions (Friedl and Wolf, 2003); all present in increased frequencies in VEGFR stimulated cultures, see arrows identifying migratory morphologies in Figure 17. In addition, VEGFR-stimulation causes increased migration of cells into the scratch-wound, oftentimes partially closing the scratch wound (Figure 17).

To obtain a quantitative measure of migration the total number of cells along the sides of the scratch-wound was counted and compared to the number of cells displaying migratory morphology along the sides of the scratch-wound. The ratio of migratory versus total cells was compared to determine the percentage change in abundance of migratory cell morphology upon VEGFR stimulation and inhibition (Figure 18).

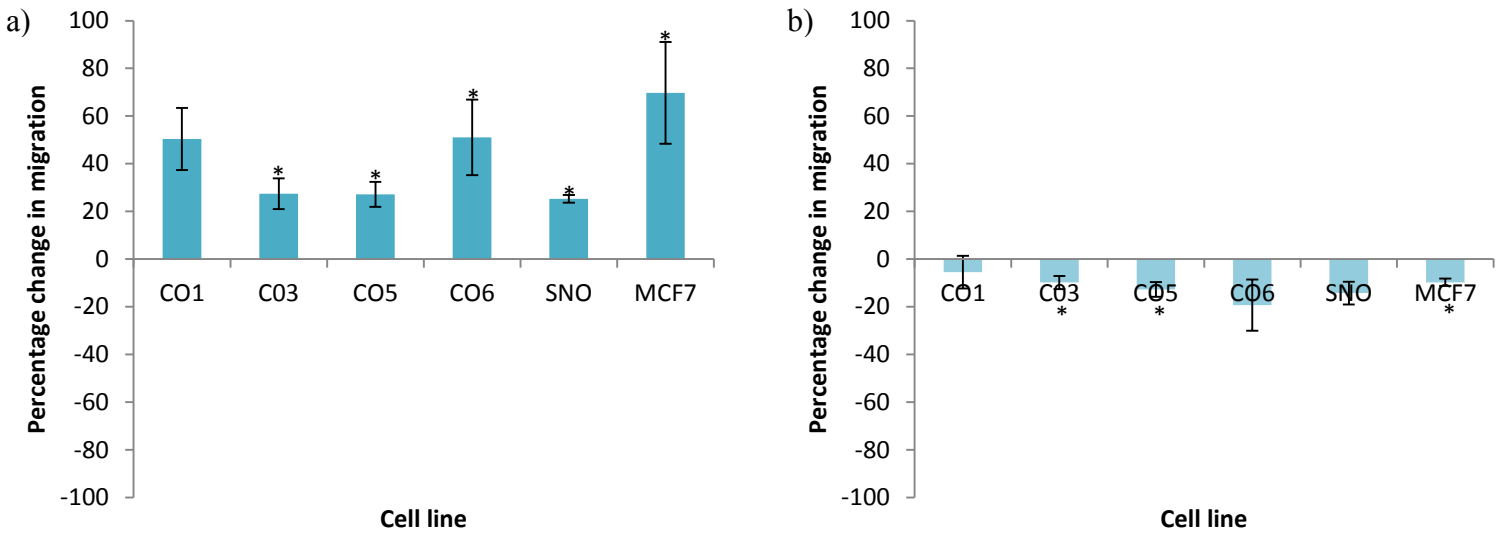

Figure 18: VEGFR signalling influences the migration of HOSCC cell lines

a) VEGFR stimulation increases migration of HOSCC cell lines (VEGFR stimulated vs control) while b) VEGFR inhibition decreases HOSCC migration (VEGFR inhibited vs control). HOSCC cell lines and the MCF7 control cell line were scratch-wounded and treated for 24 hours, after which the migratory ratio (cells displaying migratory morphology: total cells) was determined along the scratch wound ($n \geq 3$). The mean difference was represented as percentage change and standard error denoted as error bars. Significant difference at a 95 % confidence level ($p <= 0.05$) between the means of control and treated samples is indicated by an *.

Upon VEGFR-stimulation, all HOSCC cell lines displayed a marked increase in the ratio of migratory to total cells (Figure 18a). The effect of VEGFR-stimulation to enhance HOSCC cell migration was confirmed in the MCF7 control cell line (Figure 18a) known to respond to VEGFR-signal transduction (Cascio et al., 2010). Conversely, VEGFR inhibition lead to a slight decrease in cellular migration of HOSCC cell lines and the MCF7 control (Figure 18b). As cellular migration is an indicator for initiation of the invasive/metastatic response, it was concluded that VEGFR stimulation induces HOSCC cellular migration and thus triggers the invasive/metastatic response in HOSCC cell lines.

5.3.2 HOSCC cell lines contain pPKB, pGSK3βser9 and pFAK signalling intermediates putative in migration

Our research, discussed in the above chapters, found VEGFR-stimulated signalling in HOSCCs to function via PKB and GSK3β mediated signalling pathways. VEGFR signalling via these intermediates may also play a role in HOSCC migration. In addition, FAK is an important intermediate in migratory signalling (Mitra et al., 2005; Sieg et al., 2000) and was therefore included as a point of investigation in the VEGFR-induced HOSCC migratory signalling pathway. As a fresh addition to VEGFR-signalling analysis the levels of pFAK under standard HOSCC culture conditions (refer to 3.1 Tissue Culture) are presented below (Figure 19).

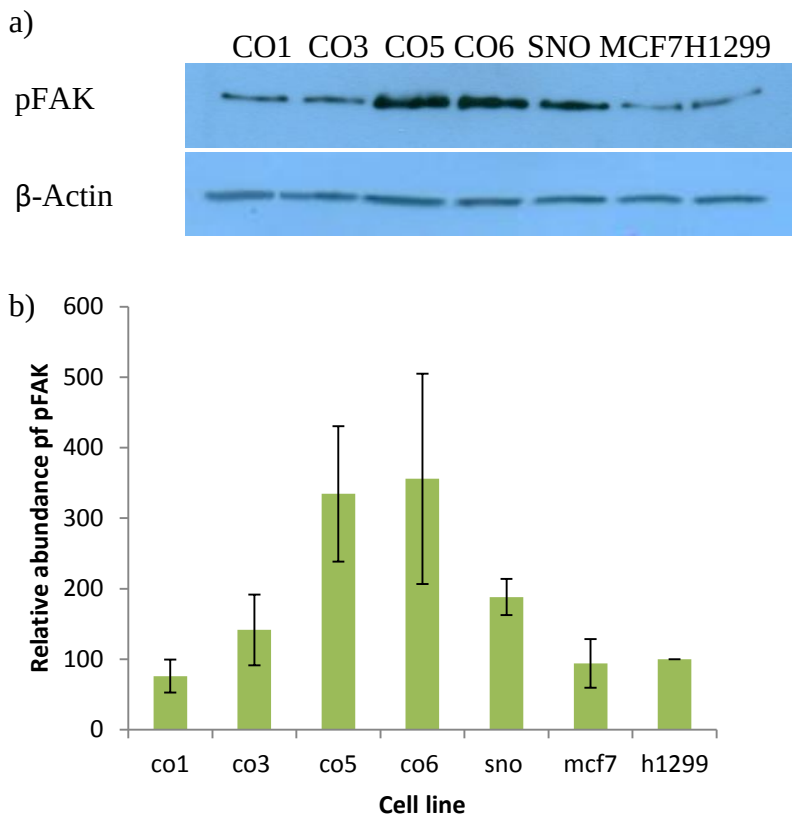

Figure 19: pFAK protein content in HOSCC cell lines

a) The HOSCC cell lines, MCF7 and H1299 control cell lines contain pFAK protein. Western blotting detected pFAK at 125 kDa. β-Actin served as the loading control. b) The mean abundance of pFAK (n ≥ 3) in each HOSCC cell line was determined via densitometric analysis, relative to the H1299 external control set at 100. Standard error denoted as error bars.

Measurable quantities of pFAK are present in HOSCC cell lines under standard culture conditions at levels equal to or higher than the control H1299 and MCF7 cell lines (Figure 19). FAK protein is therfore expressed and active (in its phosphoralated form, pFAK) under standard conditions in HOSCC, refer to (Table 1). Since active FAK is oftentimes associated with enhanced invasion and metastasis (Sieg et al., 2000), high quantities of pFAK present in HOSCC cell lines suggests these cell lines are actively migrating even under standard tissue culture conditions.

5.3.3 VEGFR signalling affects pPKB, pGSK3βser9 and pFAK signalling intermediates putative in HOSCC migration

The data presented above (Figure 18) clearly demonstrates VEGFR-stimulation induces the migration of HOSCC cell lines. Furthermore, VEGFR signalling has been shown to occur through pPKB and pGSK3βser9 mediated pathways (Chapter 2-4). An association of pPKB or pGSK3βser9 signalling with VEGFR-induced migration would suggest migration is mediated via these intermediates. In order to elucidate the signal transduction pathway through which VEGFR affects the cell migratory response of HOSCC cell lines, the change in abundance of pPKB, pGSK3βser9 and pFAK signalling intermediates putative in HOSCC migration was evaluated during VEGFR stimulation and VEGFR inhibition[1] (Figure 20).

VEGFR induced migration across the HOSCC cell lines (Figure 18a) is associated with either an increase in the activation of PKB (increase active pPKB) or an increase in the inhibition of the tumour suppressor GSK3β (increase inactive pGSK3βser9) (Figure 20a and b, refer to Table 1). In contrast, decreased migration across all the HOSCC cell lines due to inhibition of VEGFR signalling (Figure 18b) is associated with decreased PKB mediated signalling (decrease active pPKB) but negligible effect on the GSK3β tumour suppressor pathway (negligible change in inactive pGSK3βser9) (Figure 20d and e, refer to Table 1). This suggests VEGFR-induced migration occurs through a pPKB and/or pGSK3βser9 mediated signalling pathway.

[1] Note: For ease of reference Figure 20 is a reproduction of Figure 5 with the addition of corresponding pFAK data.

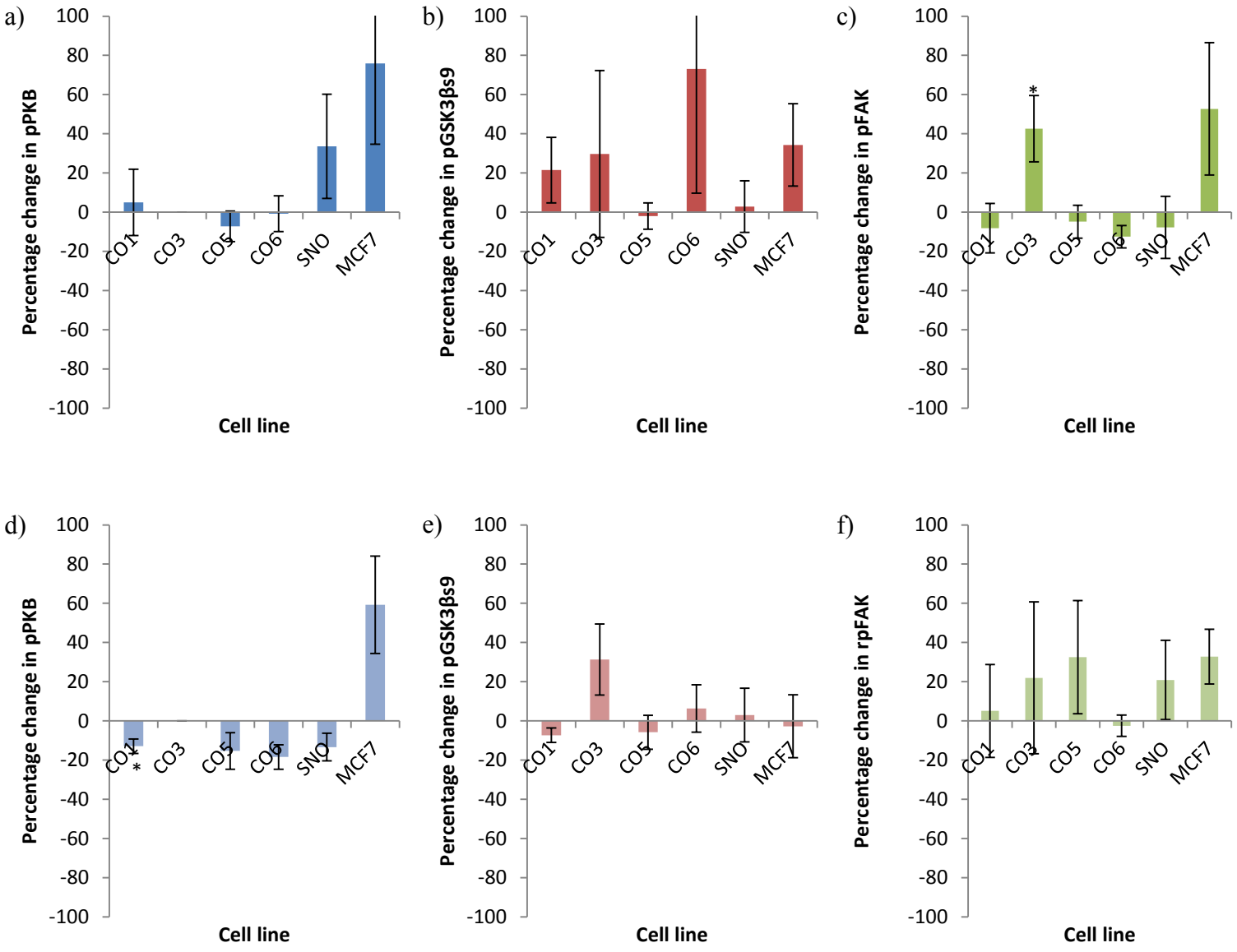

Figure 20: VEGFR signalling influences the abundance of pPKB, pGSK3βser9 and pFAK in HOSCC cell lines

a) In the majority of HOSCC cell lines VEGFR stimulation (VEGFR stimulated vs control) has negligible effect on pPKB abundance, b) increases pGSK3βser9 abundance and c) has varied effect on pFAK abundance while d) VEGFR inhibition (VEGFR inhibited vs control) decreases pPKB abundance, e) has negligible effect on pGSK3βser9 abundance and f) an equivocal effect on pFAK abundance. Abundance of pPKB, pGSK3βser9 and pFAK were determined via western blotting followed by densitometric analysis, relative to the H1299 external control set at 100. The mean difference ($n \geq 3$) was represented as percentage change and standard error denoted as error bars. Significant difference at a 95 % confidence level ($p <= 0.05$) between the means of control and treated samples is indicated by an *.

VEGFR stimulation in HOSCCs lead to an increased abundance of active FAK (pFAK) in the WHCO3 and MCF7 cell lines but a decreased active FAK in the WHCO6 cell line and had a negligible effect on abundance of active FAK in the WHCO1, WHCO5 and SNO cell lines (Figure 20c, refer to Table 1). VEGFR inhibition on the other had equivocal effect on pFAK activity across the HOSCC cell lines (Figure 20f, refer to Table 1) indicated by standard error (error bars) greater than the percentage change in pFAK (bars), detailed discussion to follow. The variable effect of VEGFR stimulation and inhibition on FAK activation seems to show VEGFR signalling may affect migration via a pathway not directly associated with FAK activity. One explanation may be that FAK functions far downstream in the VEGFR signalling cascade where crosstalk higher in the pathway clouds its association with FAK signalling.

5.4 Discussion

VEGFR-stimulated signalling has long been associated with enhanced invasion and metastasis of HOSCC (Inoue et al., 1997; Zhao et al., 2015). Indeed, this study confirms autocrine VEGFR-stimulated signal transduction induces HOSCC cell migration, an indicator of invasive and metastatic potential. In all HOSCC cell lines VEGFR-stimulated signalling in increased abundance of cell extensions and promoted cell stretching across a void (Figure 17). Quantification of this behaviour displayed a marked increase in the ratio of migratory to total cells as compared to control cultures (Figure 18a). The ability of VEGFR-stimulated signalling to induce migration of HOSCC was further evidenced by the fact that abrogation of the VEGFR signalling resulted in slightly decreased cellular migration across the HOSCC cell lines (Figure 18b). Enhanced migration of HOSCC induced by VEGFR signalling complements a recent study wherein VEGFR signalling strongly correlated with colorectal cancer cell migration and invasion (Bhattacharya et al., 2017).

VEGFR-stimulation clearly triggers a migratory response in HOSCC indicative of invasion/metastasis (Figure 18); the effect of VEGFR stimulation on migratory (FAK) signalling is however far less obvious. Despite considerable effort and time consuming biological replicates (in most cases n = 6) this study found VEGFR-stimulated signalling to have an equivocal effect on FAK migratory signalling in HOSCC cell lines (Figure 20c and f). Replicates of the same treatment often had vastly varied effects on pFAK abundance, ranging from an increase through to no change or even a decrease due to treatment, indicated by large standard error. One explanation may be that FAK functions far downstream in the VEGFR signalling cascade where crosstalk higher in the pathway clouds its association with FAK signalling. This explanation is made more reasonable by the fact that the effect of VEGFR signalling on pPKB is more consistent given its station higher upstream and closer to the receptor. Here, at PKB, the impact VEGFR-stimulation is more direct and fewer points are present upstream where pathway cross talk and salvage can confuse the effect. Indeed pGSK3βser9 slightly downstream of pPKB, although more clearly affected than pFAK is always prone to more error than pPKB. Thus the further downstream in the signalling cascade the intermediate you wish to associate with a particular behavioural response, the more subject to variation it becomes. The less than consistent effect of VEGFR signalling on pFAK is thus hardly surprising.

The finding that exacerbated VEGFR-stimulated signalling was able to induce cellular migration of all HOSCC cell lines (Figure 18), but abundance of active FAK did not associate with VEGFR-induced migration in any discernible manner (Figure 18 and Figure 20c and f), indicates that VEGFR-induced HOSCC cell migration either occurs though a mechanism where FAK is not the determining factor or the activity of FAK is spatially and temporally segregated in HOSCC. Although the mechanism by which FAK contributes to metastasis is still somewhat unclear, FAK activation is generally associated with cancer cell migration and invasion often as a result of EGFR, PDGFR and even VEGFR-stimulated signal transduction (Lee et al., 2012; Sieg et al., 2000). In contrast reduced FAK activity may act to increase migration in some instances for example by dissolving cell-cell contacts and thus promoting migration of HeLa cells (Yano et al., 2004) and inducing the formation of breast cancer invadopodia (Chan et al., 2009). It is important to note that the activation of FAK is extremely complicated with many inputs and that a variety of factors only one of which is FAK are involved in cancer cell migration (Mitra et al., 2005). Alternatively the function of FAK may be spatially and temporally segregated in HOSCC cells, being activated to aid in disassembly of focal adhesion in the trailing edge and deactivated in the leading edge for increased attachment, both of which are necessary for migration (Hood and Cheresh, 2002; Palecek et al., 1997). If FAK is being simultaneously activated and deactivated to aid in migration the level of overall active FAK may not be indicative of the local effect of VEGFR-stimulated signalling to induce migration. More focused experimentation is therefore required to determine the exact role of FAK in VEGFR-induced HOSCC migration.

As described in the previous chapters, autocrine VEGFR-stimulated signalling enhances proliferation through PKB and GSK3β mediated signalling pathways. It was therefore of interest to determine whether VEGFR-induce PKB and GSK3β mediated signalling translates to a behavioural response indicative of invasion/metastasis.

Similar to the relation of VEGFR signalling with proliferation (Chapter 2), initiation of VEGFR induced invasion and metastasis in HOSCCs (Figure 18a) is associated with an increase in either PKB mediated signalling (increase active pPKB) or an increase in the inhibition of the tumour suppressor GSK3β signalling (increase inactive pGSK3βser9) (Figure 20a and b, refer to Table 1). Also in the same way as the association with proliferation, blockade of VEGFR signalling decreases invasive/metastatic potential of the HOSCC cell lines (Figure 18b) with a corresponding decrease in PKB mediated signalling (decrease active pPKB) but had negligible effect on the GSK3β tumour suppressor pathway

(negligible change in inactive pGSK3βser9) (Figure 20d and e, refer to Table 1). VEGFR-stimulation therefore triggers initiation of HOSCC invasion and metastasis as well as proliferation through pPKB and pGSK3βser9 mediated signalling pathways. Targeting the VEGFR signalling pathway may thus have a dual effect, reducing HOSCC proliferation and metastatic initiation.

Chapter 6: The role of the VEGFR-induced PI3K/PKB signalling pathway in HOSCC migration

6.1 Introduction

The results gathered in this study clearly attest to the propensity of autocrine VEGFR-stimulated signalling to initiate the invasive/metastatic response of HOSCC cell lines (Chapter 5). Elucidating the signal transduction mechanism by which VEGFR initiates HOSCC metastasis may shed light on possible targets to prevent or reduce HOSCC metastasis. As mentioned previously it is the capacity of cancer cells to metastasise which makes cancer such a formidable disease. A treatment which hinders HOSCC metastasis to any extent would be greatly beneficial in the therapy of such an aggressive and highly metastatic cancer.

As described above, VEGFR signalling functions via the PKB and GSK3β mediated signalling pathways to enhance HOSCC proliferation and trigger the invasive/metastatic response (Chapter 2-5). The strongest association of VEGFR signalling with metastatic initiation appeared to be mediated by PKB, where abrogation of VEGFR signalling consistently reduced both migration and the abundance of active PKB across all the HOSCC cell lines (Chapter 5). It was therefore proposed that VEGFR induced PI3K/PKB signalling may be a prominent pathway in VEGFR induced HOSCCs invasion and metastasis.

Since it has already been found here (Chapter 3) that autocrine VEGFR-stimulated signalling acts via the PI3K/PKB signalling pathway to enhance proliferation of HOSCC cell lines; this pathway may also contribute towards VEGFR-stimulation enhanced HOSCC metastasis. The effect of abrogated PI3K signalling was therefore investigated with regards to migration in order to determine whether VEGFR-stimulated signalling acts via the PI3K/PKB pathway to initiate HOSCC metastasis. Furthermore, we have shown autocrine VEGFR-stimulated signalling allows HOSCC cells to compensate for the loss of PI3K signalling via the MAPK/ERK/RSK pathway, hindering the anti-proliferative effect of such therapy, refer to Chapter 3 for detailed discussion. It was therefore of interest to determine whether VEGFR signalling is similarly able to initiate a salvage pathway which could negate the anti-migratory effects of PI3K targeted therapy. In addition, this study discovered combined targeting of VEGFR signalling and the PI3K signalling pathway function together to markedly reduce HOSCC proliferation and prevent initiation of salvage pathways

(Chapter 3). The effect of combination VEGFR-PI3K targeted treatment on HOSCC migration was therefore investigated. If combined targeting of VEGFR and PI3K signalling functions in a similar manner to reduce the initiation of HOSCC invasion and metastasis, such therapy could prove to be a powerful HOSCC treatment option.

6.2 Materials and Methods

6.2.1 Tissue culture

Tissue culture of the five HOSCC cell lines as well as the H1299 control cell line was performed as described in Chapter 2, Section 2.2.1.

6.2.2 Treatment set to provide insight into VEGFR-induce PI3K/PKB signalling pathway

Cells cultured to approximately 70 % confluency in 6 cm tissue culture dishes were rinsed twice with sterile pre-warmed PBS and fresh media was provided. Cultures were then treated with each combination of the following: VEGF (Sigma-Aldrich®, V7259, at a final concentration of 50 μg/ml for 10 minutes), a VEGFR inhibitor (Axitinib) (Abcam®, ab141985, at a final concentration of 10 umol/L for an hour) and an inhibitor of PI3K (Sigma-Aldrich®, LY294002, at a final concentration of 20 μM for 1 hour). Control experiments were carried out simultaneously in the exact same manner with corresponding DMSO concentrations lacking the treatment.

6.2.3 Protein extraction

Total cellular protein was extracted from control, VEGFR stimulated, PI3K inhibited, combination VEGFR stimulated-PI3K inhibited, VEGFR inhibited and combination VEGFR inhibited-PI3K inhibited cultures according to the procedure detailed in Chapter 2, Section 2.2.3.

6.2.4 Protein concentration determination

The protein concentration of control, VEGFR stimulated, PI3K inhibited, combination VEGFR stimulated-PI3K inhibited, VEGFR inhibited and combination VEGFR inhibited-PI3K inhibited samples was determined according to the procedure detailed in Chapter 2, Section 2.2.4.

6.2.5 Sodium Dodecyl Sulphate–Polyacrylamide Gel Electrophoresis

The control, VEGFR stimulated, PI3K inhibited, combination VEGFR stimulated-PI3K inhibited, VEGFR inhibited and combination VEGFR inhibited-PI3K inhibited cell lysate samples were electrophoresed following the methodology laid out in Chapter 2, Section 2.2.5.

6.2.6 Western blot

Control, VEGFR stimulated, PI3K inhibited, combination VEGFR stimulated-PI3K inhibited, VEGFR inhibited and combination VEGFR inhibited-PI3K inhibited cell lysate samples resolved by SDS-PAGE were immunoblotted with anti-pPKB antibody, anti-pGSK3β antibody, anti-FAK antibody and anti-β-actin antibody as described in Chapter 2, Section 2.2.6.

6.2.7 Semi-quantitative analysis

Semi-quantitative analysis was carried out as described in Chapter 2, Section 2.2.7.

6.2.8 Assay of migratory cell morphology

Cellular migration was detected through a scratch-wound assay as described in Chapter 5, Section 5.2.8.

6.2.9 Comparisons and statistical analysis

The percentage change, standard error and probability of significance between treated and control samples were calculated as described in Chapter 2, Section 2.2.9.

6.3 Results

6.3.1 PI3K inhibition decreases HOSCC migration

As described in Chapter 3, VEGFR-stimulation functions via the PI3K/PKB signalling pathway to enhance HOSCC proliferation. The VEGFR induced PI3K/PKB signalling pathway may thus also mediate HOSCC migration. The effect of PI3K inhibition on HOSCC cellular migration was therefore investigated through a scratch-wound healing assay both in the presence and absence of VEGFR stimulation (Figure 21).

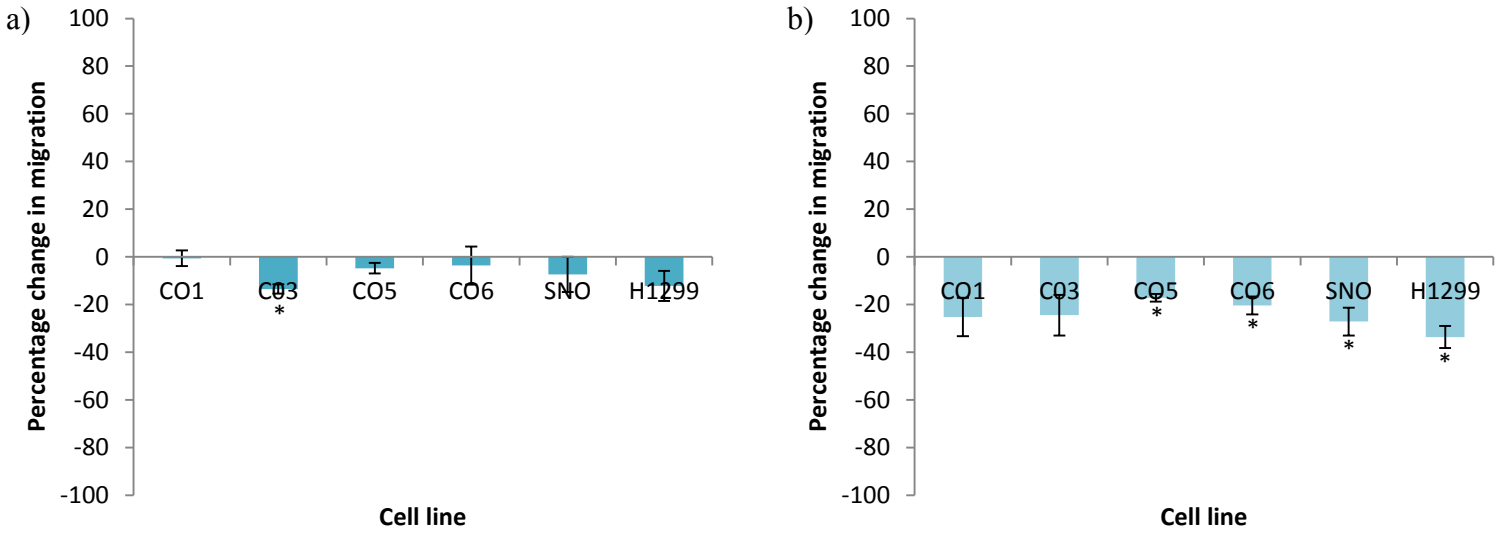

Figure 21: PI3K inhibition influences the migration of HOSCC cell lines

a) In the majority of HOSCC cell lines PI3K inhibition has a negligible effect on migration (PI3K inhibited vs control) while b) in the presence of VEGFR stimulation PI3K inhibition decreased HOSCC migration (VEGFR stimulated-PI3K inhibited vs VEGFR stimulated). HOSCC cell lines and the H1299 control cell line were scratch-wounded and treated for 24 hours, after which the migratory ratio (cells displaying migratory morphology: total cells) was determined along the scratch wound ($n \geq 3$). The mean difference was represented as percentage change and standard error denoted as error bars. Significant difference at a 95 % confidence level ($p <= 0.05$) between the means of control and treated samples is indicated by an *.

Under standard tissue culture conditions PI3K inhibition had negligible effect on HOSCC cellular migration (Figure 21a). However, during VEGFR stimulation PI3K inhibition resulted in a slight but distinct decrease in cellular migration of all HOSCC cell lines (Figure 21b). Once again the H1299 cell line, known to have a functional PI3K/PKB pathway (Choi et al., 2009; Hsieh et al., 2013) and high levels of active PKB (Figure 4b), was used as a

control for PI3K inhibition. As expected PI3K inhibition both alone and during VEGFR stimulation decreased migration of the H1299 control cell line (Figure 21). VEGFR-signalling is therefore dependent on PI3K activity in the HOSCC cell lines.

6.3.2 Effect of PI3K inhibition on signalling intermediates central to migration in HOSCC

The evidence presented above shows that PI3K inhibition reduces HOSCC migration during VEGFR stimulation (Figure 21b). The corresponding effect on signalling intermediates was therefore assessed in order to determine the role of these pathways in HOSCC cellular migration[2] (Figure 22). This study has already describe the effect of PI3K inhibition on PKB and GSK3β signalling intermediates, where VEGFR-stimulation allowed the continued inhibition of GSK3β during PI3K inhibition and thus negated the anti-proliferative effects of PI3K inhibition (Chapter 3, Figure 6 and 7). However, the effect of PI3K inhibition on pFAK and its putative association with migration required investigation (Figure 22).

[2] Note: For ease of reference Figure 22 is a reproduction of Figure 7 with the addition of corresponding pFAK data.

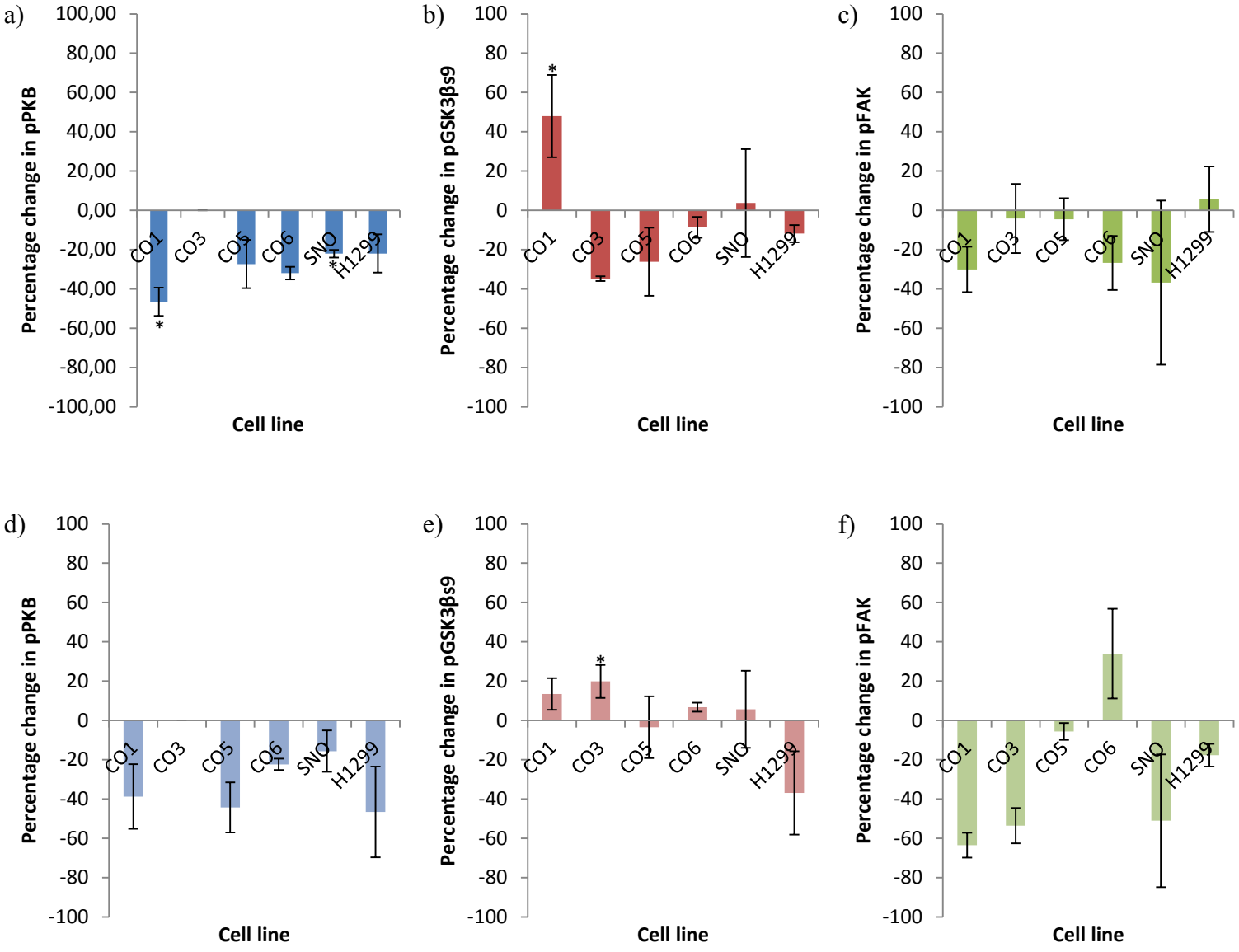

Figure 22: PI3K inhibition influences the abundance of pPKB, pGSK3βser9 and pFAK in HOSCC cell lines

a) PI3K inhibition (PI3K inhibited vs control) decreases pPKB abundance of HOSCC cell lines, b) has a varied effect on pGSK3βser9 abundance and c) equivocal effect on pFAK abundance while c) in the presence of VEGFR stimulation PI3K inhibition (VEGFR stimulated-PI3K inhibited vs VEGFR stimulated) decreases pPKB abundance e) has an enhancing or negligible effect on pGSK3βser9 and f) a varied effect on pFAK in HOSCC cell lines. Abundance of pPKB, pGSK3βser9 and pFAK were determined via western blotting followed by densitometric analysis, relative to the H1299 external control set at 100. The mean difference ($n \geq 3$) was represented as percentage change and standard error denoted as error bars. Significant difference at a 95 % confidence level ($p <= 0.05$) between the means of control and treated samples is indicated by an *.

Inhibition of PI3K signalling results in deactivated PKB mediated pathways and activated GSK3β tumour suppressor pathways as expected, indicated via a decrease in pPKB (active PKB) abundance and a decrease in pGSK3βser9 (inactive GSK3β) in the majority of HOSCC

cell lines (Figure 22a and b, refer to Table 1). However, inhibition of PI3K signalling had a varied effect on FAK mediated signalling, decreased pFAK (active FAK) abundance in some cell lines (WHCO1 and WHCO6) while having a equivocal effect on pFAK in the majority of HOSCC cell lines (WHCO3, WHCO5 and SNO) (Figure 22c). Please refer to Chapter 5 for a discussion surrounding the equivocal effects on pFAK.

Abrogation of PI3K signalling during VEGFR stimulation results in a decrease in pPKB (Figure 22d) but either increased or had negligible effect on pGSK3βser9 (Figure 22e). While abrogation of PI3K signalling during VEGFR stimulation continued to have a variable effect on FAK mediated signalling, decreasing pFAK (active FAK) abundance in the WHCO1, WHCO3 and SNO cell lines while increasing pFAK (active FAK) abundance in the WHCO6 cell line and having a negligible effect on pFAK in the WHCO5 cell line (Figure 22f).

6.3.3 Effect of PI3K inhibition in combination with VEGFR inhibition on HOSCC migration

Abrogation of VEGFR-stimulated signal transduction and abrogation of PI3K signal transduction have both been confirmed to reduce HOSCC cellular migration independently (Figure 18b and Figure 21). Chapter 3 found that combined VEGFR-PI3K inhibition dramatically reduced HOSCC proliferation more than the effect of either inhibition alone, it was thus hypothesised that combined VEGFR-PI3K inhibition would effect HOSCC migration in a similar manner. The effect of PI3K inhibition in combination with VEGFR inhibition on HOSCC migration was thus investigated via a scratch-wound healing assay (Figure 23).

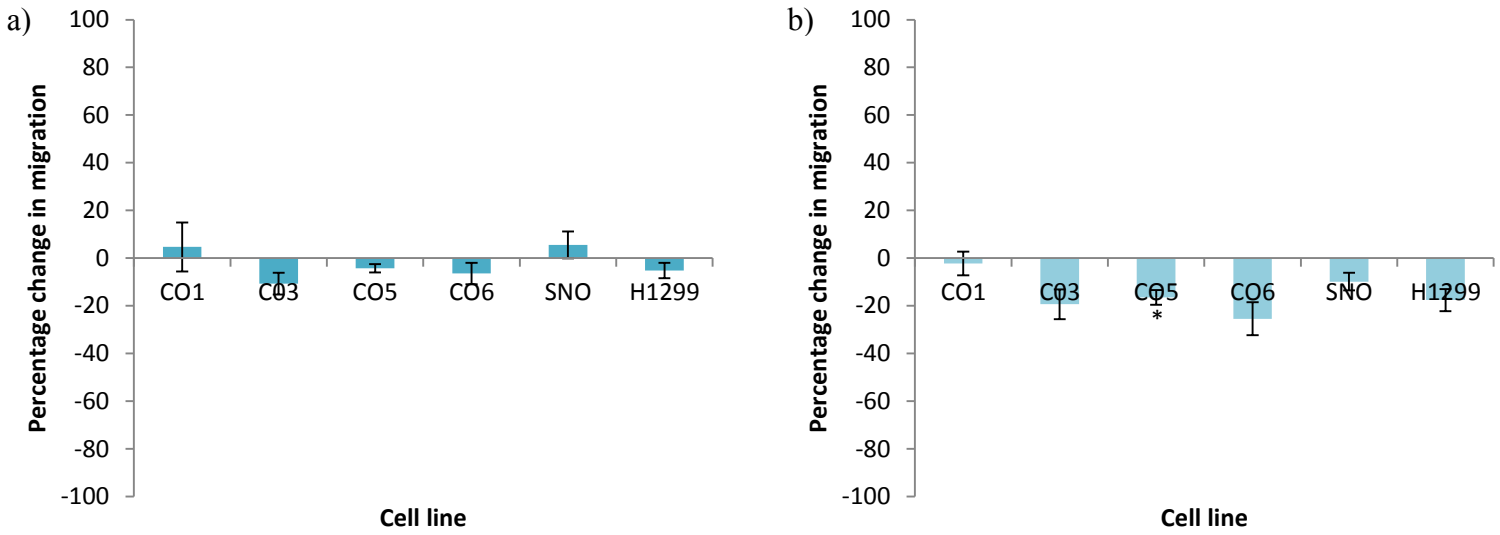

Figure 23: Combined VEGFR and PI3K inhibition influences the migration of HOSCC cell lines

a) Combined VEGFR-PI3K inhibition decreases migration of the majority of HOSCC cell lines vs VEGFR inhibition alone and b) vs control cultures. HOSCC cell lines and the H1299 control cell line were scratch-wounded and treated for 24 hours, after which the migratory ratio (cells displaying migratory morphology: total cells) was determined along the scratch wound ($n \geq 3$). The mean difference was represented as percentage change and standard error denoted as error bars. Significant difference at a 95 % confidence level ($p <= 0.05$) between the means of control and treated samples is indicated by an *.

Combined VEGFR and PI3K inhibition either causes a decrease in migration as compared to cultures in which VEGFR alone was inhibited or has negligible effect on HOSCC migration (Figure 23a). In addition, combined VEGFR and PI3K inhibition also reduces migration as compared control cultures (Figure 23b). The effect of combined VEGFR-PI3K inhibition in HOSCC is consistent with the effect on the H1299 control cell line (Figure 23). Combination VEGFR and PI3K inhibition however, did not reduce HOSCC migration more than the additive effect of each inhibition alone.

6.3.4 Effect of PI3K inhibition in combination with VEGFR inhibition on signalling intermediates central to migration in HOSCC

Since combined VEGFR and PI3K inhibition has been shown here to noticeably reduce HOSCC migration (Figure 23), the effect of PI3K inhibition in combination with VEGFR inhibition was investigated on signalling intermediates central to migration[3] (Figure 24). The results already presented above (Chapter 3, Figure 10) show combined VEGFR and PI3K

[3] Note: For ease of reference Figure 24 is a reproduction of Figure 10 with the addition of corresponding pFAK data.

inhibition consistently decreases both PKB signalling and inhibition GSK3β culminating in a marked decrease in proliferation. However, the association of such signalling as well as that of pFAK with respect to migration required investigation (Figure 24).

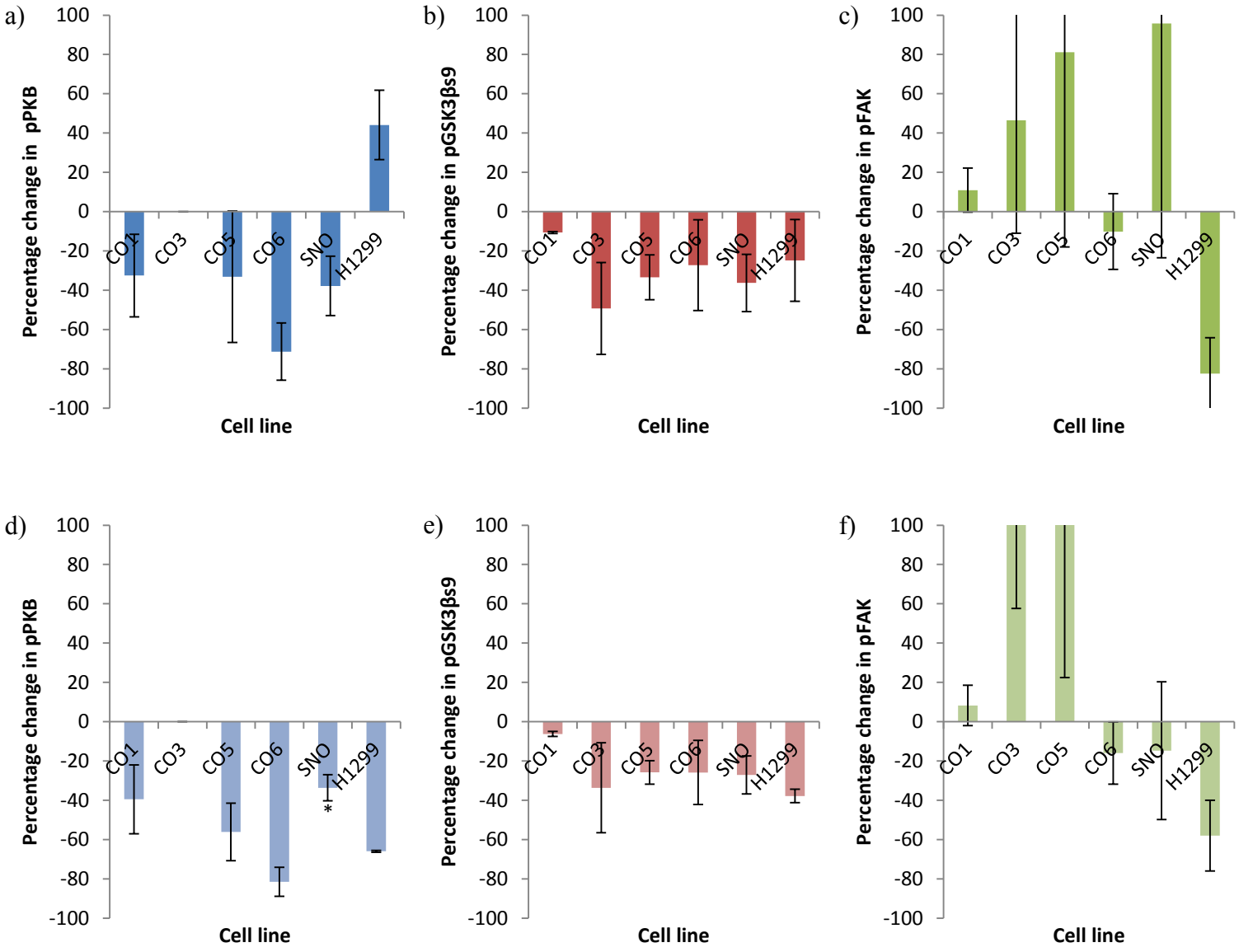

Figure 24: Combined VEGFR and PI3K inhibition influences the abundance of pPKB, pGSK3βser9 and pFAK in HOSCC cell lines

a) Combined VEGFR-PI3K inhibition decreases pPKB and b) pGSK3βser9 abundance of HOSCC cell lines vs VEGFR inhibition alone but c) has an equivocal effect on pFAK abundance while combined VEGFR-PI3K inhibition again d) decreases pPKB and e) pGSK3βser9 abundance vs control cultures and f) had an equivocal effect on pFAK abundance in HOSCC cell lines. Abundance of pPKB and pGSK3βser9 were determined via western blotting followed by densitometric analysis, relative to the H1299 external control set at 100. The mean difference ($n \geq 3$) was represented as percentage change and standard error denoted as error bars. Significant difference at a 95 % confidence level ($p <= 0.05$) between the means of control and treated samples is indicated by an *.

Combined VEGFR and PI3K inhibition results in deactivated PKB mediated pathways and activated GSK3β tumour suppressor pathways as expected, indicated via a decrease in pPKB (active PKB) abundance and a decrease in pGSK3βser9 (inactive GSK3β) across all HOSCC cell lines and the H1299 control cell line, as compared to cultures in which VEGFR alone was inhibited (Figure 24a and b, refer to Table 1). However, combined VEGFR and PI3K inhibition had an equivocal effect on pFAK as compared to cultures in which VEGFR alone was inhibited (Figure 24c). Please refer to Chapter 5 for a discussion surrounding the equivocal effects on pFAK.

Furthermore, combined VEGFR and PI3K inhibition also reduced both active PKB (decreased pPKB) and inactive GSK3β (decreased pGSK3βser9) signalling across all HOSCC cell lines and the H1299 control cell line as compared to control cultures (Figure 24d and e). Yet again, the effect of combined VEGFR and PI3K inhibition on pFAK was equivocal as compared to control cultures (Figure 24f).

6.4 Discussion

The VEGFR-induced PI3K signalling pathway was proposed to be integral for the initiation of the invasive/metastatic response in HOSCCs. Abrogation of VEGFR-induced PI3K signalling was therefore predicted to reduce HOSCC migration as an indicator of invasive/metastatic potential. Indeed the behavioural experiments presented in this thesis found abrogation of VEGFR-stimulated PI3K/PKB signalling caused a marked decline in the portion of cells displaying migratory morphology as compared to VEGFR stimulated cultures (Figure 21). VEGFR signalling thus triggers the invasive/metastatic response of HOSCCs via a PI3K dependent pathway.

One a related note, we theorise that the metastatic potential of untreated HOSCC cells is primarily due to VEGFR-induced PI3K signalling. This theory is motivated by the slight decrease in HOSCC migration upon abrogation of PI3K signalling (under standard tissue culture conditions) (Figure 21a) being of similar extent to the aforementioned slight decrease in HOSCC migration upon inhibition of VEGFR signalling (Figure 18b). As we have shown VEGF to be constitutively expressed in HOSCC cell lines, autocrine VEGFR-stimulated signalling is almost certainly occurring in untreated HOSCC cultures. The loss of low level autocrine VEGFR signalling induce PI3K signalling, either though VEGFR or PI3K inhibition, would therefore result in reduced HOSCC migration to a similar extent as demonstrated here (Figure 18b and Figure 21a).

The evidence gathered in this study shows autocrine VEGFR-stimulated signalling initiates the invasive/metastatic response of HOSCC cell line via a PI3K/PKB mediated signalling pathway. Abrogation of VEGFR-induce PI3K signalling was found to lead to a distinct decrease in both cellular migration (Figure 21b) and PKB mediated signalling across all the HOSCC cell lines as well as the control H1299 cell line (Figure 22a and d). Taken together with the finding that VEGFR-inhibition also unfailingly reduces both HOSCC cellular migration and PKB mediated signalling (Figure 18b and Figure 20d), it was concluded that autocrine VEGFR signalling functions through a PI3K/PKB dependent pathway to initiate HOSCC metastasis.

As described earlier, some HOSCC cell lines (WHCO1 and WHCO3) are able to compensate for the loss of PI3K/PKB signalling with enhanced inhibition of the GSK3β tumour suppressor during VEGFR stimulation (Chapter 3). In these cell lines, VEGFR stimulation acted via a MAPK/ERK/RSK salvage pathway to somewhat negate the anti-proliferative

effect of PI3K abrogation; refer to Chapters 3 and 4 for more details. Migration of HOSCC cell lines was however, not reduced any less by loss of PI3K/PKB signalling in cell lines able to compensate via MAPK/ERK/RSK inhibition of GSK3β than it was in the remaining HOSCC cell lines where inhibition of GSK3β signalling is maintained not heightened (Figure 21, Figure 22b and e). The initiation of a VEGFR-induced GSK3β mediated salvage pathway therefore does not negate the anti-migration effects of anti-PI3K/PKB therapy. Further evidencing the fact that GSK3β signalling is not involved in initiation of VEGFR induced HOSCC metastasis.

Surprisingly, FAK signalling originally suspected to be a prominent mediator of HOSCC metastatic initiation, did not correspond to HOSCC migration in any discernible manner throughout the course of this investigation. More specifically PI3K inhibition both alone, during VEGFR stimulation or in combination with VEGFR inhibition had either a varied or equivocal effects on FAK mediated signalling (Figure 22c and f; and Figure 24c and f), apparently not associated with the consistent effect of reduced HOSCC migration (Figure 21 and Figure 23). It was therefore concluded that VEGFR signalling triggers the invasive/metastatic response of HOSCCs via a PI3K/PKB dependent pathway while GSK3β and FAK are likely not major contributing factors towards initiation of VEGFR induced HOSCC metastasis.

Moreover, we have shown combined inhibition of VEGFR-stimulated signalling and PI3K mediated signalling consistently reduces HOSCC cellular migration (Figure 23b). However, the reduction in HOSCC migration due to combined VEGFR-PI3K inhibition is not more than the reduction due to either VEGFR inhibition (Figure 23a) or PI3K inhibition alone. Combined inhibition of VEGFR and PI3K is however able to curb salvage pathway compensation for the loss of PI3K signalling, indicated by consistently decreased PKB mediated signalling (decreased active pPKB) and decreased inhibition of the tumour suppressor GSK3β (decreased inactive pGSK3βser9) as described in Chapter 3. Nevertheless as VEGFR-stimulation does not appear to compensate for the anti-migratory effect of anti-PI3K treatment (discussed above; Figure 21, Figure 22b and e), single target therapy aimed at either VEGFR or the PI3K/PKB signalling pathway would likely be enough to effectively reduce initiation of HOSCC metastasis. Regardless, the consistent decline in initiation of HOSCC invasive/metastatic response afforded by inhibition of VEGFR and/or PI3K signalling suggests its potential as a therapeutic strategy aimed at preventing or reducing HOSCC invasion and metastasis.

Chapter 7: General discussion

The current thesis describes an autocrine VEGF/VEGFR signalling axis in human oesophageal squamous cell carcinoma cells, wherein HOSCC cells are able to both produce VEGF and respond to its stimulus, as discussed in Chapter 2. Furthermore, autocrine VEGFR signalling was discovered to both increase HOSCC proliferation and trigger the invasive/metastatic response of HOSCC cells, as described in Chapters 2 and 5 respectively. However, abrogation of VEGFR signalling lead to only a slight decrease in proliferation of HOSCC cell lines and an equally slight reduction in initiation of the HOSCC metastatic response, also described in Chapters 2 and 5. The efficacy of a therapeutic solely targeting VEGFR-stimulation with the aim of reducing HOSCC proliferation and metastasis would thus likely be marginal.

Investigation of the autocrine VEGFR signalling mechanism in HOSCC found VEGFR signalling to function via both the P13K/PKB and MAPK/ERK/RSK signalling pathways, refer to Chapter 3 and 4 respectively. An intricate balancing was revealed to exist between these pathways wherein if one pathway is shutdown, VEGFR produced by HOSCC cell may act in an autocrine manner upon the HOSCCs to initiate the other pathway to compensate for loss of the targeted pathway (Chapter 3 and 4). Furthermore, this study found VEGFR-stimulated signal transduction contributes to HOSCC proliferation via both the PI3K/PKB and MAPK/ERK/RSK signalling pathways (Chapter 3 and 4) and triggers the invasive/metastatic response of HOSCC cell lines through the PI3K/PKB signalling pathway (Chapter 6). The redundancies of VEGFR-stimulated signalling pathways lead us to investigate combination targeting as a means to potentially prevent pathway compensation and thus resistance to treatment.

The potential of combination therapy aimed at both the PI3K/PKB and MAPK/ERK/RSK signalling pathways was dismissed as an option due to the fact that both these pathways are prominent players in cell proliferation and survival (Jope et al., 2007; Vara et al., 2004). Combined shutdown of the PI3K/PKB and MAPK/ERK/RSK signalling pathways would thus almost certainly lead to devastating effects on cell signalling. Systemic treatment with such a combination of inhibitors would undoubtedly have toxic effect on both cancerous and non-cancerous cells throughout the body leading to pronounced side effects.

Conversely, a potential combination therapy involving VEGFR inhibition was hypothesised to be favourable. VEGFR signalling is has few roles in the adult human body outside of wound healing and female reproductive cycling (Hanahan and Folkman, 1996). However, as demonstrated in this study autocrine VEGFR signalling is a major player in HOSCC proliferation and metastatic initiation, refer to Chapters 2 and 5. Shutting down the VEGFR signal transduction pathway is therefore expected to have a little effect on non-cancerous adult body cells while having a more profound effect on cancerous HOSCC cells. There are already several clinically approved drugs targeting VEGFR-stimulation, developed with the aim of eliminating VEGFR-induced angiogenesis (Ellis and Hicklin, 2008a). The effectivity of these agents could be utilised to block autocrine VEGFR stimulated signalling in HOSCCs while also hindering the paracrine effect of VEGFR to induce angiogenesis (Ellis and Hicklin, 2008a). In addition, the frequent resistance to anti-VEGFR therapy could theoretically be circumvented and the effectivity of these agents further improved by combination with inhibitors targeting other points in the VEGFR signalling pathway.

Indeed our study revealed combined inhibition of VEGFR and PI3K prevented the initiation of salvage pathways culminating in PKB and GSK3β and thereby prevented salvage of HOSCC proliferation; refer to Chapter 3. The inability of HOSCC to compensate for loss of signals during combined VEGFR-PI3K inhibition would hopefully translate *in vivo* to less incidences of therapeutic resistance. In addition, as discussed in Chapter 6 combined abrogation of VEGFR and PI3K pathways lead to a consistent decline in initiation of the invasive/metastatic response across all the HOSCC cell lines. The results presented in Chapter 3 further support the potential of combination VEGFR-PI3K therapy, as combined inhibition of VEGFR and PI3K/PKB signalling was found to synergistically reduce HOSCC proliferation. Combined VEGFR-PI3K inhibition would however only act synergistically to reduce proliferation in cells where both VEGFR signalling is occurring as well as PI3K signalling for example in HOSCC cells which were found in this study to possess an autocrine VEGF/VEGFR signalling axis and a PI3K/PKB signalling axis. Although PI3K/PKB signalling occurs ubiquitously in the majority of human body cells, most of these cells do not possess a VEGF/VEGFR signalling axis and would thus have a less intense reduction in proliferation due to combined VEGFR-PI3K inhibition. The small but consistent decrease in HOSCC proliferation and migration due to loss of either VEGFR signalling or PI3K mediated signalling individually, refer to Chapters 2, 3, 5 and 6, is also probably safer than if the individual treatments greatly reduced proliferation and migration. A dramatic

reduction in proliferation would likely be a result of toxicity and would not be limited to cancerous cells but likely affect all human body cells. Non-cancerous cells need to be able to survive systemic treatment with the desired chemotherapeutic agents. This is what makes combined targeting of VEGFR and PI3K such a promising HOSCC therapeutic as VEGFR signalling for the most part is limited to cancer cells and thus the drugs would act in combination only in HOSCC cells.

The finding gathered in Chapter 4, indicate combined inhibition of VEGFR and RSK does decrease HOSCC proliferation, although not more than either inhibition alone. In addition, combined VEGFR-RSK inhibition did not entirely prevent the activity of salvage pathways culminating in PKB and GSK3β. Treatment of HOSCC with a combination of VEGFR and RSK inhibitors may therefore lead to development of drug resistance, possibly in the form of enhanced survival, refer to Chapter 4 for a more detailed discussion. Furthermore, we have shown VEGFR triggers the invasive/metastatic response of HOSCC predominantly through the PI3K/PKB pathway unaffected by MAPK/ERK/RSK compensation (Chapter 6). The MAPK/ERK/RSK signalling pathway therefore has little or no influence on initiation of HOSCC metastasis and so combined VEGFR-RSK inhibition is unlikely to decrease HOSCC metastasis more than VEGFR inhibition alone. For these reasons combined inhibition of VEGFR and PI3K rather than RSK, is preferred as a potential HOSCC treatment strategy.

The promise of combination therapy aimed VEGFR and PI3K may not be limited to HOSCC. Many other cancer types are known to have an autocrine VEGF/VEGFR signalling axis for example colon, breast and lung cancers express both VEGF and the VEGF receptor suggesting the existence of an autocrine VEGFR signalling axis (Carrillo de Santa Pau et al., 2009; Decaussin et al., 1999; Ghosh et al., 2008; de Jong et al., 1998; Seto et al., 2006; Takahashi et al., 1995). The PI3K/PKB signalling pathway is also frequently disrupted in human tumours including breast, prostate, ovarian, cervical and colorectal cancers (Bellacosa et al., 1995; Carpten et al., 2007; Ma et al., 2000; Shayesteh et al., 1999; Vara et al., 2004). Cancers, in which both autocrine VEGFR signalling and disrupted PI3K/PKB signalling is occurring, may respond to combined VEGFR-PI3K inhibition in a similar manner to HOSCC. Such cancers may fail to respond to anti-VEGFR targeted therapy but could potentially benefit from combination therapy aimed at both the VEGFR and PI3K/PKB signalling pathways. In this case the dual pathway shutdown would prevent the initiation of alternative salvage pathways, reduce proliferation and metastasis of these cancers.

7.1 Conclusion

The insight provided by this study with regards to VEGF receptor-stimulated signal transduction in human oesophageal squamous cell carcinoma, sheds light on the signalling mechanisms by which autocrine VEGFR signalling contributes to HOSCC progression and metastatic initiation. More than purely the acquisition of cancer cell biology knowledge, the value of this study lies in its translatability into a clinical context. In particular, the finding that combined VEGFR and PI3K inhibition lessens HOSCC proliferation, combats drug resistance and abates initiation of the invasive/metastatic response of HOSCC cell lines is of clinical value. Of course, animal bases *in vivo* studies are required to confirm the applicability of such combination therapy. Nevertheless, based on the results of this study we strongly believe a therapeutic strategy combining drugs targeting the VEGFR signalling pathway and the PI3K/PKB signalling pathway is a promising option in the treatment of human oesophageal squamous cell carcinoma.

References

American Cancer Society (2010). The global economic cost of cancer (Atlanta: American Cancer Society). Available: http://phrma-docs.phrma.org/sites/default/files/pdf/08-17-2010_economic_impact_study.pdf. [Accessed 23 Jan. 2015].

Aurello, P., D'Angelo, F., Nigri, G., Bellagamba, R., Cicchini, C., Ruzzetti, R., and Ramacciato, G. (2006). Comparison between site N-category and number N-category for nodal staging in carcinoma of the gastroesophageal junction: our experience and literature review. Am. Surg. *72*, 118–123.

Bachelder, R.E., Crago, A., Chung, J., Wendt, M.A., Shaw, L.M., Robinson, G., and Mercurio, A.M. (2001). Vascular endothelial growth factor is an autocrine survival factor for neuropilin-expressing breast carcinoma cells. Cancer Res. *61*, 5736–5740.

Bachelder, R.E., Wendt, M.A., and Mercurio, A.M. (2002). Vascular endothelial growth factor promotes breast carcinoma invasion in an autocrine manner by regulating the chemokine receptor CXCR4. Cancer Res. *62*, 7203–7206.

Ban, K.C., Singh, H., Krishnan, R., and Seow, H.F. (2003). GSK-3beta phosphorylation and alteration of beta-catenin in hepatocellular carcinoma. Cancer Lett. *199*, 201–208.

Batchelor, T.T., Sorensen, A.G., di Tomaso, E., Zhang, W.-T., Duda, D.G., Cohen, K.S., Kozak, K.R., Cahill, D.P., Chen, P.-J., Zhu, M., et al. (2007). AZD2171, a Pan-VEGF Receptor Tyrosine Kinase Inhibitor, Normalizes Tumor Vasculature and Alleviates Edema in Glioblastoma Patients. Cancer Cell *11*, 83–95.

Bates, R.C., Goldsmith, J.D., Bachelder, R.E., Brown, C., Shibuya, M., Oettgen, P., and Mercurio, A.M. (2003). Flt-1-dependent survival characterizes the epithelial-mesenchymal transition of colonic organoids. Curr. Biol. CB *13*, 1721–1727.

Beck, B., Driessens, G., Goossens, S., Youssef, K.K., Kuchnio, A., Caauwe, A., Sotiropoulou, P.A., Loges, S., Lapouge, G., Candi, A., et al. (2011). A vascular niche and a VEGF–Nrp1 loop regulate the initiation and stemness of skin tumours. Nature *478*, 399–403.

Bellacosa, A., De Feo, D., Godwin, A.K., Bell, D.W., Cheng, J.Q., Altomare, D.A., Wan, M., Dubeau, L., Scambia, G., Masciullo, V., et al. (1995). Molecular alterations of theAKT2 oncogene in ovarian and breast carcinomas. Int. J. Cancer *64*, 280–285.

Bergers, G., and Benjamin, L.E. (2003). Angiogenesis: Tumorigenesis and the angiogenic switch. Nat. Rev. Cancer *3*, 401–410.

Bergers, G., and Hanahan, D. (2008). Modes of resistance to anti-angiogenic therapy. Nat. Rev. Cancer *8*, 592–603.

Beurel, E., Kornprobst, M., Blivet-Van Eggelpoël, M.-J., Ruiz-Ruiz, C., Cadoret, A., Capeau, J., and Desbois-Mouthon, C. (2004). GSK-3β inhibition by lithium confers resistance to chemotherapy-induced apoptosis through the repression of CD95 (Fas/APO-1) expression. Exp. Cell Res. *300*, 354–364.

Beurel, E., Kornprobst, M., Blivet-Van Eggelpoël, M.-J., Cadoret, A., Capeau, J., and Desbois-Mouthon, C. (2005). GSK-3beta reactivation with LY294002 sensitizes hepatoma cells to chemotherapy-induced apoptosis. Int. J. Oncol. *27*, 215–222.

Bey, E., Alexander, J., Whitcutt, J.M., Hunt, J.A., and Gear, J.H.S. (1976). Carcinoma of the esophagus in africans: Establishment of a continuously growing cell line from a tumor specimen. In Vitro *12*, 107–114.

Bhattacharya, R., Ye, X.C., Wang, R., Ling, X., McManus, M., Fan, F., Boulbes, D., and Ellis, L.M. (2016). Intracrine VEGF Signaling Mediates the Activity of Pro-survival Pathways in Human Colorectal Cancer Cells. Cancer Res. *76 (10)*, 3014-24.

Bhattacharya, R., Fan, F., Wang, R., Ye, X, Xia, L., Boulbes, D., and Ellis, L.M. (2017). Intracrine VEGF signalling mediates colorectal cancer cell migration and invasion. Br. J. Cancer *117(6)*, 848-855.

Bianchi, M., De Lucchini, S., Marin, O., Turner, D.L., Hanks, S.K., and Villa-Moruzzi, E. (2005). Regulation of FAK Ser-722 phosphorylation and kinase activity by GSK3 and PP1 during cell spreading and migration. Biochem. J. *391*, 359–370.

Blot, W.J. (1994). Esophageal cancer trends and risk factors. Semin. Oncol. *21*, 403–410.

Blume-Jensen, P., and Hunter, T. (2001). Oncogenic kinase signalling. Nature *411*, 355–365.

Brakebusch, C., and Fässler, R. (2003). The integrin-actin connection, an eternal love affair. EMBO J. *22*, 2324–2333.

Bramhall, S., Noack, N., Wu, M., and Loewenberg, J.R. (1969). A simple colorimetric method for determination of protein. Anal. Biochem. *31*, 146–148.

Burris, H., and Rocha-Lima, C. (2008). New Therapeutic Directions for Advanced Pancreatic Cancer: Targeting the Epidermal Growth Factor and Vascular Endothelial Growth Factor Pathways. The Oncologist *13*, 289–298.

Cance, W.G., Harris, J.E., Iacocca, M.V., Roche, E., Yang, X., Chang, J., Simkins, S., and Xu, L. (2000). Immunohistochemical analyses of focal adhesion kinase expression in benign and malignant human breast and colon tissues: correlation with preinvasive and invasive phenotypes. Clin. Cancer Res. Off. J. Am. Assoc. Cancer Res. *6*, 2417–2423.

Cao, Y., E, G., Wang, E., Pal, K., Dutta, S.K., Bar-Sagi, D., and Mukhopadhyay, D. (2012). VEGF exerts an angiogenesis-independent function in cancer cells to promote their malignant progression. Cancer Res. *72*, 3912–3918.

Carpten, J.D., Faber, A.L., Horn, C., Donoho, G.P., Briggs, S.L., Robbins, C.M., Hostetter, G., Boguslawski, S., Moses, T.Y., Savage, S., et al. (2007). A transforming mutation in the pleckstrin homology domain of AKT1 in cancer. Nature *448*, 439–444.

Carrillo de Santa Pau, E., Arias, F.C., Caso Peláez, E., Muñoz Molina, G.M., Sánchez Hernández, I., Muguruza Trueba, I., Moreno Balsalobre, R., Sacristán López, S., Gómez Pinillos, A., and del Val Toledo Lobo, M. (2009). Prognostic significance of the expression of vascular endothelial growth factors A, B, C, and D and their receptors R1, R2, and R3 in patients with nonsmall cell lung cancer. Cancer *115*, 1701–1712.

Cascio, S., D'Andrea, A., Ferla, R., Surmacz, E., Gulotta, E., Amodeo, V., Bazan, V., Gebbia, N., and Russo, A. (2010). miR-20b modulates VEGF expression by targeting HIF-1α and STAT3 in MCF-7 breast cancer cells. J. Cell. Physiol. n/a – n/a.

Chan, K.T., Cortesio, C.L., and Huttenlocher, A. (2009). FAK alters invadopodia and focal adhesion composition and dynamics to regulate breast cancer invasion. J. Cell Biol. *185*, 357–370.

Chen, H.C., and Guan, J.L. (1994). Association of focal adhesion kinase with its potential substrate phosphatidylinositol 3-kinase. Proc. Natl. Acad. Sci. U. S. A. *91*, 10148–10152.

Cheng, J.Q., Ruggeri, B., Klein, W.M., Sonoda, G., Altomare, D.A., Watson, D.K., and Testa, J.R. (1996). Amplification of AKT2 in human pancreatic cells and inhibition of AKT2 expression and tumorigenicity by antisense RNA. Proc. Natl. Acad. Sci. U. S. A. *93*, 3636–3641.

Chin, Y.R., and Toker, A. (2009). Function of Akt/PKB signaling to cell motility, invasion and the tumor stroma in cancer. Cell. Signal. *21*, 470–476.

Chodniewicz, D., and Klemke, R.L. (2004). Regulation of integrin-mediated cellular responses through assembly of a CAS/Crk scaffold. Biochim. Biophys. Acta *1692*, 63–76.

Choi, U.-J., Jee, B.-K., Lim, Y., and Lee, K.-H. (2009). KAI1/CD82 decreases Rac1 expression and cell proliferation through PI3K/Akt/mTOR pathway in H1299 lung carcinoma cells. Cell Biochem. Funct. *27*, 40–47.

Cohen, P., and Frame, S. (2001). The renaissance of GSK3. Nat. Rev. Mol. Cell Biol. *2*, 769–776.

Cross, D.A.E., Alessi, D.R., Cohen, P., Andjelkovich, M., and Hemmings, B.A. (1995). Inhibition of glycogen synthase kinase-3 by insulin mediated by protein kinase B. Nature *378*, 785–789.

Decaussin, M., Sartelet, H., Robert, C., Moro, D., Claraz, C., Brambilla, C., and Brambilla, E. (1999). Expression of vascular endothelial growth factor (VEGF) and its two receptors (VEGF-R1-Flt1 and VEGF-R2-Flk1/KDR) in non-small cell lung carcinomas (NSCLCs): correlation with angiogenesis and survival. J. Pathol. *188*, 369–377.

De Jong, J.S., van Diest, P.J., van der Valk, P., and Baak, J.P.A. (1998). Expression of growth factors, growth inhibiting factors, and their receptors in invasive breast cancer. I: An inventory in search of autocrine and paracrine loops. J. Pathol. *184*, 44–52.

Driessens, G., Beck, B., Caauwe, A., Simons, B.D., and Blanpain, C. (2012). Defining the mode of tumour growth by clonal analysis. Nature *488*, 527–530.

Du Plessis, L., Dietzsch, E., Van Gele, M., Van Roy, N., Van Helden, P., Parker, M.I., Mugwanya, D.K., De Groot, M., Marx, M.P., Kotze, M.J., et al. (1999). Mapping of novel regions of DNA gain and loss by comparative genomic hybridization in esophageal carcinoma in the Black and Colored populations of South Africa. Cancer Res. *59*, 1877–1883.

Ellis, L.M., and Hicklin, D.J. (2008a). VEGF-targeted therapy: mechanisms of anti-tumour activity. Nat. Rev. Cancer *8*, 579–591.

Ellis, L.M., and Hicklin, D.J. (2008b). Pathways Mediating Resistance to Vascular Endothelial Growth Factor-Targeted Therapy. Clin. Cancer Res. *14*, 6371–6375.

Enomoto, A., Murakami, H., Asai, N., Morone, N., Watanabe, T., Kawai, K., Murakumo, Y., Usukura, J., Kaibuchi, K., and Takahashi, M. (2005). Akt/PKB regulates actin organization and cell motility via Girdin/APE. Dev. Cell *9*, 389–402.

Etienne-Manneville, S., and Hall, A. (2003). Cdc42 regulates GSK-3beta and adenomatous polyposis coli to control cell polarity. Nature *421*, 753–756.

Ferlay, J., Soerjomataram, I., Ervik, M., Dikshit, R., Eser, S., Mathers, C., Rebelo, M., Parkin, D.M., Forman, D., and Bray, F. (2013). GLOBOCAN 2012 v1.0, Cancer Incidence and Mortality Worldwide: IARC CancerBase No. 11 [Internet] (Lyon, France: International Agency for Research on Cancer).

Fidler, I.J. (2003). The pathogenesis of cancer metastasis: the "seed and soil" hypothesis revisited. Nat. Rev. Cancer *3*, 453–458.

Folkman, J. (1990). What Is the Evidence That Tumors Are Angiogenesis Dependent? J. Natl. Cancer Inst. *82*, 4–7.

Force, T., and Woodgett, J.R. (2009). Unique and Overlapping Functions of GSK-3 Isoforms in Cell Differentiation and Proliferation and Cardiovascular Development. J. Biol. Chem. *284*, 9643–9647.

Friedl, P., and Wolf, K. (2003). Tumour-cell invasion and migration: diversity and escape mechanisms. Nat. Rev. Cancer *3*, 362–374.

Gabarra-Niecko, V., Schaller, M.D., and Dunty, J.M. (2003). FAK regulates biological processes important for the pathogenesis of cancer. Cancer Metastasis Rev. *22*, 359–374.

Ganguly, K.K., Pal, S., Moulik, S., and Chatterjee, A. (2013). Integrins and metastasis. Cell Adhes. Migr. *7*, 251–261.

Geretti, E., Shimizu, A., and Klagsbrun, M. (2008). Neuropilin structure governs VEGF and semaphorin binding and regulates angiogenesis. Angiogenesis *11*, 31–39.

Ghosh, S., Sullivan, C.A.W., Zerkowski, M.P., Molinaro, A.M., Rimm, D.L., Camp, R.L., and Chung, G.G. (2008). High levels of vascular endothelial growth factor and its receptors (VEGFR-1, VEGFR-2, neuropilin-1) are associated with worse outcome in breast cancer. Hum. Pathol. *39*, 1835–1843.

Giatromanolaki, A., Koukourakis, M.I., Turley, H., Sivridis, E., Harris, A.L., and Gatter, K.C. (2006). Phosphorylated KDR expression in endometrial cancer cells relates to HIF1α/VEGF pathway and unfavourable prognosis. Mod. Pathol. *19*, 701–707.

Giatromanolaki, A., Koukourakis, M.I., Sivridis, E., Chlouverakis, G., Vourvouhaki, E., Turley, H., Harris, A.L., Gatter, K.C., and for the "Tumour and Angiogenesis Research

Group" (2007). Activated Vegfr2/kdr Pathway In Tumour Cells And Tumour Associated Vessels Of Colorectal Cancer. Eur. J. Clin. Invest. *37*, 878–886.

Goel, H.L., and Mercurio, A.M. (2013). VEGF targets the tumour cell. Nat. Rev. Cancer *13*, 871–882.

Goel, H.L., Pursell, B., Chang, C., Shaw, L.M., Mao, J., Simin, K., Kumar, P., Kooi, C.W.V., Shultz, L.D., Greiner, D.L., et al. (2013). GLI1 regulates a novel neuropilin-2/α6β1 integrin based autocrine pathway that contributes to breast cancer initiation: NRP2 in the initiation of breast tumours. EMBO Mol. Med. *5*, 488–508.

Gong, Y., and Zhang, Z. (2005). Alternative signaling pathways: When, where and why? FEBS Lett. *579*, 5265–5274.

Goto, H., Kawano, K., Kobayashi, I., Sakai, H., and Yanagisawa, S. (2002). Expression of cyclin D1 and GSK-3beta and their predictive value of prognosis in squamous cell carcinomas of the tongue. Oral Oncol. *38*, 549–556.

Grille, S.J., Bellacosa, A., Upson, J., Klein-Szanto, A.J., Van Roy, F., Lee-Kwon, W., Donowitz, M., Tsichlis, P.N., and Larue, L. (2003). The protein kinase Akt induces epithelial mesenchymal transition and promotes enhanced motility and invasiveness of squamous cell carcinoma lines. Cancer Res. *63*, 2172–2178.

Grimes, C.A., and Jope, R.S. (2001). The multifaceted roles of glycogen synthase kinase 3beta in cellular signaling. Prog. Neurobiol. *65*, 391–426.

Gupta, G.P., and Massagué, J. (2006). Cancer Metastasis: Building a Framework. Cell *127*, 679–695.

Hanahan, D., and Folkman, J. (1996). Patterns and Emerging Mechanisms of the Angiogenic Switch during Tumorigenesis. Cell *86*, 353–364.

Hanahan, D., and Weinberg, R.A. (2011). Hallmarks of Cancer: The Next Generation. Cell *144*, 646–674.

Harari, D., and Yarden, Y. (2000). Molecular mechanisms underlying ErbB2/HER2 action in breast cancer. Oncogene *19*, 6102–6114.

Hathout, Y. (2007). Approaches to the study of the cell secretome. Expert Rev. Proteomics *4*, 239–248.

Hauck, C.R., Hsia, D.A., Ilic, D., and Schlaepfer, D.D. (2002). v-Src SH3-enhanced Interaction with Focal Adhesion Kinase at 1 Integrin-containing Invadopodia Promotes Cell Invasion. J. Biol. Chem. *277*, 12487–12490.

Hood, J.D., and Cheresh, D.A. (2002). Role of Integrins in Cell Invasion and Migration. Nat. Rev. Cancer *2*, 91–100.

Houck, K.A., Ferrara, N., Winer, J., Cachianes, G., Li, B., and Leung, D.W. (1991). The Vascular Endothelial Growth Factor Family: Identification of a Fourth Molecular Species and Characterization of Alternative Splicing of RNA. Mol. Endocrinol. *5*, 1806–1814.

Hsia, D.A., Mitra, S.K., Hauck, C.R., Streblow, D.N., Nelson, J.A., Ilic, D., Huang, S., Li, E., Nemerow, G.R., Leng, J., et al. (2003). Differential regulation of cell motility and invasion by FAK. J. Cell Biol. *160*, 753–767.

Hsieh, M.-J., Tsai, T.-L., Hsieh, Y.-S., Wang, C.-J., and Chiou, H.-L. (2013). Dioscin-induced autophagy mitigates cell apoptosis through modulation of PI3K/Akt and ERK and JNK signaling pathways in human lung cancer cell lines. Arch. Toxicol. *87*, 1927–1937.

Huang, J., Zhang, X., Tang, Q., Zhang, F., Li, Y., Feng, Z., and Zhu, J. (2011). Prognostic significance and potential therapeutic target of VEGFR2 in hepatocellular carcinoma. J. Clin. Pathol. *64*, 343–348.

Inoki, K., Li, Y., Zhu, T., Wu, J., and Guan, K.-L. (2002). TSC2 is phosphorylated and inhibited by Akt and suppresses mTOR signalling. Nat. Cell Biol. *4*, 648–657.

Inoue, K., Ozeki, Y., Suganuma, T., Sugiura, Y., and Tanaka, S. (1997). Vascular endothelial growth factor expression in primary esophageal squamous cell carcinoma. Cancer *79*, 206–213.

Jain, R.K., Duda, D.G., Clark, J.W., and Loeffler, J.S. (2006). Lessons from phase III clinical trials on anti-VEGF therapy for cancer. Nat. Clin. Pract. Oncol. *3*, 24–40.

Ji, Y., Chen, S., Li, K., Xiao, X., Xu, T., and Zheng, S. (2014). Upregulated autocrine vascular endothelial growth factor (VEGF)/VEGF receptor-2 loop prevents apoptosis in haemangioma-derived endothelial cells. Br. J. Dermatol. *170*, 78–86.

Jope, R.S., and Johnson, G.V.W. (2004). The glamour and gloom of glycogen synthase kinase-3. Trends Biochem. Sci. *29*, 95–102.

Jope, R.S., Yuskaitis, C.J., and Beurel, E. (2007). Glycogen Synthase Kinase-3 (GSK3): Inflammation, Diseases, and Therapeutics. Neurochem. Res. *32*, 577–595.

Kandasamy, K., and Srivastava, R.K. (2002). Role of the phosphatidylinositol 3'-kinase/PTEN/Akt kinase pathway in tumor necrosis factor-related apoptosis-inducing ligand-induced apoptosis in non-small cell lung cancer cells. Cancer Res. *62*, 4929–4937.

Karihaloo, A., Karumanchi, S.A., Cantley, W.L., Venkatesha, S., Cantley, L.G., and Kale, S. (2005). Vascular Endothelial Growth Factor Induces Branching Morphogenesis/ Tubulogenesis in Renal Epithelial Cells in a Neuropilin-Dependent Fashion. Mol. Cell. Biol. *25*, 7441–7448.

Karkkainen, M.J., and Petrova, T.V. (2000). Vascular endothelial growth factor receptors in the regulation of angiogenesis and lymphangiogenesis. Oncogene *19*, 5598–5605.

Keyt, B.A., Berleau, L.T., Nguyen, H.V., Chen, H., Heinsohn, H., Vandlen, R., and Ferrara, N. (1996). The carboxyl-terminal domain (111-165) of vascular endothelial growth factor is critical for its mitogenic potency. J. Biol. Chem. *271*, 7788–7795.

Kim, D., Kim, S., Koh, H., Yoon, S.O., Chung, A.S., Cho, K.S., and Chung, J. (2001). Akt/PKB promotes cancer cell invasion via increased motility and metalloproteinase production. FASEB J. Off. Publ. Fed. Am. Soc. Exp. Biol. *15*, 1953–1962.

Klimstra, D.S. (1994). Pathologic prognostic factors in esophageal carcinoma. Semin. Oncol. *21*, 425–430.

Koch, S., and Claesson-Welsh, L. (2012). Signal Transduction by Vascular Endothelial Growth Factor Receptors. Cold Spring Harb. Perspect. Med. *2*, a006502–a006502.

Kowanetz, M. (2006). Vascular Endothelial Growth Factor Signaling Pathways: Therapeutic Perspective. Clin. Cancer Res. *12*, 5018–5022.

Kristensen, T.B., Knutsson, M.L.T., Wehland, M., Laursen, B.E., Grimm, D., Warnke, E., and Magnusson, N.E. (2014). Anti-vascular endothelial growth factor therapy in breast cancer. Int. J. Mol. Sci. *15*, 23024–23041.

Kyzas, P.A. (2005). Prognostic Significance of Vascular Endothelial Growth Factor Immunohistochemical Expression in Head and Neck Squamous Cell Carcinoma: A Meta-Analysis. Clin. Cancer Res. *11*, 1434–1440.

Lahlou, H., Sanguin-Gendreau, V., Zuo, D., Cardiff, R.D., McLean, G.W., Frame, M.C., and Muller, W.J. (2007). Mammary epithelial-specific disruption of the focal adhesion kinase blocks mammary tumor progression. Proc. Natl. Acad. Sci. U. S. A. *104*, 20302–20307.

Lantuéjoul, S., Constantin, B., Drabkin, H., Brambilla, C., Roche, J., and Brambilla, E. (2003). Expression of VEGF, semaphorin SEMA3F, and their common receptors neuropilins NP1 and NP2 in preinvasive bronchial lesions, lung tumours, and cell lines. J. Pathol. *200*, 336–347.

Lark, A.L., Livasy, C.A., Dressler, L., Moore, D.T., Millikan, R.C., Geradts, J., Iacocca, M., Cowan, D., Little, D., Craven, R.J., et al. (2005). High focal adhesion kinase expression in invasive breast carcinomas is associated with an aggressive phenotype. Mod. Pathol. Off. J. U. S. Can. Acad. Pathol. Inc *18*, 1289–1294.

Lauffenburger, D.A., and Horwitz, A.F. (1996). Cell Migration: A Physically Integrated Molecular Process. Cell *84*, 359–369.

Lee, J., Ku, T., Yu, H., Chong, K., Ryu, S.-W., Choi, K., and Choi, C. (2012). Blockade of VEGF-A suppresses tumor growth via inhibition of autocrine signaling through FAK and AKT. Cancer Lett. *318*, 221–225.

Liang, C.-C., Park, A.Y., and Guan, J.-L. (2007). In vitro scratch assay: a convenient and inexpensive method for analysis of cell migration in vitro. Nat. Protoc. *2*, 329–333.

Lichtenberger, B.M., Tan, P.K., Niederleithner, H., Ferrara, N., Petzelbauer, P., and Sibilia, M. (2010). Autocrine VEGF Signaling Synergizes with EGFR in Tumor Cells to Promote Epithelial Cancer Development. Cell *140*, 268–279.

Liu, P., Zhou, J., Zhu, H., Xie, L., Wang, F., Liu, B., Shen, W., Ye, W., Xiang, B., Zhu, X., et al. (2011). VEGF-C promotes the development of esophageal cancer via regulating CNTN-1 expression. Cytokine *55*, 8–17.

Logue, J.S., and Morrison, D.K. (2012). Complexity in the signaling network: insights from the use of targeted inhibitors in cancer therapy. Genes Dev. *26*, 641–650.

Ma, Y.-Y., Wei, S.-J., Lin, Y.-C., Lung, J.-C., Chang, T.-C., Whang-Peng, J., Liu, J.M., Yang, D.-M., Yang, W.K., and Shen, C.-Y. (2000). PIK3CA as an oncogene in cervical cancer. Oncogene *19*, 2739–2744.

Mak, P., Leav, I., Pursell, B., Bae, D., Yang, X., Taglienti, C.A., Gouvin, L.M., Sharma, V.M., and Mercurio, A.M. (2010). ERβ Impedes Prostate Cancer EMT by Destabilizing HIF-1α and Inhibiting VEGF-Mediated Snail Nuclear Localization: Implications for Gleason Grading. Cancer Cell *17*, 319–332.

Mandard, A.-M., Hainaut, P., and Hollstein, M. (2000). Genetic steps in the development of squamous cell carcinoma of the esophagus. Mutat. Res. Mutat. Res. *462*, 335–342.

Meier, R., and Hemmings, B.A. (1999). Regulation of Protein Kinase B. J. Recept. Signal Transduct. *19*, 121–128.

Mimeault, M., and Batra, S.K. (2013). Hypoxia-inducing factors as master regulators of stemness properties and altered metabolism of cancer- and metastasis-initiating cells. J. Cell. Mol. Med. *17*, 30–54.

Mitra, S.K., Hanson, D.A., and Schlaepfer, D.D. (2005). Focal adhesion kinase: in command and control of cell motility. Nat. Rev. Mol. Cell Biol. *6*, 56–68.

Mulholland, D.J., Dedhar, S., Wu, H., and Nelson, C.C. (2006). PTEN and GSK3beta: key regulators of progression to androgen-independent prostate cancer. Oncogene *25*, 329–337.

Mylona, E., Alexandrou, P., Giannopoulou, I., Liapis, G., Sofia, M., Keramopoulos, A., and Nakopoulou, L. (2007). The prognostic value of vascular endothelial growth factors (VEGFs)-A and -B and their receptor, VEGFR-1, in invasive breast carcinoma. Gynecol. Oncol. *104*, 557–563.

Nakopoulou, L., Stefanaki, K., Panayotopoulou, E., Giannopoulou, I., Athanassiadou, P., Gakiopoulou-Givalou, H., and Louvrou, A. (2002). Expression of the vascular endothelial growth factor receptor-2/Flk-1 in breast carcinomas: Correlation with proliferation. Hum. Pathol. *33*, 863–870.

Owens, L.V., Xu, L., Craven, R.J., Dent, G.A., Weiner, T.M., Kornberg, L., Liu, E.T., and Cance, W.G. (1995). Overexpression of the focal adhesion kinase (p125FAK) in invasive human tumors. Cancer Res. *55*, 2752–2755.

Ozdemir, F., Akdogan, R., Aydin, F., Reis, A., Kavgaci, H., Gul, S., and Akdogan, E. (2006). The effects of VEGF and VEGFR-2 on survival in patients with gastric cancer. J. Exp. Clin. Cancer Res. CR *25*, 83–88.

Palazzo, A.F., Eng, C.H., Schlaepfer, D.D., Marcantonio, E.E., and Gundersen, G.G. (2004). Localized stabilization of microtubules by integrin- and FAK-facilitated Rho signaling. Science *303*, 836–839.

Palecek, S.P., Loftus, J.C., Ginsberg, M.H., Lauffenburger, D.A., Horwitz, A.F., and others (1997). Integrin-ligand binding properties govern cell migration speed through cell-substratum adhesiveness. Nature *385*, 537–540.

Park, B.K., Zeng, X., and Glazer, R.I. (2001). Akt1 induces extracellular matrix invasion and matrix metalloproteinase-2 activity in mouse mammary epithelial cells. Cancer Res. *61*, 7647–7653.

Polakis, P. (1999). The oncogenic activation of beta-catenin. Curr. Opin. Genet. Dev. *9*, 15–21.

Popov, I. (2005). Signal transduction inhibition. Arch. Oncol. *13*, 48–50.

Price, D.J., Miralem, T., Jiang, S., Steinberg, R., and Avraham, H. (2001). Role of vascular endothelial growth factor in the stimulation of cellular invasion and signaling of breast cancer cells. Cell Growth Differ. Mol. Biol. J. Am. Assoc. Cancer Res. *12*, 129–135.

Prud'homme, G.J., and Glinka, Y. (2012). Neuropilins are multifunctional coreceptors involved in tumor initiation, growth, metastasis and immunity. Oncotarget *3*, 921.

Rapisarda, A., and Melillo, G. (2012). Role of the VEGF / VEGFR Axis in Cancer Biology and Therapy (Elsevier Inc.).

Riedel, F., Götte, K., Schwalb, J., Wirtz, H., Bergler, W., and Hörmann, K. (2000). Serum levels of vascular endothelial growth factor in patients with head and neck cancer. Eur. Arch. Otorhinolaryngol. *257*, 332–336.

Rodríguez-Antona, C., Pallares, J., Montero-Conde, C., Inglada-Pérez, L., Castelblanco, E., Landa, I., Leskelä, S., Leandro-García, L.J., López-Jiménez, E., Letón, R., et al. (2010). Overexpression and activation of EGFR and VEGFR2 in medullary thyroid carcinomas is related to metastasis. Endocr. Relat. Cancer *17*, 7–16.

Rousseau, S., Houle, F., Kotanides, H., Witte, L., Waltenberger, J., Landry, J., and Huot, J. (2000). Vascular endothelial growth factor (VEGF)-driven actin-based motility is mediated by VEGFR2 and requires concerted activation of stress-activated protein kinase 2 (SAPK2/p38) and geldanamycin-sensitive phosphorylation of focal adhesion kinase. J. Biol. Chem. *275*, 10661–10672.

Samuel, S., Fan, F., Dang, L.H., Xia, L., Gaur, P., and Ellis, L.M. (2010). Intracrine vascular endothelial growth factor signaling in survival and chemoresistance of human colorectal cancer cells. Oncogene *30*, 1205–1212.

Samuel, S., Fan, F., Dang, L.H., Xia, L., Gaur, P., and Ellis, L.M. (2011). Intracrine vascular endothelial growth factor signaling in survival and chemoresistance of human colorectal cancer cells. Oncogene *30*, 1205–1212.

Schaller, M.D., Hildebrand, J.D., Shannon, J.D., Fox, J.W., Vines, R.R., and Parsons, J.T. (1994). Autophosphorylation of the focal adhesion kinase, pp125FAK, directs SH2-dependent binding of pp60src. Mol. Cell. Biol. *14*, 1680–1688.

Schlaepfer, D.D., Mitra, S.K., and Ilic, D. (2004). Control of motile and invasive cell phenotypes by focal adhesion kinase. Biochim. Biophys. Acta *1692*, 77–102.

Schottenfeld, D. (1984). Epidemiology of cancer of the esophagus. Semin. Oncol. *11*, 92–100.

Sefton, B.M. (1998). Overview of Protein Phosphorylation. Curr. Protoc. Cell Biol. *00*, 14.1.1–14.1.3.

Senger, D.R. (2010). Vascular endothelial growth factor: much more than an angiogenesis factor. Mol. Biol. Cell *21*, 377–379.

Seto, T., Higashiyama, M., Funai, H., Imamura, F., Uematsu, K., Seki, N., Eguchi, K., Yamanaka, T., and Ichinose, Y. (2006). Prognostic value of expression of vascular endothelial growth factor and its flt-1 and KDR receptors in stage I non-small-cell lung cancer. Lung Cancer *53*, 91–96.

Sever, R., and Brugge, J.S. (2015). Signal Transduction in Cancer. Cold Spring Harb. Perspect. Med. *5*, a006098–a006098.

Shaw, N. (2011). PI3K in human oesophageal squamous carcinoma cells : a critical modulator in the PKB signalling pathway. Doctoral Thesis. University of the Witwatersrand.

Shayesteh, L., Lu, Y., Kuo, W.-L., Baldocchi, R., Godfrey, T., Collins, C., Pinkel, D., Powell, B., Mills, G.B., and Gray, J.W. (1999). PIK3CA is implicated as an oncogene in ovarian cancer. Nat. Genet. *21*, 99–102.

Shin, I., Yakes, F.M., Rojo, F., Shin, N.-Y., Bakin, A.V., Baselga, J., and Arteaga, C.L. (2002). PKB/Akt mediates cell-cycle progression by phosphorylation of p27Kip1 at threonine 157 and modulation of its cellular localization. Nat. Med. *8*, 1145–1152.

Shojaei, F., and Ferrara, N. (2008). Role of the microenvironment in tumor growth and in refractoriness/resistance to anti-angiogenic therapies. Drug Resist. Updat. *11*, 219–230.

Sieg, D.J., Hauck, C.R., Ilic, D., Klingbeil, C.K., Schaefer, E., Damsky, C.H., and Schlaepfer, D.D. (2000). FAK integrates growth-factor and integrin signals to promote cell migration. Nat. Cell Biol. *2*, 249–256.

Simpson, L., and Parsons, R. (2001). PTEN: Life as a Tumor Suppressor. Exp. Cell Res. *264*, 29–41.

Soker, S., Takashima, S., Miao, H.Q., Neufeld, G., and Klagsbrun, M. (1998). Neuropilin-1 Is Expressed by Endothelial and Tumor Cells as an Isoform-Specific Receptor for Vascular Endothelial Growth Factor. Cell *92*, 735–745.

Sons, H.U. (1987). Etiologic and epidemiologic factors of carcinoma of the esophagus. Surg. Gynecol. Obstet. *165*, 183–190.

Spannuth, W.A., Nick, A.M., Jennings, N.B., Armaiz-Pena, G.N., Mangala, L.S., Danes, C.G., Lin, Y.G., Merritt, W.M., Thaker, P.H., Kamat, A.A., et al. (2009). Functional significance of VEGFR-2 on ovarian cancer cells. Int. J. Cancer *124*, 1045–1053.

Staal, S.P. (1987). Molecular cloning of the akt oncogene and its human homologues AKT1 and AKT2: amplification of AKT1 in a primary human gastric adenocarcinoma. Proc. Natl. Acad. Sci. U. S. A. *84*, 5034–5037.

Stewart, B.W., and Wild, C.P. (2014). World cancer report 2014.

Stoner, G.D., and Gupta, A. (2001). Etiology and chemoprevention of esophageal squamous cell carcinoma. Carcinogenesis *22*, 1737–1746.

Strizzi, L., Catalano, A., Vianale, G., Orecchia, S., Casalini, A., Tassi, G., Puntoni, R., Mutti, L., and Procopio, A. (2001). Vascular endothelial growth factor is an autocrine growth factor in human malignant mesothelioma. J. Pathol. *193*, 468–475.

Su, J.-L., Yang, P.-C., Shih, J.-Y., Yang, C.-Y., Wei, L.-H., Hsieh, C.-Y., Chou, C.-H., Jeng, Y.-M., Wang, M.-Y., and Chang, K.-J. (2006). The VEGF-C/Flt-4 axis promotes invasion and metastasis of cancer cells. Cancer Cell *9*, 209–223.

Sun, C., and Bernards, R. (2014). Feedback and redundancy in receptor tyrosine kinase signaling: relevance to cancer therapies. Trends Biochem. Sci. *39*, 465–474.

Sun, M., Wang, G., Paciga, J.E., Feldman, R.I., Yuan, Z.-Q., Ma, X.-L., Shelley, S.A., Jove, R., Tsichlis, P.N., Nicosia, S.V., et al. (2001). AKT1/PKBα Kinase Is Frequently Elevated in Human Cancers and Its Constitutive Activation Is Required for Oncogenic Transformation in NIH3T3 Cells. Am. J. Pathol. *159*, 431–437.

Takahashi, K., Sawasaki, Y., Hata, J.-I., Mukai, K., and Goto, T. (1990). Spontaneous transformation and immortalization of human endothelial cells. In Vitro Cell. Dev. Biol. *26*, 265–274.

Takahashi, Y., Kitadai, Y., Bucana, C.D., Cleary, K.R., and Ellis, L.M. (1995). Expression of vascular endothelial growth factor and its receptor, KDR, correlates with vascularity, metastasis, and proliferation of human colon cancer. Cancer Res. *55*, 3964–3968.

Talmadge, J.E., and Fidler, I.J. (2010). AACR Centennial Series: The Biology of Cancer Metastasis: Historical Perspective. Cancer Res. *70*, 5649–5669.

Tanno, S., Tanno, S., Mitsuuchi, Y., Altomare, D.A., Xiao, G.H., and Testa, J.R. (2001). AKT activation up-regulates insulin-like growth factor I receptor expression and promotes invasiveness of human pancreatic cancer cells. Cancer Res. *61*, 589–593.

Turner, C.E. (2000). Paxillin and focal adhesion signalling. Nat. Cell Biol. *2*, E231.

Van Nimwegen, M.J., Verkoeijen, S., van Buren, L., Burg, D., and van de Water, B. (2005). Requirement for focal adhesion kinase in the early phase of mammary adenocarcinoma lung metastasis formation. Cancer Res. *65*, 4698–4706.

Van Zijl, F., Krupitza, G., and Mikulits, W. (2011). Initial steps of metastasis: Cell invasion and endothelial transmigration. Mutat. Res. Mutat. Res. *728*, 23–34.

Vara, J.Á.F., Casado, E., de Castro, J., Cejas, P., Belda-Iniesta, C., and González-Barón, M. (2004). PI3K/Akt signalling pathway and cancer. Cancer Treat. Rev. *30*, 193–204.

Veale, R.B., and Thornley, A.L. (1989). Increased Single Class Low-Affinity Egf Receptors Expressed by Human Esophageal Squamous Carcinoma Cell-Lines. South Afr. J. Sci. *85*, 375–379.

Viatour, P., Dejardin, E., Warnier, M., Lair, F., Claudio, E., Bureau, F., Marine, J.-C., Merville, M.-P., Maurer, U., Green, D., et al. (2004). GSK3-mediated BCL-3 phosphorylation modulates its degradation and its oncogenicity. Mol. Cell *16*, 35–45.

Watcharasit, P., Bijur, G.N., Song, L., Zhu, J., Chen, X., and Jope, R.S. (2003). Glycogen synthase kinase-3beta (GSK3beta) binds to and promotes the actions of p53. J. Biol. Chem. *278*, 48872–48879.

Webb, D.J., Donais, K., Whitmore, L.A., Thomas, S.M., Turner, C.E., Parsons, J.T., and Horwitz, A.F. (2004). FAK-Src signalling through paxillin, ERK and MLCK regulates adhesion disassembly. Nat. Cell Biol. *6*, 154–161.

Wei, S.-C. (2005). Placenta growth factor expression is correlated with survival of patients with colorectal cancer. Gut *54*, 666–672.

Weigand, M., Hantel, P., Kreienberg, R., and Waltenberger, J. (2005). Autocrine vascular endothelial growth factor signalling in breast cancer. Evidence from cell lines and primary breast cancer cultures in vitro. Angiogenesis *8*, 197–204.

Welsh, G.I., and Proud, C.G. (1993). Glycogen synthase kinase-3 is rapidly inactivated in response to insulin and phosphorylates eukaryotic initiation factor eIF-2B. Biochem. J. *294 (Pt 3)*, 625–629.

Wolf, K., and Friedl, P. (2006). Molecular mechanisms of cancer cell invasion and plasticity. Br. J. Dermatol. *154 Suppl 1*, 11–15.

Xia, G., Kumar, S.R., Hawes, D., Cai, J., Hassanieh, L., Groshen, S., Zhu, S., Masood, R., Quinn, D.I., Broek, D., et al. (2006). Expression and Significance of Vascular Endothelial Growth Factor Receptor 2 in Bladder Cancer. J. Urol. *175*, 1245–1252.

Yamaguchi, H., Wyckoff, J., and Condeelis, J. (2005). Cell migration in tumors. Curr. Opin. Cell Biol. *17*, 559–564.

Yang, F., Tang, X., Riquelme, E., Behrens, C., Nilsson, M.B., Giri, U., Varella-Garcia, M., Byers, L.A., Lin, H.Y., Wang, J., et al. (2011). Increased VEGFR-2 Gene Copy Is Associated with Chemoresistance and Shorter Survival in Patients with Non-Small-Cell Lung Carcinoma Who Receive Adjuvant Chemotherapy. Cancer Res. *71*, 5512–5521.

Yano, H., Mazaki, Y., Kurokawa, K., Hanks, S.K., Matsuda, M., and Sabe, H. (2004). Roles played by a subset of integrin signaling molecules in cadherin-based cell-cell adhesion. J. Cell Biol. *166*, 283–295.

Zeng, H., Dvorak, H.F., and Mukhopadhyay, D. (2001). Vascular Permeability Factor (VPF)/Vascular Endothelial Growth Factor (VEGF) Receptor-1 Down-modulates VPF/VEGF Receptor-2-mediated Endothelial Cell Proliferation, but Not Migration, through Phosphatidylinositol 3-Kinase-dependent Pathways. J. Biol. Chem. *276*, 26969–26979.

Zhang, X., Chattopadhyay, A., Ji, Q.S., Owen, J.D., Ruest, P.J., Carpenter, G., and Hanks, S.K. (1999). Focal adhesion kinase promotes phospholipase C-gamma1 activity. Proc. Natl. Acad. Sci. U. S. A. *96*, 9021–9026.

Zhao, Z.-H., Tian, Y., Yang, J.-P., Zhou, J., and Chen, K.-S. (2015). RhoC, vascular endothelial growth factor and microvascular density in esophageal squamous cell carcinoma. World J Gastroenterol *21*, 905–912.

Zhou, B.P., Liao, Y., Xia, W., Spohn, B., Lee, M.-H., and Hung, M.-C. (2001). Cytoplasmic localization of p21Cip1/WAF1 by Akt-induced phosphorylation in HER-2/neu-overexpressing cells. Nat. Cell Biol. *3*, 245–252.

Zhou, B.P., Deng, J., Xia, W., Xu, J., Li, Y.M., Gunduz, M., and Hung, M.-C. (2004). Dual regulation of Snail by GSK-3beta-mediated phosphorylation in control of epithelial-mesenchymal transition. Nat. Cell Biol. *6*, 931–940.

Appendix A

1. DMEM / Hams F12 (3:1) tissue culture media

Dulbecco's Modified Eagle Medium (DMEM) solution:

1.37 %	DMEM
0.37 %	Sodium Bicarbonate
2 %	Penicillin (500 U/ml)/Streptomycin solution (0.5 %)

Make up to final volume with distilled water (dH_2O)

Hams F12 medium solution:

1.07 %	Hams F12 medium
0.118 %	Sodium bicarbonate
2 %	Penicillin (500 U/ml)/Streptomycin solution (0.5 %)

Make up to final volume with dH_2O

Mix DMEM / Hams F12 medium solutions in a 3:1 ratio
Filter sterilise
Store at 4 °C

2. Phosphate buffered saline (PBS) 1x

136.90 mM	Sodium chloride
2.68 mM	Potassium chloride
10.10 mM	Disodium hydrogen phosphate dodecohydrate
1.769 mM	Potassium dihydrogen phosphate

Adjust to a pH of 7.2 - 7.3
Make up to final volume with dH_2O
Autoclave to sterilise
Store at 4 °C

3. Trypsin / Ethylenediaminetetra-acetic acid (EDTA)

Trypsin solution:

0.010 % Trypsin

Make up to final volume with PBS

EDTA solution:

0.004 % EDTA

Make up to final volume with PBS
Mix Trypsin/ EDTA solutions in a 1:1 ratio
Store at 4 °C

4. PMSF (100 mM)

100 mM PMSF

Make up to final volume with methanol
Store at 4 °C
Use at working concentration of 1 mM

5. Sodium Orthovanadate (Na3VO4) (200 mM)

200 mM Na_3VO_4

Adjust pH of dH_2O to approximately 10
Dissolve in Na_3VO_4 dH_2O
If yellow boil for 10 minutes
Cool and check pH (readjust to 10 if necessary)
Re-boil and adjust pH till solution stays clear
Make up to final volume with dH_2O
Store aliquots at -20 °C
Use at working concentration of 10 mM

6. Sodium Fluoride (NaF) (1M)

1 M	NaF

Make up to final volume with dH_2O

Store aliquots at -20 °C

Use at working concentration of 5 mM

7. Laemmli double lysis buffer

125 mM	Tris-HCl pH 6.8
4 %	SDS
20 %	Glycerol
10 %	β-mercaptoethanol

Make up to final volume with dH_2O

Store at 4 °C

8. 7.5 % Trichloroacetic acid

7.5 %	Trichloroacetic acid

Make up to final volume with dH_2O

9. 0.25 % Coomassie Brilliant Blue solution

0.25 %	Coomassie Brilliant Blue G250 powder
50 %	Methanol
10 %	Glacial acetic acid

Make up to final volume with dH_2O

10. Destain solution (Protein Determination)

10 %	Glacial acetic acid
12 %	Methanol

Make up to final volume with dH_2O

11. Elution solution

66 %	Methanol
33 %	dH_2O
1 %	Ammonia

12. SDS overlay

0.2 %	SDS

Make up to final volume with dH_2O

13. Separating gel

10 %	Acrylamide
0.1 %	N,N'-methylenebisacrylamide
375 mM	Tris- HCl pH 8.8
0.2 %	SDS

Make up to final volume with dH_2O

Just prior to use add:

1 mM	Ammonium Persulphate
0.25 %	N,N,N',N'-tetramethylethylenediamine (TEMED)

14. Stacking gel

5 %	Acrylamide
0.1 %	N,N'-methylenebisacrylamide
125 mM	Tris- HCl pH 6.8
0.2 %	SDS

Make up to final volume with dH_2O

Just prior to use add:

1 mM	Ammonium Persulphate
0.25 %	N,N,N',N'-tetramethylethylenediamine (TEMED)

15. Destain solution (SDS-PAGE)

10 %	Acetic acid
10 %	Methanol

Make up to final volume with dH_2O

16. Electrophoresis running buffer

3.74 mM	SDS
25 mM	Tris-HCl pH 8.3
192.5 mM	Glycine

Make up to final volume with dH_2O

17. Transfer buffer

25 mM	Tris-HCl pH 8.3
1.41 %	Glycine
20 %	Methanol

Make up to final volume with dH_2O
Store at 4 °C

18. Tris-buffered saline (TBS)

50.00 mM	Tris- HCl (pH 7.8)
150.00 mM	Sodium Chloride
2.00 mM	Calcium chloride dihydrate

Make up to final volume with dH_2O
Autoclave to sterilise
Store at 4 °C

19. Tris-buffered saline with Tween®20 (TBST)

50.00 mM	Tris- HCl (pH 7.8)
150.00 mM	Sodium Chloride
2.00 mM	Calcium chloride dihydrate
0.10 %	Tween®20

Make up to final volume with dH_2O

Autoclave to sterilise

Store at 4 °C

20. Blocking Buffer

150 mM	NaCl
50 mM	Tris-HCl pH 7.8
2 mM	Calcium chloride dehydrate
0.05 %	Triton X-100

Make up to final volume with dH_2O

Store at 4 °C

21. SuperSignalTM West Pico Chemiluminescent Substrate

From the SuperSignal™ West Pico Chemiluminescent Substrate Kit

50 %	Luminol enhancer solution
50 %	Stable peroxide buffer

Prepare immediately before use

Store in the dark

22. Developer solution

6.4 M	Metol
0.6 M	Anhydrous sodium sulphite
80 mM	Hydroquinone
0.45 mM	Anhydrous sodium carbonate
34 mM	Potassium bromide

Make up to final volume with dH_2O

Store in the dark

23. Fixer solution

0.8 M	Sodium thiosulphate
0.2 M	Sodium metasulphite

Make up to final volume with dH_2O

Store in the dark

24. MTT solution (60 mM)

60 mM MTT

Make up to final volume with PBS

Vortex

Store at 4 °C in the dark

Use at working concentration of 6 mM

25. 4 % Paraformaldehyde solution

4 % Paraformaldehyde

Make up to final volume with PBS

Appendix B

1. Protein concentration determination from standard curve

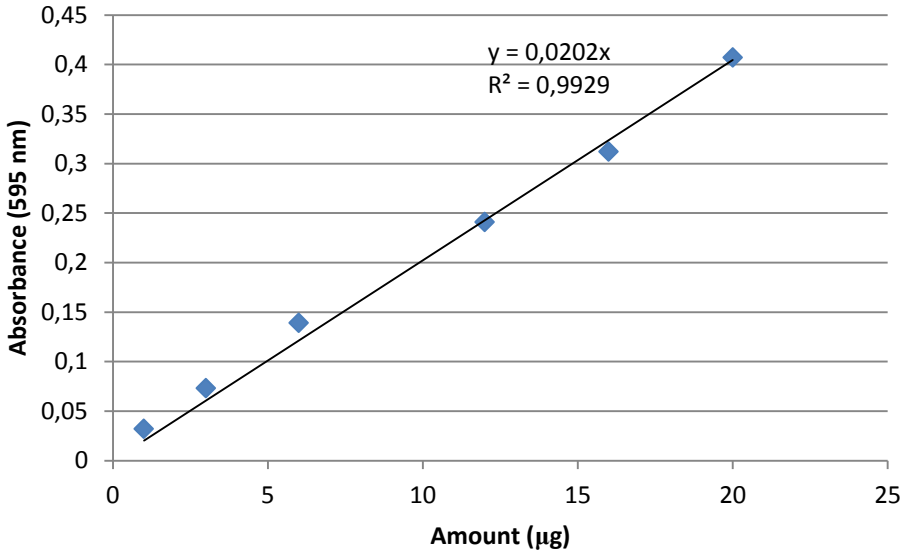

Figure B1: Example of a standard curve for protein concentration determination of cell lysate samples

BSA standards of known varying amounts (1, 3, 6, 12, 16, 20 µg) and their corresponding absorbance (at 595 nm) was used to construct the standard curve. The equation of the curve (y = 0,0202x) was used to calculate the amount of protein and thus protein concentration of cell lysate samples. The R^2 linear regression value was 0.9929 which indicates strong positive linear correlation of the data points.

The equation of the standard curve was used to calculate the amount of protein present in a specified volume of a cell lysate sample from its absorbance value as described in equation 1.

Equation 1: $y = mx$

$$Absorbance = Gradient\ of\ standard\ curve \times Amount\ (\mu g)$$

$$Amount\ (\mu g) = \frac{Absorbance}{Gradient\ of\ standard\ curve}$$

where y is the sample's absorbance (at 595 nm);

m is the gradient of the standard curve;

and x is the amount of protein present in the cell lysate sample.

The amount of protein present in the cell lysate sample was then used to calculate the protein concentration of the sample as described in Equation 2.

Equation 2: $Concentration\ (\mu g/\mu l) = \frac{Amount\ (\mu g)}{Volume\ (\mu l)}$

where volume is the volume of cell lysate sample dotted i.e. 2 µl.

The volume to be loaded into a SDS-PAGE gel was then calculated as described in equation 3.

Equation 3: $Volume\ to\ load\ (\mu l) = \frac{Amount\ to\ load\ (\mu g)}{Concentration\ (\mu g/\mu l)}$

where the amount to be loaded was 40 µg unless stated otherwise.

2. Normalisation of densitometry results

Table B1: Example of densitometry results and normalisation

a)

	CO6	H1299
Replicate 1	12.65	100
Replicate 2	22.52	100
Replicate 3	23.13	100
Replicate 4	30.17	100
Mean	22.12	100

b)

		CO1 control	CO1 PI3K inhibited	CO6	H1299	Ratio (r)
Standard HOSCC culture conditions				22.12	100	
Replicate 1	Original	137.43	91.81	109.94	100	22.12 / 109.94 = 0.2012006549
	% change	-33.19				
	Normalised	137.43 x r = 27.65	91.81 x r = 18.47	109.94 x r = 22.12	100	
	% change	-33.19				
Replicate 2	Original	125.58	64.88	92.67	100	22.12 / 92.67 = 0.2386964498
	% change	-48.33				
	Normalised	125.58 x r = 29.97	64.88 x r = 15.48	92.67 x r = 22.12	100	
	% change	-48.33				
Replicate 3	Original	121.90	51.09	128.47	100	22.12 / 128.47 = 0.1721802756
	% change	-58.08				
	Normalised	121.90 x r = 20.99	51.09 x r = 8.80	128.47 x r = 22.12	100	
	% change	-58.08				

a) Relative abundance of pPKB in untreated WHCO6 and H1299 cell lines under standard HOSCC culture conditions. The relative protein abundance was always measured relative to the positive control untreated H1299 cell lysate (set at 100), thus allowing comparison of the relative expression levels of a particular protein across multiple blots. b) In order to give a more reliable estimate of the relative protein abundance of control and treatment samples for statistical analysis the ratio of an untreated WHCO6 internal control to the H1299 positive control was adjusted to match the corresponding ratio under standard HOSCC culture conditions.

It should be noted that while the normalised estimates of relative protein abundance are more consistent allowing for more accurate statistical comparison, the percentage change due to treatment was not altered as these samples were always run together on the same blot and thus multiplied by the same factor.

Appendix C

1. SDS-PAGE

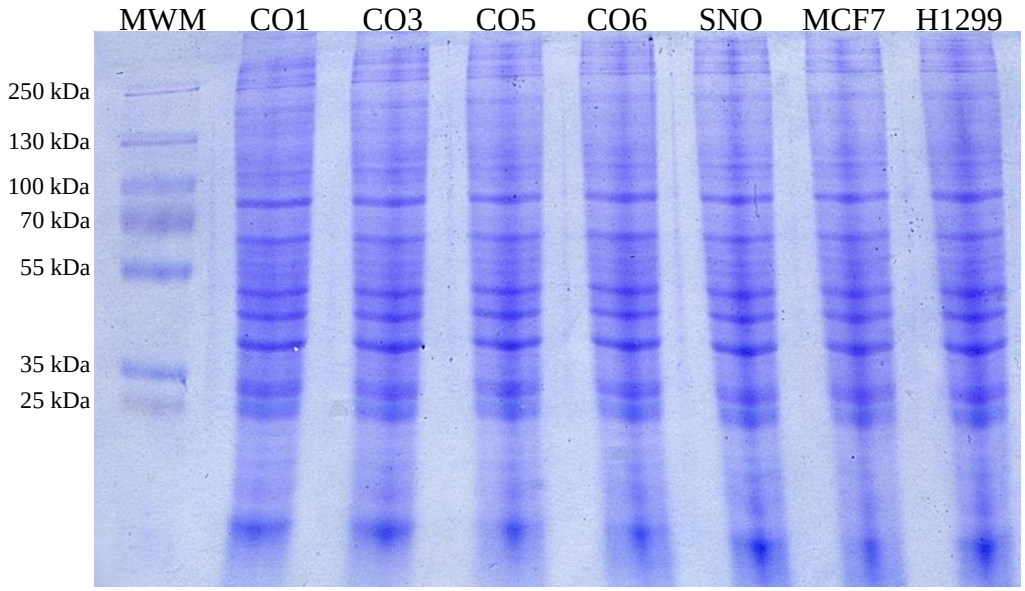

Figure C1: SDS-PAGE resolved whole cell protein extracts

SDS-PAGE resolved whole cell protein extracts of the HOSCC cell lines, the MCF7 and H1299 control cell lines. Equivalent amounts (10 µg) of total cellular protein derived from whole cell lysis were resolved on a 10 % SDS-PAGE gel electrophoresed at constant current of 21 mA and stained with coomassie blue. MWM refers to the molecular weight marker PageRuler^{TM} Prestained Protein Ladder (Fermentas Life Science).

2. VEGF Dot Blot

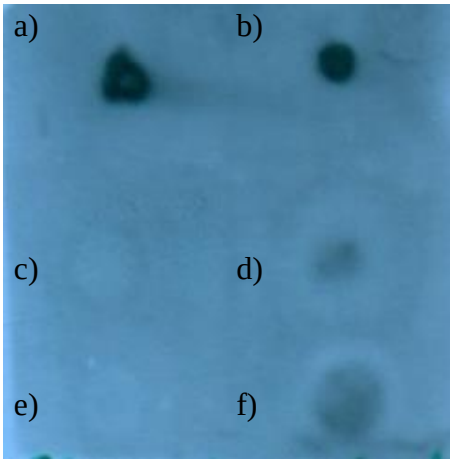

Figure C2: Dot blot confirming functionality of the anti-VEGF antibody

Dot blot confirming functionality of the anti-VEGF antibody and presence of VEGF in the MCF7 positive control cell line and the SNO HOSCC cell line. The following were dotted onto a nitrocellulose membrane: a) 2 µl of anti-VEGF antibody (positive), b) 2 µl of purified VEGF (positive), c) 2 µl of MCF7 cell lysate (negative/ negligible), d) 10 µl of MCF7 cell lysate (weak positive), e) 2 µl of SNO cell lysate (negative/ negligible) and f) 10 µl of SNO cell lysate (positive). The membrane was then dried and immunoblotted with anti-VEGF antibody (1:200).

Appendix D

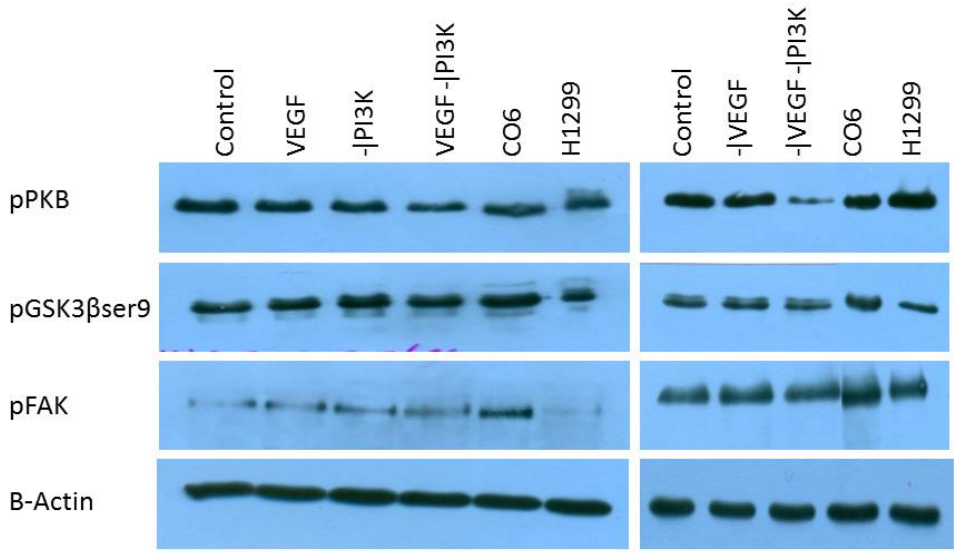

Figure D1: Representative blots showing the influence of VEGFR and PI3K signalling on the abundance of pPKB, pGSK3βser9 and pFAK in HOSCC cell lines

The abundance of pPKB (56 kDa), pGSK3βser9 (48 kDa) and pFAK (125 kDa) was detected by western blotting. β-Actin served as the loading control. The abundance of pPKB, pGSK3βser9 and pFAK was determined in WHCO1 control, VEGFR stimulated, PI3K inhibited, VEGFR stimulated-PI3K inhibited, VEGFR inhibited and VEGFR inhibited-PI3K inhibited HOSCC samples.

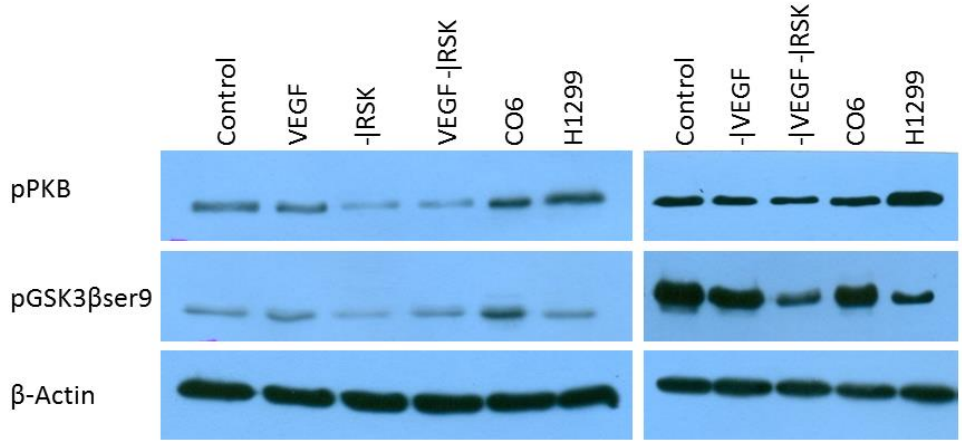

Figure D2: Representative blots showing the influence of VEGFR and RSK signalling on the abundance of pPKB and pGSK3βser9 in HOSCC cell lines

The abundance of pPKB (56 kDa) and pGSK3βser9 (48 kDa) was detected by western blotting. β-Actin served as the loading control. The abundance of pPKB and pGSK3βser9 was determined in WHCO1 control, VEGFR stimulated, RSK inhibited, VEGFR stimulated-RSK inhibited, VEGFR inhibited and VEGFR inhibited-RSK inhibited HOSCC samples.

The data set for each figure is presented below. Each data item represents an experimental repeat ($n \geq 3$). In addition the mean value, standard error (SE), percentage change due to treatment (% Change) and student's T-test probability of significance (p) were calculated and are also presented below.

Data Table for Figure 2: VEGF protein content in HOSCC cell lines

	CO1	CO3	CO5	CO6	SNO	MCF7	H1299
	110.22	301.70	235.04	125.55	131.63	41.94	100
	23.82	67.29	34.72	19.24	21.88	28.19	100
	25.08	19.67	10.69	15.88	6.27	1.26	100
Mean	53.04	129.55	93.48	53.56	53.26	23.80	100
SE	28.59	87.17	71.12	36.01	39.44	11.95	0

Data Table for Figure 3: VEGFR signalling influences the proliferation of HOSCC cell lines

CO1	Control	VEGFR stimulated	% Change
	0.50	0.49	-2.58
	0.47	0.54	15.57
	0.32	0.37	14.42
	0.30	0.37	25.08
	0.26	0.31	19.38
	0.43	0.43	2.12
Mean	0.38	0.42	12.33
SE			4.30
p			0.04
CO3	Control	VEGFR stimulated	% Change
	0.68	0.66	-3.39
	0.20	0.28	40.59
	0.26	0.28	10.59

CO1	Control	VEGFR inhibited	% Change
	0.44	0.43	-4.28
	0.47	0.38	-20.04
	0.24	0.21	-11.98
	0.16	0.14	-7.74
	0.15	0.14	-5.88
	0.13	0.17	29.92
Mean	0.27	0.24	-3.33
SE			7.04
p			0.29
CO3	Control	VEGFR inhibited	% Change
	0.62	0.44	-28.43
	0.59	0.44	-24.66
	0.57	0.56	-1.93

	0.73	0.77	5.20
	0.76	0.72	-5.26
	0.72	0.74	2.35
Mean	0.56	0.58	8.35
SE			6.86
p			0.39
CO5	Control	VEGFR stimulated	% Change
	0.95	1.25	31.23
	0.77	0.91	18.35
	0.89	0.86	-3.48
	0.15	0.16	4.73
	0.35	0.86	148.99
	0.30	0.38	28.52
	0.32	0.30	-4.42
Mean	0.53	0.68	31.99
SE			20.25
p			0.11
CO6	Control	VEGFR stimulated	% Change
	0.84	0.88	3.91
	0.68	0.67	-1.03
	0.67	0.64	-4.02
	0.67	0.81	21.44
	0.51	0.50	-0.98
	0.81	0.81	0.74
	0.60	0.63	4.81
Mean	0.68	0.71	3.55
SE			3.19
p			0.29
SNO	Control	VEGFR stimulated	% Change
	1.09	1.11	2.39

	0.47	0.43	-8.49
	0.46	0.41	-10.63
	0.20	0.20	-3.43
Mean	0.49	0.41	-12.93
SE			4.52
p			0.06
CO5	Control	VEGFR inhibited	% Change
	0.31	0.30	-3.28
	0.23	0.22	-6.49
	0.35	0.32	-7.98
	0.17	0.16	-6.63
	0.12	0.11	-0.87
	0.15	0.11	-23.65
Mean	0.22	0.20	-8.15
SE			3.28
p			0.02
CO6	Control	VEGFR inhibited	% Change
	0.17	0.16	-4.09
	0.24	0.23	-5.42
	0.28	0.27	-3.90
	0.37	0.35	-4.09
	0.35	0.33	-6.25
	0.16	0.14	-10.69
Mean	0.26	0.25	-5.74
SE			1.06
p			0.00
SNO	Control	VEGFR inhibited	% Change
	0.38	0.36	-4.76

	0.62	0.77	23.63
	0.45	0.73	61.83
	0.12	0.17	40.16
	1.03	1.05	2.13
	1.01	1.09	7.75
	0.92	1.12	21.55
Mean	0.75	0.86	22.78
SE			8.31
p			0.02
MCF7	Control	VEGFR stimulated	% Change
	0.15	0.19	23.33
	0.19	0.21	10.99
	0.18	0.21	11.41
Mean	0.18	0.20	15.25
SE			4.04
p			0.03
H1299	Control	VEGFR stimulated	% Change
	0.24	0.21	-10.97
	0.29	0.26	-8.77
	0.30	0.22	-27.39
	0.18	0.20	12.92
Mean	0.25	0.22	-8.55
SE			8.28
p			0.29

	0.49	0.39	-20.00
	0.43	0.39	-9.45
	0.27	0.25	-9.56
	0.29	0.29	-1.03
	0.15	0.15	-0.68
Mean	0.34	0.30	-7.58
SE			2.94
p			0.09
MCF7	Control	VEGFR inhibited	% Change
	0.15	0.13	-15.33
	0.19	0.18	-8.38
	0.18	0.18	-3.26
Mean	0.18	0.16	-8.99
SE			3.50
p			0.09
H1299	Control	VEGFR inhibited	% Change
	0.24	0.27	15.19
	0.29	0.30	3.51
	0.30	0.24	-20.13
	0.18	0.18	3.37
Mean	0.25	0.25	0.48
SE			7.41
p			0.92

Data Table for Figure 4: pPKB and pGSK3βser9 protein content in HOSCC cell lines

pPKB:

	CO1	CO3	CO5	CO6	SNO	MCF7	H1299
	20.40	0.71	7.43	12.65	22.12	1.94	100
	62.71	0.24	42.52	22.52	32.78	7.03	100
	45.61	0.34	69.30	23.13	38.01	1.44	100
	12.51	-0.03	46.55	30.17	41.04	26.65	100
Mean	35.31	0.31	41.45	22.12	33.49	9.26	100
SE	11.54	0.15	12.78	3.60	4.15	5.93	0.00

pGSK3βser9:

	CO1	CO3	CO5	CO6	SNO	MCF7	H1299
	187.50	30.08	135.00	192.50	221.67	152.50	100
	150.00	126.61	170.97	107.26	118.55	118.55	100
	52.88	79.20	106.27	98.25	106.52	88.97	100
Mean	130.13	78.63	137.41	132.67	148.91	120.01	100
SE	40.11	27.87	18.72	30.03	36.54	18.35	0

Data Table for Figure 5: VEGFR signalling influences the abundance of pPKB and pGSK3βser9 in HOSCC cell lines

pPKB:

CO1	Control	VEGFR stimulated	% Change
	24.65	16.95	-31.24
	23.95	23.81	-0.59
	24.75	22.36	-9.66
	57.63	69.63	20.83
	9.77	20.82	113.10
	35.86	28.28	-21.15
	29.97	18.51	-38.24

CO1	Control	VEGFR inhibited	% Change
	18.40	15.52	-15.61
	66.04	61.50	-6.88
	25.50	24.93	-2.21
	23.04	16.56	-28.13
	20.99	17.49	-16.67
	34.40	33.82	-1.70
	57.63	46.42	-19.44

	20.99	22.49	7.19
Mean	28.45	27.86	5.03
SE			16.93
p			0.85
CO3	Control	VEGFR stimulated	% Change
	0	0	0
	0	0	0
	0	0	0
Mean	0	0	0
SE			0
p			-
CO5	Control	VEGFR stimulated	% Change
	38.84	26.43	-31.94
	24.59	17.63	-28.30
	145.82	113.34	-22.27
	14.36	15.26	6.31
	25.13	31.14	23.95
	31.66	31.88	0.68
	44.09	44.58	1.12
Mean	46.35	40.04	-7.21
SE			7.82
p			0.25
CO6	Control	VEGFR stimulated	% Change
	23.93	19.98	-16.52
	15.76	13.08	-16.98
	14.48	19.32	33.42
	26.49	32.20	21.56
	18.56	16.46	-11.35
	36.73	31.16	-15.18
Mean	22.66	22.03	-0.84

Mean	35.14	30.89	-12.95
SE			3.69
p			0.02
CO3	Control	VEGFR inhibited	% Change
	0	0	0
	0	0	0
	0	0	0
Mean	0	0	0
SE			0
p			-
CO5	Control	VEGFR inhibited	% Change
	21.69	11.59	-46.57
	35.11	32.42	-7.65
	192.94	162.69	-15.68
	44.07	53.67	21.77
	50.41	42.61	-15.48
	145.82	104.15	-28.57
Mean	81.67	67.86	-15.36
SE			9.29
p			0.13
CO6	Control	VEGFR inhibited	% Change
	69.88	39.83	-43.00
	22.44	17.39	-22.49
	114.28	92.77	-18.82
	36.37	37.44	2.93
	36.51	33.31	-8.76
	24.09	19.16	-20.49
Mean	50.60	39.98	-18.44

SE			9.13
p			0.76
SNO	Control	VEGFR stimulated	% Change
	8.35	16.25	94.59
	17.56	22.31	27.05
	15.65	11.32	-27.71
	36.53	37.03	1.38
	22.98	22.98	0.00
	23.58	18.01	-23.63
	30.20	79.57	163.44
Mean	22.12	29.64	33.59
SE			26.65
p			0.34
MCF7	Control	VEGFR stimulated	% Change
	5.57	6.22	11.72
	20.80	33.97	63.29
	9.28	23.43	152.48
Mean	11.88	21.21	75.83
SE			41.12
p			0.17
H1299	Control	VEGFR stimulated	% Change
	41.29	36.13	-12.50
	79.98	72.94	-8.80
	95.50	99.95	4.66
Mean	72.25	69.67	-5.54
SE			5.21
p			0.54

SE			6.26
p			0.09
SNO	Control	VEGFR inhibited	% Change
	53.90	50.46	-6.37
	44.23	41.84	-5.42
	24.75	16.23	-34.43
	22.34	20.70	-7.32
Mean	36.30	32.31	-13.39
SE			7.03
p			0.08
MCF7	Control	VEGFR inhibited	% Change
	14.04	21.65	54.17
	9.26	18.89	103.92
	18.24249088	21.8155029	19.59
Mean	13.85	20.78	59.22
SE			24.48
p			0.06
H1299	Control	VEGFR inhibited	% Change
	28237.32	4960.32	-82.43
	41.29	8.81	-78.66
	298.05	202.96	-31.90
Mean	9525.55	1724.03	-64.33
SE			16.25
p			0.42

pGSK3βser9:

CO1	Control	VEGFR stimulated	% Change
	70.30	69.68	-0.88
	95.23	72.85	-23.50
	208.01	175.59	-15.58
	398.82	416.45	4.42
	59.96	125.36	109.06
	96.39	102.89	6.74
	85.10	94.26	10.77
	41.18	74.32	80.48
Mean	131.87	141.42	21.44
SE			16.73
p			0.41
CO3	Control	VEGFR stimulated	% Change
	96.88	123.41	27.39
	98.52	75.79	-23.07
	31.35	91.90	193.14
	57.58	31.65	-45.03
	100.80	96.75	-4.02
Mean	77.03	83.90	29.68
SE			42.56
p			0.70
CO5	Control	VEGFR stimulated	% Change
	166.98	175.37	5.02
	411.16	445.88	8.44
	41.04	50.35	22.69
	252.31	196.63	-22.07
	186.15	137.81	-25.97
	98.17	88.22	-10.14

CO1	Control	VEGFR inhibited	% Change
	133.58	119.04	-10.88
	193.70	201.66	4.11
	121.40	128.33	5.71
	155.72	150.08	-3.62
	193.62	166.99	-13.76
	146.11	127.29	-12.88
	398.82	318.78	-20.07
Mean	191.85	173.17	-7.34
SE			3.66
p			0.15
CO3	Control	VEGFR inhibited	% Change
	122.26	138.74	13.48
	30.11	63.81	111.89
	78.46	83.67	6.64
	52.10	79.25	52.10
	120.41	108.59	-9.82
	116.66	132.67	13.73
Mean	86.67	101.12	31.34
SE			18.12
p			0.08
CO5	Control	VEGFR inhibited	% Change
	150.84	95.41	-36.75
	236.84	290.27	22.56
	163.12	143.54	-12.00
	118.53	132.21	11.54
	134.04	130.84	-2.38
	252.31	207.29	-17.84

	102.40	110.77	8.18
Mean	179.74	172.15	-1.98
SE			6.75
p			0.57
CO6	Control	VEGFR stimulated	% Change
	106.40	76.77	-27.85
	119.94	145.70	21.47
	88.25	100.60	13.99
	87.38	130.38	49.21
	51.89	285.19	449.57
	122.13	122.13	0.00
	129.89	136.55	5.13
Mean	100.84	142.47	73.07
SE			63.36
p			0.25
SNO	Control	VEGFR stimulated	% Change
	113.25	136.98	20.95
	190.82	138.12	-27.62
	9.95	14.82	48.96
	127.57	139.05	9.00
	206.15	124.50	-39.60
	90.76	95.48	5.20
Mean	123.08	108.16	2.82
SE			13.20
p			0.42
MCF7	Control	VEGFR stimulated	% Change
	147.66	160.40	8.63
	106.61	126.15	18.33
	74.03	130.30	76.00
Mean	109.43	138.95	34.32

Mean	175.95	166.60	-5.81
SE			8.67
p			0.59
CO6	Control	VEGFR inhibited	% Change
	232.17	185.74	-20.00
	220.82	359.72	62.90
	204.44	220.75	7.98
	234.27	236.21	0.83
	270.51	231.68	-14.35
	153.25	153.71	0.30
Mean	219.24	231.30	6.28
SE			12.10
p			0.68
SNO	Control	VEGFR inhibited	% Change
	357.78	591.12	65.22
	435.56	497.78	14.29
	349.21	320.81	-8.13
	163.88	115.11	-29.76
	78.82	70.63	-10.40
	132.67	114.63	-13.60
Mean	252.99	285.01	2.94
SE			13.72
p			0.49
MCF7	Control	VEGFR inhibited	% Change
	191.83	133.56	-30.37
	315.09	394.45	25.19
	327.91	317.90	-3.05
Mean	278.28	281.97	-2.75

SE			21.03
p			0.16
H1299	Control	VEGFR stimulated	% Change
	572.82	599.53	4.66
	251.37	234.91	-6.55
	782.32	358.44	-54.18
Mean	535.50	397.63	-18.69
SE			18.04
p			0.44

SE			16.04
p			0.94
H1299	Control	VEGFR inhibited	% Change
	572.82	655.92	14.51
	71.10	79.16	11.34
	782.32	844.79	7.98
Mean	475.41	526.62	11.28
SE			1.88
p			0.15

Data Table for Figure 6: PI3K inhibition influences the proliferation of HOSCC cell lines

CO1	Control	PI3K inhibited	% Change
	0.50	0.43	-13.72
	0.47	0.46	-2.56
	0.32	0.38	17.55
Mean	0.43	0.42	0.43
SE			9.15
p			0.84
CO3	Control	PI3K inhibited	% Change
	0.68	0.63	-6.78
	0.20	0.14	-29.21
	0.26	0.24	-7.06
Mean	0.38	0.34	-14.35
SE			7.43

CO1	VEGFR stimulated	VEGFR stimulated - PI3K inhibited	% Change
	0.49	0.46	-5.71
	0.54	0.49	-10.33
	0.69	0.64	-7.49
Mean	0.58	0.53	-7.85
SE			1.34
p			0.04
CO3	VEGFR stimulated	VEGFR stimulated - PI3K inhibited	% Change
	0.66	0.51	-22.14
	0.28	0.22	-22.89
	0.28	0.26	-7.09
Mean	0.41	0.33	-17.37
SE			5.14

p			0.08
CO5	Control	PI3K inhibited	% Change
	0.95	0.66	-30.29
	0.77	0.82	6.10
	0.89	0.89	-0.22
	0.15	0.14	-7.43
Mean	0.69	0.63	-7.96
SE			7.94
p			0.46
CO6	Control	PI3K inhibited	% Change
	0.84	0.86	2.01
	0.67	0.62	-7.45
	0.67	0.71	5.70
Mean	0.73	0.73	0.09
SE			3.92
p			0.96
SNO	Control	PI3K inhibited	% Change
	0.62	0.62	-0.80
	0.45	0.69	54.46
	0.12	0.10	-16.39
Mean	0.40	0.47	12.42
SE			21.50
p			0.48
H1299	Control	PI3K inhibited	% Change

p			0.17
CO5	VEGFR stimulated	VEGFR stimulated - PI3K inhibited	% Change
	1.25	0.45	-63.92
	0.91	0.84	-7.67
	0.86	0.85	-1.40
	0.16	0.13	-13.55
Mean	0.79	0.57	-21.63
SE			14.31
p			0.32
CO6	VEGFR stimulated	VEGFR stimulated - PI3K inhibited	% Change
	0.88	0.74	-15.39
	0.64	0.58	-9.63
	0.81	0.58	-28.15
Mean	0.78	0.64	-17.72
SE			5.47
p			0.10
SNO	VEGFR stimulated	VEGFR stimulated - PI3K inhibited	% Change
	1.11	0.52	-53.23
	0.73	0.69	-4.83
	0.17	0.11	-35.67
Mean	0.67	0.44	-31.24
SE			14.15
p			0.33
H1299	VEGFR stimulated	VEGFR stimulated	% Change

	0.24	0.15	-36.29
	0.29	0.19	-32.98
	0.30	0.19	-38.61
Mean	0.28	0.18	-35.96
SE			1.63
p			0.01

		- PI3K inhibited	
	0.21	0.16	-22.27
	0.26	0.18	-29.62
	0.22	0.16	-25.91
Mean	0.23	0.17	-25.93
SE			2.12
p			0.02

Data Table for Figure 7: PI3K inhibition influences the abundance of pPKB and pGSK3βser9 in HOSCC cell lines

pPKB:

CO1	Control	PI3K inhibited	% Change
	27.65	18.47	-33.19
	29.97	15.48	-48.33
	20.99	8.80	-58.08
Mean	26.20	14.25	-46.54
SE			7.24
p			0.02
CO3	Control	PI3K inhibited	% Change
	0	0	0
	0	0	0
	0	0	0
Mean	0	0	0
SE			0

CO1	VEGFR stimulated	VEGFR stimulated - PI3K inhibited	% Change
	21.06	14.59	-30.73
	18.51	15.71	-15.14
	22.49	6.65	-70.45
Mean	20.69	12.31	-38.77
SE			16.46
p			0.16
CO3	VEGFR stimulated	VEGFR stimulated - PI3K inhibited	% Change
	0	0	0
	0	0	0
	0	0	0
Mean	0	0	0
SE			0

p			-	p			-
CO5	Control	PI3K inhibited	% Change	**CO5**	VEGFR stimulated	VEGFR stimulated - PI3K inhibited	% Change
	14.36	13.84	-3.60		15.26	9.71	-36.36
	25.13	13.90	-44.67		31.14	9.58	-69.23
	27.39	18.16	-33.70		18.57	13.49	-27.32
Mean	22.29	15.30	-27.33	Mean	21.66	10.93	-44.30
SE			12.28	SE			12.73
p			0.17	p			0.19
CO6	Control	PI3K inhibited	% Change	**CO6**	VEGFR stimulated	VEGFR stimulated - PI3K inhibited	% Change
	42.17	29.54	-29.97		32.20	23.21	-27.92
	18.56	13.43	-27.66		16.46	13.06	-20.64
	36.73	22.69	-38.22		31.16	25.39	-18.52
Mean	32.49	21.89	-31.95	Mean	26.61	20.55	-22.36
SE			3.21	SE			2.85
p			0.06	p			0.06
SNO	Control	PI3K inhibited	% Change	**SNO**	VEGFR stimulated	VEGFR stimulated - PI3K inhibited	% Change
	36.53	29.49	-19.27		37.03	33.01	-10.86
	22.98	17.06	-25.79		22.98	14.74	-35.85
	23.58	18.61	-21.06		18.01	17.97	-0.23
Mean	27.70	21.72	-22.04	Mean	26.01	21.91	-15.65
SE			1.94	SE			10.56
p			0.01	p			0.23
H1299	Control	PI3K inhibited	% Change	**H1299**	VEGFR stimulated	VEGFR stimulated - PI3K	% Change

	79.98	64.03	-19.94
	58.87	35.43	-39.81
	46.58	43.72	-6.13
Mean	61.81	47.73	-21.96
SE			9.77
p			0.14

		inhibited	
	314.98	23.19	-92.64
	72.94	53.94	-26.05
	428.16	338.27	-20.99
Mean	272.03	138.47	-46.56
SE			23.09
p			0.24

pGSK3βser9:

CO1	Control	PI3K inhibited	% Change
	96.39	121.30	25.84
	85.10	109.10	28.21
	41.18	78.17	89.84
Mean	74.22	102.86	47.96
SE			20.95
p			0.02
CO3	Control	PI3K inhibited	% Change
	922.61	622.93	-32.48
	57.58	37.03	-35.69
	100.80	64.31	-36.21
Mean	360.33	241.42	-34.79
SE			1.17
p			0.32
CO5	Control	PI3K inhibited	% Change
	186.15	79.40	-57.35

CO1	VEGFR stimulated	VEGFR stimulated - PI3K inhibited	% Change
	102.89	108.30	5.26
	94.26	99.50	5.56
	74.32	96.34	29.63
Mean	90.49	101.38	13.48
SE			8.07
p			0.19
CO3	VEGFR stimulated	VEGFR stimulated - PI3K inhibited	% Change
	31.65	41.19	30.14
	96.75	106.02	9.58
Mean	64.20	73.60	19.86
SE			10.28
p			0.01
CO5	VEGFR stimulated	VEGFR stimulated - PI3K inhibited	% Change
	137.81	89.99	-34.70

	98.17	74.96	-23.65		88.22	96.18	9.02
	102.40	104.98	2.52		110.77	127.52	15.12
Mean	128.91	86.44	-26.16	Mean	112.27	104.56	-3.52
SE			17.33	SE			15.69
p			0.33	p			0.74
CO6	Control	PI3K inhibited	% Change	**CO6**	VEGFR stimulated	VEGFR stimulated - PI3K inhibited	% Change
	152.70	155.41	1.77		155.95	169.49	8.68
	122.13	106.91	-12.46		122.13	124.86	2.24
	129.89	109.91	-15.38		136.55	149.32	9.35
Mean	134.91	124.08	-8.69	Mean	138.21	147.89	6.76
SE			5.30	SE			2.27
p			0.26	p			0.11
SNO	Control	PI3K inhibited	% Change	**SNO**	VEGFR stimulated	VEGFR stimulated - PI3K inhibited	% Change
	127.57	141.60	11.00		139.05	151.16	8.72
	206.15	109.05	-47.10		124.50	87.47	-29.74
	90.76	133.67	47.29		95.48	131.66	37.89
Mean	141.49	128.11	3.73	Mean	119.68	123.43	5.62
SE			27.49	SE			19.59
p			0.78	p			0.88
H1299	Control	PI3K inhibited	% Change	**H1299**	VEGFR stimulated	VEGFR stimulated - PI3K inhibited	% Change
	251.37	199.50	-20.63		253.49	106.13	-58.13
	121.00	111.78	-7.61		234.91	198.00	-15.71
	126.53	117.31	-7.28	Mean	244.20	152.07	-36.92
Mean	166.30	142.87	-11.84	SE			21.21
SE			4.40	p			0.34

p			0.24				

Data Table for Figure 8: Combined VEGFR and PI3K inhibition influences the proliferation of HOSCC cell lines

CO1	VEGFR inhibited	Combined VEGFR - PI3K inhibited	% Change
	0.43	0.26	-40.00
	0.38	0.21	-42.93
	0.21	0.18	-16.90
Mean	0.34	0.22	-33.28
SE			8.23
p			0.11

CO1	Control	Combined VEGFR - PI3K inhibited	% Change
	0.44	0.26	-42.57
	0.47	0.21	-54.37
	0.24	0.18	-26.86
Mean	0.39	0.22	-41.27
SE			7.97
p			0.09

CO3	VEGFR inhibited	Combined VEGFR - PI3K inhibited	% Change
	0.44	0.38	-13.77
	0.44	0.37	-17.61
	0.56	0.22	-61.11
Mean	0.48	0.32	-30.83
SE			15.18
p			0.22

CO3	Control	Combined VEGFR - PI3K inhibited	% Change
	0.62	0.38	-38.29
	0.59	0.37	-37.93
	0.57	0.22	-61.86
Mean	0.59	0.32	-46.03
SE			7.92
p			0.02

CO5	VEGFR inhibited	Combined VEGFR - PI3K inhibited	% Change
	0.30	0.14	-54.24
	0.22	0.16	-26.39
	0.32	0.21	-34.37
Mean	0.28	0.17	-38.33
SE			8.28

CO5	Control	Combined VEGFR - PI3K inhibited	% Change
	0.31	0.14	-55.74
	0.23	0.16	-31.17
	0.35	0.21	-39.60
Mean	0.30	0.17	-42.17
SE			7.21

p			0.07
CO6	VEGFR inhibited	Combined VEGFR - PI3K inhibited	% Change
	0.16	0.13	-21.95
	0.23	0.16	-31.28
	0.27	0.14	-48.71
Mean	0.22	0.14	-33.98
SE			7.84
p			0.10
SNO	VEGFR inhibited	Combined VEGFR - PI3K inhibited	% Change
	0.36	0.32	-10.28
	0.39	0.34	-12.24
	0.39	0.28	-29.77
Mean	0.38	0.31	-17.43
SE			6.20
p			0.11
H1299	VEGFR inhibited	Combined VEGFR - PI3K inhibited	% Change
	0.27	0.13	-50.92
	0.30	0.16	-47.12
	0.24	0.18	-26.03
Mean	0.27	0.16	-41.36
SE			7.74
p			0.05

p			0.05
CO6	Control	Combined VEGFR - PI3K inhibited	% Change
	0.17	0.13	-25.15
	0.24	0.16	-35.00
	0.28	0.14	-50.71
Mean	0.23	0.14	-36.95
SE			7.44
p			0.09
SNO	Control	Combined VEGFR - PI3K inhibited	% Change
	0.38	0.32	-14.55
	0.49	0.34	-29.80
	0.43	0.28	-36.41
Mean	0.43	0.31	-26.92
SE			6.47
p			0.07
H1299	Control	Combined VEGFR - PI3K inhibited	% Change
	0.24	0.13	-43.46
	0.29	0.16	-45.26
	0.30	0.18	-40.92
Mean	0.28	0.16	-43.22
SE			1.26
p			0.00

Data Table for Figure 9: Combined inhibition of both VEGFR and PI3K signalling synergistically reduces proliferation of HOSCC cell lines

	CO1	CO3	CO5	CO6	SNO	H1299
VEGFR inhibition (x)	-3.33	-12.93	-8.15	-5.74	-7.58	0.484
PI3K inhibition during VEGFR stimulation (y)	-7.85	-17.37	-21.63	-17.72	-31.24	-25.93
Combined VEGFR and PI3K inhibition (z)	-41.27	-46.03	-42.17	-36.95	-26.92	-43.22
Decrease not accounted for by additive effect of VEGFR inhibition and PI3K inhibition (d=z-(x+y))	-30.08	-15.72	-12.39	-13.49	11.90	-17.77

Data Table for Figure 10: Combined VEGFR and PI3K inhibition influences the abundance of pPKB and pGSK3βser9 in HOSCC cell lines

pPKB:

CO1	VEGFR inhibited	Combined VEGFR - PI3K inhibited	% Change
	15.52	14.67	-5.48
	61.50	50.31	-18.18
	24.93	6.50	-73.94
Mean	33.98	23.83	-32.53
SE			21.02
p			0.18
CO3	VEGFR inhibited	Combined VEGFR	% Change

CO1	Control	Combined VEGFR - PI3K inhibited	% Change
	18.40	14.67	-20.23
	66.04	50.31	-23.81
	25.50	6.50	-74.51
Mean	36.64	23.83	-39.52
SE			17.53
p			0.11
CO3	Control	Combined VEGFR	% Change

		- PI3K inhibited	
	0	0	0
	0	0	0
	0	0	0
Mean	0	0	0
SE			0
P			-
CO5	VEGFR inhibited	Combined VEGFR - PI3K inhibited	% Change
	11.59	15.42	33.03
	32.42	13.85	-57.28
	162.69	40.40	-75.17
Mean	68.90	23.22	-33.14
SE			33.48
p			0.36
CO6	VEGFR inhibited	Combined VEGFR - PI3K inhibited	% Change
	39.83	22.89	-42.54
	17.39	3.31	-80.99
	92.77	9.08	-90.22
Mean	50.00	11.76	-71.25
SE			14.60
p			0.23
SNO	VEGFR inhibited	Combined VEGFR - PI3K inhibited	% Change
	66.57	21.69	-67.42
	50.46	41.66	-17.45

		- PI3K inhibited	
	0	0	0
	0	0	0
	0	0	0
Mean	0	0	0
SE			0
p			-
CO5	Control	Combined VEGFR - PI3K inhibited	% Change
	21.69	15.42	-28.92
	35.11	13.85	-60.55
	192.94	40.40	-79.06
Mean	83.25	23.22	-56.18
SE			14.64
p			0.33
CO6	Control	Combined VEGFR - PI3K inhibited	% Change
	69.88	22.89	-67.25
	22.44	3.31	-85.26
	114.28	9.08	-92.06
Mean	68.87	11.76	-81.52
SE			7.40
p			0.15
SNO	Control	Combined VEGFR - PI3K inhibited	% Change
	39.94	21.69	-45.70
	53.90	41.66	-22.71

	41.84	29.86	-28.63
Mean	52.96	31.07	-37.83
SE			15.14
p			0.20
H1299	VEGFR inhibited	Combined VEGFR - PI3K inhibited	% Change
	8.81	14.25	61.79
	11.60	14.67	26.46
Mean	10.20	14.46	44.12
SE			17.66
p			0.17

	44.23	29.86	-32.50
Mean	46.02	31.07	-33.64
SE			6.66
p			0.01
H1299	Control	Combined VEGFR - PI3K inhibited	% Change
	41.29	14.25	-65.48
	298.05	100.06	-66.43
Mean	169.67	57.16	-65.95
SE			0.48
p			0.41

pGSK3βser9:

CO1	VEGFR inhibited	Combined VEGFR - PI3K inhibited	% Change
	201.66	179.10	-11.18
	128.33	115.33	-10.14
Mean	164.99	147.21	-10.66
SE			0.52
p			0.17
CO3	VEGFR inhibited	Combined VEGFR - PI3K inhibited	% Change
	138.74	29.83	-78.50
	63.81	21.49	-66.33
	83.67	81.07	-3.11
Mean	95.41	44.13	-49.31
SE			23.37

CO1	Control	Combined VEGFR - PI3K inhibited	% Change
	193.70	179.10	-7.53
	121.40	115.33	-5.00
Mean	157.55	147.21	-6.27
SE			1.27
p			0.25
CO3	Control	Combined VEGFR - PI3K inhibited	% Change
	122.26	29.83	-75.60
	30.11	21.49	-28.65
	78.46	81.07	3.32
Mean	76.95	44.13	-33.64
SE			22.92

p			0.24
CO5	VEGFR inhibited	Combined VEGFR - PI3K inhibited	% Change
	290.27	160.27	-44.79
	143.54	112.01	-21.97
Mean	216.90	136.14	-33.38
SE			11.41
p			0.35
CO6	VEGFR inhibited	Combined VEGFR - PI3K inhibited	% Change
	185.74	184.41	-0.71
	359.72	96.16	-73.27
	220.75	203.35	-7.88
Mean	255.40	161.31	-27.29
SE			23.08
p			0.38
SNO	VEGFR inhibited	Combined VEGFR - PI3K inhibited	% Change
	591.12	204.00	-65.49
	497.78	393.34	-20.98
	320.81	248.96	-22.40
Mean	469.90	282.10	-36.29
SE			14.61
p			0.20
H1299	VEGFR inhibited	Combined VEGFR - PI3K	% Change

p			0.39
CO5	Control	Combined VEGFR - PI3K inhibited	% Change
	150.84	129.94	-13.86
	236.84	160.27	-32.33
	163.12	112.01	-31.33
Mean	183.60	134.07	-25.84
SE			6.00
p			0.09
CO6	Control	Combined VEGFR - PI3K inhibited	% Change
	232.17	184.41	-20.57
	220.82	96.16	-56.45
	204.44	203.35	-0.53
Mean	219.14	161.31	-25.85
SE			16.36
p			0.25
SNO	Control	Combined VEGFR - PI3K inhibited	% Change
	357.78	204.00	-42.98
	435.56	393.34	-9.69
	349.21	248.96	-28.71
Mean	380.85	282.10	-27.13
SE			9.64
p			0.09
H1299	Control	Combined VEGFR - PI3K	% Change

		inhibited	
	92.13	88.45	-4.00
	844.79	459.58	-45.60
Mean	468.46	274.01	-24.80
SE			20.80
p			0.49

		inhibited	
	134.88	88.45	-34.43
	782.32	459.58	-41.25
Mean	458.60	274.01	-37.84
SE			3.41
p			0.41

Data Table for Figure 12: RSK inhibition influences the proliferation of HOSCC cell lines

CO1	Control	RSK inhibited	% Change
	0.30	0.20	-34.45
	0.26	0.20	-24.03
	0.43	0.26	-38.12
Mean	0.33	0.22	-32.20
SE			4.22
p			0.06
CO3	Control	RSK inhibited	% Change
	0.73	0.31	-58.28
	0.76	0.33	-56.84
	0.72	0.32	-56.49
Mean	0.74	0.32	-57.20
SE			0.55
p			0.00
CO5	Control	RSK inhibited	% Change

CO1	VEGFR stimulated	VEGFR stimulated - RSK inhibited	% Change
	0.37	0.28	-26.47
	0.31	0.21	-33.44
	0.43	0.27	-38.71
Mean	0.37	0.25	-32.87
SE			3.54
p			0.03
CO3	VEGFR stimulated	VEGFR stimulated - RSK inhibited	% Change
	0.77	0.40	-47.98
	0.72	0.43	-40.00
	0.74	0.36	-50.88
Mean	0.74	0.40	-46.29
SE			3.25
p			0.01
CO5	VEGFR stimulated	VEGFR stimulated - RSK inhibited	% Change

	0.15	0.10	-35.81
	0.30	0.22	-26.51
	0.32	0.19	-41.01
Mean	0.25	0.17	-34.44
SE			4.24
p			0.06
CO6	Control	RSK inhibited	% Change
	0.51	0.36	-29.08
	0.81	0.42	-48.39
	0.60	0.33	-44.61
Mean	0.64	0.37	-40.69
SE			5.91
p			0.06
SNO	Control	RSK inhibited	% Change
	1.03	0.70	-32.01
	1.01	0.66	-34.56
	0.92	0.60	-34.39
Mean	0.99	0.65	-33.65
SE			0.82
p			0.00
H1299	Control	RSK inhibited	% Change
	0.18	0.17	-3.93
	0.24	0.13	-45.99
	0.29	0.18	-36.49
Mean	0.23	0.16	-28.81

	0.86	0.57	-33.91
	0.38	0.22	-43.60
	0.30	0.19	-37.62
Mean	0.52	0.33	-38.38
SE			2.82
p			0.07
CO6	VEGFR stimulated	VEGFR stimulated - RSK inhibited	% Change
	0.50	0.41	-19.25
	0.81	0.49	-39.53
	0.63	0.41	-35.13
Mean	0.65	0.44	-31.30
SE			6.16
p			0.08
SNO	VEGFR stimulated	VEGFR stimulated - RSK inhibited	% Change
	1.05	0.77	-26.97
	1.09	0.70	-35.67
	1.12	0.58	-47.72
Mean	1.09	0.68	-36.79
SE			6.01
p			0.03
H1299	VEGFR stimulated	VEGFR stimulated - RSK inhibited	% Change
	0.20	0.13	-34.33
	0.21	0.25	18.96
	0.26	0.27	3.08
Mean	0.22	0.22	-4.10

SE			12.74	SE			15.80
p			0.16	p			0.85

Data Table for Figure 13: RSK inhibition influences the abundance of pPKB and pGSK3βser9 in HOSCC cell lines

pPKB:

CO1	Control	RSK inhibited	% Change	**CO1**	VEGFR stimulated	VEGFR stimulated - RSK inhibited	% Change
	24.65	6.48	-73.71		16.95	7.70	-54.57
	23.95	2.86	-88.06		23.81	2.73	-88.52
	24.75	9.01	-63.57		22.36	8.33	-62.73
Mean	24.45	6.12	-75.12	Mean	21.04	6.26	-68.61
SE			7.10	SE			10.23
p			0.01	p			0.05
CO3	Control	RSK inhibited	% Change	**CO3**	VEGFR stimulated	VEGFR stimulated - RSK inhibited	% Change
	0	0	0		0	0	0
	0	0	0		0	0	0
	0	0	0		0	0	0
Mean	0	0	0	Mean	0	0	0
SE			0	SE			0
p			-	p			-
CO5	Control	RSK inhibited	% Change	**CO5**	VEGFR stimulated	VEGFR stimulated - RSK inhibited	% Change
	38.84	17.35	-55.32		26.43	14.89	-43.67
	24.59	10.34	-57.94		17.63	7.48	-57.57
	25.74	19.94	-22.54		113.34	150.10	32.43
Mean	29.73	15.88	-45.27	Mean	52.47	57.49	-22.94

SE			11.39
p			0.09
CO6	Control	RSK inhibited	% Change
	23.93	25.32	5.80
	15.76	22.30	41.51
	14.48	17.54	21.15
Mean	18.06	21.72	22.82
SE			10.34
p			0.14
SNO	Control	RSK inhibited	% Change
	8.35	11.89	42.34
	14.40	20.29	40.88
	15.65	16.23	3.67
Mean	12.80	16.13	28.96
SE			12.65
p			0.16
H1299	Control	RSK inhibited	% Change
	28237.32	23405.84	-17.11
	41.29	20.15	-51.19
	90.95	55.88	-38.56
Mean	9456.52	7827.29	-35.62
SE			9.95
p			0.42

SE			27.97
p			0.78
CO6	VEGFR stimulated	VEGFR stimulated - RSK inhibited	% Change
	19.98	20.30	1.60
	13.08	16.69	27.56
	22.80	16.37	-28.22
Mean	18.62	17.79	0.31
SE			16.12
p			0.80
SNO	VEGFR stimulated	VEGFR stimulated - RSK inhibited	% Change
	22.31	20.19	-9.48
	13.93	15.02	7.84
	11.32	16.09	42.13
Mean	15.85	17.10	13.50
SE			15.17
p			0.59
H1299	VEGFR stimulated	VEGFR stimulated - RSK inhibited	% Change
	24801.60	6957.33	-71.95
	36.13	20.40	-43.54
Mean	12418.86	3488.87	-57.74
SE			14.21
p			0.50

pGSK3βser9:

CO1	Control	RSK inhibited	% Change
	81.59	35.00	-57.10
	70.30	31.25	-55.56
	95.23	29.06	-69.49
Mean	82.37	31.77	-60.71
SE			4.41
p			0.02
CO3	Control	RSK inhibited	% Change
	245.36	237.24	-3.31
	98.52	14.84	-84.93
	62.19	61.89	-0.49
Mean	135.36	104.66	-29.58
SE			27.69
p			0.37
CO5	Control	RSK inhibited	% Change
	41.04	24.06	-41.37
	166.98	155.54	-6.85
	252.31	197.82	-21.60
Mean	153.44	125.81	-23.27
SE			10.00
p			0.18
CO6	Control	RSK inhibited	% Change

CO1	VEGFR stimulated	VEGFR stimulated - RSK inhibited	% Change
	61.97	48.02	-22.51
	69.68	52.82	-24.20
	72.85	44.28	-39.22
Mean	68.17	48.37	-28.64
SE			5.31
p			0.05
CO3	VEGFR stimulated	VEGFR stimulated - RSK inhibited	% Change
	123.41	92.46	-25.08
	75.79	63.58	-16.12
	91.90	79.30	-13.71
Mean	97.04	78.45	-18.30
SE			3.46
p			0.10
CO5	VEGFR stimulated	VEGFR stimulated - RSK inhibited	% Change
	175.37	150.20	-14.35
	445.88	51.53	-88.44
	50.35	40.46	-19.64
Mean	223.86	80.73	-40.81
SE			23.87
p			0.37
CO6	VEGFR stimulated	VEGFR stimulated	% Change

	106.40	119.20	12.03
	119.94	132.52	10.49
	120.12	156.87	30.60
Mean	115.49	136.20	17.70
SE			6.46
p			0.12
SNO	Control	RSK inhibited	% Change
	89.03	99.50	11.76
	113.25	142.38	25.71
	136.42	147.12	7.84
Mean	112.90	129.66	15.11
SE			5.42
p			0.11
H1299	Control	RSK inhibited	% Change
	572.82	560.94	-2.07
	782.32	483.38	-38.21
Mean	677.57	522.16	-20.14
SE			18.07
p			0.47

	76.77	138.06	79.82
	145.70	152.73	4.83
	105.78	121.01	14.41
Mean	109.41	137.27	33.02
SE			23.56
p			0.24
SNO	VEGFR stimulated	VEGFR stimulated - RSK inhibited	% Change
	94.26	108.23	14.81
	136.98	92.87	-32.20
	91.20	170.76	87.24
Mean	107.48	123.95	23.28
SE			34.74
p			0.69
H1299	VEGFR stimulated	VEGFR stimulated - RSK inhibited	% Change
	599.53	498.62	-16.83
	117.28	90.89	-22.50
	214.48	146.67	-31.62
Mean	310.43	245.39	-23.65
SE			4.31
p			0.09

Data Table for Figure 14: Combined VEGFR and RSK inhibition influences the proliferation of HOSCC cell lines

CO1	VEGFR inhibited	Combined VEGFR - RSK inhibited	% Change
	0.14	0.14	-4.90
	0.14	0.13	-6.94
	0.13	0.13	-0.79
Mean	0.14	0.13	-4.21
SE			1.81
p			0.15
CO3	VEGFR inhibited	Combined VEGFR - RSK inhibited	% Change
	0.43	0.28	-35.96
	0.41	0.32	-23.30
	0.20	0.14	-29.95
Mean	0.35	0.24	-29.74
SE			3.66
p			0.07
CO5	VEGFR inhibited	Combined VEGFR - RSK inhibited	% Change
	0.16	0.12	-23.87
	0.11	0.10	-15.79
	0.11	0.11	0.00
Mean	0.13	0.11	-13.22
SE			7.01
p			0.23
CO6	VEGFR	Combined	% Change

CO1	Control	Combined VEGFR - RSK inhibited	% Change
	0.16	0.14	-12.26
	0.15	0.13	-12.42
	0.17	0.13	-23.64
Mean	0.16	0.13	-16.10
SE			3.77
p			0.06
CO3	Control	Combined VEGFR - RSK inhibited	% Change
	0.47	0.28	-41.40
	0.46	0.32	-31.45
	0.20	0.14	-32.35
Mean	0.38	0.24	-35.07
SE			3.18
p			0.07
CO5	Control	Combined VEGFR - RSK inhibited	% Change
	0.17	0.12	-28.92
	0.12	0.10	-16.52
	0.15	0.11	-23.65
Mean	0.14	0.11	-23.03
SE			3.59
p			0.06
CO6	Control	Combined	% Change

	inhibited	VEGFR - RSK inhibited	
	0.35	0.27	-24.72
	0.33	0.28	-15.45
	0.14	0.13	-7.04
Mean	0.27	0.23	-15.74
SE			5.10
p			0.16
SNO	VEGFR inhibited	Combined VEGFR - RSK inhibited	% Change
	0.25	0.22	-10.57
	0.29	0.19	-34.60
	0.15	0.12	-17.81
Mean	0.23	0.18	-20.99
SE			7.12
p			0.18
H1299	VEGFR inhibited	Combined VEGFR - RSK inhibited	% Change
	0.18	0.15	-20.65
	0.27	0.26	-6.59
	0.30	0.22	-24.07
Mean	0.25	0.21	-17.10
SE			5.35
p			0.11

		VEGFR - RSK inhibited	
	0.37	0.27	-27.79
	0.35	0.28	-20.74
	0.16	0.13	-16.98
Mean	0.29	0.23	-21.84
SE			3.17
p			0.09
SNO	Control	Combined VEGFR - RSK inhibited	% Change
	0.27	0.22	-19.12
	0.29	0.19	-35.27
	0.15	0.12	-18.37
Mean	0.24	0.18	-24.25
SE			5.51
p			0.11
H1299	Control	Combined VEGFR - RSK inhibited	% Change
	0.18	0.15	-17.98
	0.24	0.26	7.59
	0.29	0.22	-21.40
Mean	0.23	0.21	-10.60
SE			9.15
p			0.39

Data Table for Figure 15: Combined VEGFR and RSK inhibition influences the abundance of pPKB and pGSK3βser9 in HOSCC cell lines

pPKB:

CO1	VEGFR inhibited	Combined VEGFR - RSK inhibited	% Change
	16.56	0.13	-99.20
	17.49	0.26	-98.51
	33.82	21.77	-35.64
Mean	22.62	7.39	-77.79
SE			21.07
p			0.01

CO1	Control	Combined VEGFR - RSK inhibited	% Change
	23.04	0.13	-99.43
	20.99	0.26	-98.76
	34.40	21.77	-36.73
Mean	26.14	7.39	-78.31
SE			20.79
p			0.03

CO3	VEGFR inhibited	Combined VEGFR - RSK inhibited	% Change
	0	0	0
	0	0	0
	0	0	0
Mean	0	0	0
SE			0
p			-

CO3	Control	Combined VEGFR - RSK inhibited	% Change
	0	0	0
	0	0	0
	0	0	0
Mean	0	0	0
SE			0
p			-

CO5	VEGFR inhibited	Combined VEGFR - RSK inhibited	% Change
	53.67	55.62	3.64
	42.61	57.08	33.97
	104.15	94.35	-9.41
Mean	66.81	69.02	9.40
SE			12.85
p			0.78

CO5	Control	Combined VEGFR - RSK inhibited	% Change
	44.07	55.62	26.20
	50.41	57.08	13.23
	145.82	94.35	-35.29
Mean	80.10	69.02	1.38
SE			18.71
p			0.64

CO6	VEGFR inhibited	Combined VEGFR - RSK inhibited	% Change
	37.44	16.65	-55.52
	33.31	21.72	-34.80
	19.16	16.39	-14.43
Mean	29.97	18.25	-34.92
SE			11.86
p			0.15
SNO	VEGFR inhibited	Combined VEGFR - RSK inhibited	% Change
	16.23	16.77	3.35
	15.68	16.95	8.09
	20.70	17.21	-16.84
Mean	17.54	16.98	-1.80
SE			7.64
p			0.74
H1299	VEGFR inhibited	Combined VEGFR - RSK inhibited	% Change
	8.81	8.86	0.56
	64.70	22.12	-65.81
Mean	36.75	15.49	-32.63
SE			33.19
p			0.50

CO6	Control	Combined VEGFR - RSK inhibited	% Change
	36.37	16.65	-54.21
	36.51	21.72	-40.51
	24.09	16.39	-31.97
Mean	32.32	18.25	-42.23
SE			6.48
p			0.06
SNO	Control	Combined VEGFR - RSK inhibited	% Change
	24.75	16.77	-32.23
	12.33	16.95	37.50
	22.34	17.21	-22.93
Mean	19.80	16.98	-5.89
SE			21.86
p			0.54
H1299	Control	Combined VEGFR - RSK inhibited	% Change
	28237.32	10425.26	-63.08
	41.29	8.86	-78.54
	90.95	22.12	-75.68
Mean	9456.52	3485.41	-72.43
SE			4.75
p			0.42

pGSK3βser9:

CO1	VEGFR inhibited	Combined VEGFR - RSK inhibited	% Change
	150.08	96.30	-35.84
	166.99	63.52	-61.96
	318.78	236.03	-25.96
Mean	211.95	131.95	-41.25
SE			10.74
p			0.03
CO3	VEGFR inhibited	Combined VEGFR - RSK inhibited	% Change
	79.25	93.26	17.68
	108.59	82.32	-24.19
	132.67	93.78	-29.31
Mean	106.83	89.79	-11.94
SE			14.88
p			0.40
CO5	VEGFR inhibited	Combined VEGFR - RSK inhibited	% Change
	132.21	110.33	-16.55
	130.84	147.26	12.54
	207.29	216.77	4.57
Mean	156.78	158.12	0.19
SE			8.68
p			0.92
CO6	VEGFR inhibited	Combined VEGFR	% Change

CO1	Control	Combined VEGFR - RSK inhibited	% Change
	155.72	96.30	-38.16
	193.62	63.52	-67.20
	398.82	236.03	-40.82
Mean	249.39	131.95	-48.72
SE			9.27
p			0.06
CO3	Control	Combined VEGFR - RSK inhibited	% Change
	52.10	93.26	78.99
	120.41	82.32	-31.64
	116.66	93.78	-19.61
Mean	96.39	89.79	9.25
SE			35.04
p			0.81
CO5	Control	Combined VEGFR - RSK inhibited	% Change
	118.53	110.33	-6.92
	134.04	147.26	9.86
	252.31	216.77	-14.08
Mean	168.29	158.12	-3.71
SE			7.10
p			0.55
CO6	Control	Combined VEGFR	% Change

		- RSK inhibited	
	236.21	142.38	-39.73
	231.68	198.03	-14.53
	153.71	143.19	-6.85
Mean	207.20	161.20	-20.37
SE			9.93
p			0.21
SNO	VEGFR inhibited	Combined VEGFR - RSK inhibited	% Change
	115.11	88.19	-23.39
	70.63	90.53	28.18
	114.63	120.46	5.09
Mean	100.12	99.72	3.29
SE			14.91
p			0.98
H1299	VEGFR inhibited	Combined VEGFR - RSK inhibited	% Change
	655.92	501.59	-23.53
	844.79	324.23	-61.62
Mean	750.36	412.91	-42.57
SE			19.05
p			0.32

		- RSK inhibited	
	234.27	142.38	-39.23
	270.51	198.03	-26.79
	153.25	143.19	-6.57
Mean	219.35	161.20	-24.20
SE			9.52
p			0.14
SNO	Control	Combined VEGFR - RSK inhibited	% Change
	163.88	88.19	-46.19
	78.82	90.53	14.85
	132.67	120.46	-9.20
Mean	125.12	99.72	-13.51
SE			17.75
p			0.43
H1299	Control	Combined VEGFR - RSK inhibited	% Change
	572.82	501.59	-12.44
	134.88	134.14	-0.55
	782.32	324.23	-58.56
Mean	496.67	319.99	-23.85
SE			17.69
p			0.34

Data Table for Figure 18: VEGFR signalling influences the migration of HOSCC cell lines

CO1	Control	VEGFR stimulated	% Change
	27.50	47.35	72.14
	28.18	35.81	27.10
	32.38	49.19	51.93
Mean	29.35	44.12	50.39
SE			13.03
p			0.06
CO3	Control	VEGFR stimulated	% Change
	52.91	64.84	22.54
	53.18	63.59	19.58
	43.49	60.95	40.13
Mean	49.86	63.13	27.42
SE			6.42
p			0.03
CO5	Control	VEGFR stimulated	% Change
	33.42	40.40	20.91
	36.87	50.74	37.62
	36.70	45.12	22.94
Mean	35.66	45.42	27.16
SE			5.27
p			0.04
CO6	Control	VEGFR stimulated	% Change
	29.94	54.55	82.19
	40.22	56.67	40.89
	47.33	61.62	30.19
Mean	39.16	57.61	51.09
SE			15.85

CO1	Control	VEGFR inhibited	% Change
	36.66	30.80	-15.98
	28.76	30.89	7.43
	32.38	29.78	-8.03
Mean	32.60	30.49	-5.53
SE			6.87
p			0.46
CO3	Control	VEGFR inhibited	% Change
	37.60	32.17	-14.44
	53.18	50.56	-4.93
	45.59	40.94	-10.20
Mean	45.45	41.22	-9.86
SE			2.75
p			0.04
CO5	Control	VEGFR inhibited	% Change
	43.65	38.92	-10.85
	39.04	31.68	-18.86
	36.70	33.53	-8.63
Mean	39.80	34.71	-12.78
SE			3.11
p			0.05
CO6	Control	VEGFR inhibited	% Change
	44.35	26.93	-39.28
	36.84	30.82	-16.35
	44.34	43.29	-2.37
Mean	41.84	33.68	-19.33
SE			10.76

p			0.03
SNO	Control	VEGFR stimulated	% Change
	23.28	29.54	26.90
	29.88	37.92	26.93
	52.37	63.89	22.00
Mean	35.18	43.78	25.27
SE			1.64
p			0.03
MCF7	Control	VEGFR stimulated	% Change
	40.00	52.67	31.68
	36.19	62.21	71.91
	25.86	53.13	105.47
Mean	34.02	56.00	69.68
SE			21.33
p			0.04
H1299	Control	VEGFR stimulated	% Change
	44.01	47.35	7.58
	40.90	55.47	35.62
	45.13	53.53	18.61
Mean	43.35	52.12	20.60
SE			8.16
p			0.11

p			0.23
SNO	Control	VEGFR inhibited	% Change
	25.05	23.69	-5.43
	31.37	26.43	-15.76
	52.37	41.01	-21.68
Mean	36.26	30.38	-14.29
SE			4.75
p			0.18
MCF7	Control	VEGFR inhibited	% Change
	41.96	39.20	-6.58
	46.06	41.01	-10.98
	52.14	46.07	-11.65
Mean	46.72	42.09	-9.73
SE			1.59
p			0.04
H1299	Control	VEGFR inhibited	% Change
	44.01	37.24	-15.40
	40.90	34.76	-15.03
	45.13	40.95	-9.25
Mean	43.35	37.65	-13.23
SE			1.99
p			0.02

Data Table for Figure 19: pFAK protein content in HOSCC cell lines

pFAK:

	CO1	CO3	CO5	CO6	SNO	MCF7	H1299
	120.07	107.62	420.07	349.44	239.78	68.40	100
	40.63	240.54	143.24	100.90	166.67	162.16	100
	67.52	76.92	440.17	617.52	158.55	51.71	100
Mean	76.08	141.69	334.50	355.95	188.33	94.09	100
SE	23.33	50.21	95.80	149.17	25.83	34.37	0

Data Table for Figure 20: VEGFR signalling influences the abundance of pPKB, pGSK3βser9 and pFAK in HOSCC cell lines

pFAK:

CO1	Control	VEGFR stimulated	% Change
	235.51	203.19	-13.72
	157.13	130.84	-16.73
	110.89	167.30	50.86
	368.40	395.78	7.43
	244.80	240.91	-1.59
	201.13	88.86	-55.82
	294.35	135.70	-53.90
	204.93	241.64	17.91
Mean	227.14	200.53	-8.19
SE			12.62
p			0.35
CO3	Control	VEGFR stimulated	% Change
	165.36	238.81	44.41
	154.35	311.07	101.53
	652.13	709.19	8.75
	85.37	126.70	48.41

CO1	Control	VEGFR inhibited	% Change
	233.08	183.68	-21.20
	76.46	76.09	-0.48
	261.14	310.88	19.05
	34.66	82.08	136.82
	27.69	13.60	-50.88
	368.40	338.53	-8.11
	71.80	43.20	-39.83
Mean	153.32	149.72	5.05
SE			23.70
p			0.81
CO3	Control	VEGFR inhibited	% Change
	10.75	19.14	77.93
	34.89	95.93	174.96
	114.05	102.61	-10.03
	30.57	40.13	31.28

	335.82	368.30	9.67
Mean	278.61	350.81	42.56
SE			16.94
p			0.03
CO5	Control	VEGFR stimulated	% Change
	456.76	374.86	-17.93
	322.69	236.86	-26.60
	303.80	223.44	-26.45
	1256.31	1428.31	13.69
	282.13	377.05	33.64
	430.52	413.64	-3.92
	180.27	168.34	-6.62
Mean	461.78	460.36	-4.88
SE			8.37
p			0.97
CO6	Control	VEGFR stimulated	% Change
	432.60	339.07	-21.62
	476.42	463.49	-2.71
	383.95	304.64	-20.66
	520.24	555.84	6.84
	163.71	162.71	-0.61
	101.59	63.88	-37.12
	513.54	452.36	-11.91
Mean	370.29	334.57	-12.54
SE			5.71
p			0.09
SNO	Control	VEGFR stimulated	% Change
	120.92	172.99	43.05
	289.87	291.37	0.52

	132.74	42.48	-67.99
	165.58	42.26	-74.48
Mean	81.43	57.09	21.95
SE			38.75
p			0.43
CO5	Control	VEGFR inhibited	% Change
	439.56	407.89	-7.20
	183.29	405.36	121.16
	15.60	32.45	108.05
	353.89	397.34	12.28
	318.70	399.41	25.32
	1256.31	444.94	-64.58
Mean	427.89	347.90	32.51
SE			28.89
p			0.62
CO6	Control	VEGFR inhibited	% Change
	429.27	460.62	7.30
	388.60	326.42	-16.00
	353.34	337.63	-4.44
	130.52	134.01	2.67
	246.99	283.31	14.71
	331.26	267.33	-19.30
Mean	313.33	301.55	-2.51
SE			5.44
p			0.54
SNO	Control	VEGFR inhibited	% Change
	255.01	262.98	3.13
	203.23	229.08	12.72

	217.78	222.28	2.07
	838.05	594.41	-29.07
	146.50	158.61	8.26
	2652.03	757.05	-71.45
Mean	710.86	366.12	-7.77
SE			15.83
p			0.32
MCF7	Control	VEGFR stimulated	% Change
	21.36	28.43	33.10
	23.54	56.46	139.84
	72.53	116.36	60.42
	127.45	98.75	-22.52
Mean	61.22	75.00	52.71
SE			33.78
p			0.46
H1299	Control	VEGFR stimulated	% Change
	650.69	467.05	-28.22
	156.97	156.39	-0.37
	543.54	617.53	13.61
	308.01	320.20	3.96
	512.94	339.85	-33.74
	699.35	626.06	-10.48
	1372.49	1935.99	41.06
Mean	606.29	637.58	-2.03
SE		0.75	9.64
p			0.75

	66.51	70.02	5.27
	226.29	189.42	-16.29
	113.40	226.29	99.55
Mean	172.89	195.56	20.87
SE			20.24
p			0.41
MCF7	Control	VEGFR inhibited	% Change
	137.00	176.81	29.06
	21.36	33.87	58.56
	57.47	63.60	10.68
Mean	71.94	91.42	32.77
SE			13.95
p			0.20
H1299	Control	VEGFR inhibited	% Change
	650.69	546.40	-16.03
	543.54	77.48	-85.74
	512.94	247.27	-51.79
	699.35	249.17	-64.37
	1372.49	6.19	-99.55
Mean	755.80	225.30	-63.50
SE			14.47
p			0.07

Data Table for Figure 21: PI3K inhibition influences the migration of HOSCC cell lines

CO1	Control	PI3K inhibited	% Change
	27.50	29.12	5.86
	28.18	27.39	-2.78
	32.38	30.79	-4.92
Mean	29.35	29.10	-0.61
SE			3.30
p			0.82
CO3	Control	PI3K inhibited	% Change
	52.91	44.50	-15.89
	53.18	48.10	-9.55
	43.49	36.96	-15.03
Mean	49.86	43.19	-13.49
SE			1.99
p			0.02
CO5	Control	PI3K inhibited	% Change
	33.42	31.89	-4.57
	36.87	36.48	-1.06
	36.70	33.50	-8.71
Mean	35.66	33.96	-4.78
SE			2.21
p			0.17
CO6	Control	PI3K inhibited	% Change

CO1	VEGFR stimulated	VEGFR stimulated - PI3K inhibited	% Change
	47.35	29.82	-37.02
	35.81	32.31	-9.79
	49.19	35.06	-28.72
Mean	44.12	32.40	-25.18
SE			8.06
p			0.11
CO3	VEGFR stimulated	VEGFR stimulated - PI3K inhibited	% Change
	64.84	51.41	-20.71
	63.59	56.03	-11.90
	60.95	36.06	-40.84
Mean	63.13	47.83	-24.48
SE			8.57
p			0.10
CO5	VEGFR stimulated	VEGFR stimulated - PI3K inhibited	% Change
	40.40	34.47	-14.69
	50.74	40.48	-20.23
	45.12	37.64	-16.57
Mean	45.42	37.53	-17.16
SE			1.63
p			0.02
CO6	VEGFR stimulated	VEGFR stimulated	% Change

	29.94	32.48	8.49
	40.22	39.96	-0.65
	47.33	38.48	-18.71
Mean	39.16	36.97	-3.62
SE			7.99
p			0.59
SNO	Control	PI3K inhibited	% Change
	23.28	24.47	5.13
	29.88	23.82	-20.28
	52.37	48.73	-6.95
Mean	35.18	32.34	-7.37
SE			7.34
p			0.32
H1299	Control	PI3K inhibited	% Change
	44.01	34.84	-20.85
	40.90	34.42	-15.85
	45.13	45.15	0.04
Mean	43.35	38.13	-12.22
SE			6.30
p			0.20

		- PI3K inhibited	
	54.55	39.97	-26.73
	56.67	48.96	-13.61
	61.62	48.80	-20.81
Mean	57.61	45.91	-20.38
SE			3.79
p			0.03
SNO	VEGFR stimulated	VEGFR stimulated - PI3K inhibited	% Change
	29.54	22.80	-22.83
	37.92	23.24	-38.71
	63.89	51.14	-19.96
Mean	43.78	32.39	-27.17
SE			5.83
p			0.04
H1299	VEGFR stimulated	VEGFR stimulated - PI3K inhibited	% Change
	47.35	31.02	-34.50
	55.47	32.59	-41.25
	53.53	40.03	-25.21
Mean	52.12	34.55	-33.65
SE			4.65
p			0.02

Data Table for Figure 22: PI3K inhibition influences the abundance of pPKB, pGSK3βser9 and pFAK in HOSCC cell lines

pFAK:

CO1	Control	PI3K inhibited	% Change
	244.80	213.66	-12.72
	294.35	140.93	-52.12
	204.93	152.88	-25.40
Mean	248.03	169.16	-30.08
SE			11.61
p			0.17

CO1	VEGFR stimulated	VEGFR stimulated - PI3K inhibited	% Change
	240.91	87.80	-63.55
	135.70	64.43	-52.52
	241.64	61.80	-74.42
Mean	206.08	71.34	-63.50
SE			6.32
p			0.05

CO3	Control	PI3K inhibited	% Change
	119.88	106.15	-11.45
	85.37	59.43	-30.39
	335.82	434.55	29.40
Mean	180.36	200.04	-4.15
SE			17.64
p			0.67

CO3	VEGFR stimulated	VEGFR stimulated - PI3K inhibited	% Change
	90.84	29.84	-67.15
	126.70	54.60	-56.90
	368.30	233.19	-36.68
Mean	195.28	105.88	-53.58
SE			8.95
p			0.06

CO5	Control	PI3K inhibited	% Change
	282.13	329.59	16.82
	430.52	360.18	-16.34
	180.27	155.04	-13.99
Mean	297.64	281.60	-4.50
SE			10.68
p			0.69

CO5	VEGFR stimulated	VEGFR stimulated - PI3K inhibited	% Change
	377.05	353.32	-6.29
	413.64	422.08	2.04
	168.34	146.79	-12.81
Mean	319.68	307.39	-5.69
SE			4.30
p			0.36

CO6	Control	PI3K inhibited	% Change
	163.71	83.61	-48.93
	101.59	71.19	-29.92
	513.54	506.12	-1.44
Mean	259.61	220.31	-26.77
SE			13.80
p			0.21
SNO	Control	PI3K inhibited	% Change
	146.50	153.76	4.96
	2652.03	568.96	-78.55
Mean	1399.26	361.36	-36.79
SE			41.75
p			0.50
H1299	Control	PI3K inhibited	% Change
	156.97	128.38	-18.22
	103.63	142.83	37.83
	250.07	243.31	-2.70
Mean	170.22	171.51	5.64
SE			16.71
p			0.95

CO6	VEGFR stimulated	VEGFR stimulated - PI3K inhibited	% Change
	162.71	176.73	8.62
	63.88	114.68	79.52
	452.36	515.39	13.93
Mean	226.32	268.93	34.02
SE			22.80
p			0.10
SNO	VEGFR stimulated	VEGFR stimulated - PI3K inhibited	% Change
	158.61	184.03	16.03
	1259.03	109.20	-91.33
	757.05	166.93	-77.95
Mean	724.89	153.39	-51.08
SE			33.78
p			0.23
H1299	VEGFR stimulated	VEGFR stimulated - PI3K inhibited	% Change
	156.39	137.71	-11.94
	617.53	472.47	-23.49
Mean	386.96	305.09	-17.72
SE			5.78
p			0.42

Data Table for Figure 23: Combined VEGFR and PI3K inhibition influences the migration of HOSCC cell lines

CO1	VEGFR inhibited	Combined VEGFR - PI3K inhibited	% Change
	30.80	38.57	25.21
	30.89	28.63	-7.32
	29.78	28.60	-3.94
Mean	30.49	31.93	4.65
SE			10.33
p			0.69
CO3	VEGFR inhibited	Combined VEGFR - PI3K inhibited	% Change
	32.17	28.07	-12.74
	50.56	49.50	-2.09
	40.94	33.80	-17.44
Mean	41.22	37.12	-10.76
SE			4.54
p			0.14
CO5	VEGFR inhibited	Combined VEGFR - PI3K inhibited	% Change
	38.92	35.93	-7.68
	31.68	30.77	-2.87
	33.53	32.82	-2.13
Mean	34.71	33.17	-4.23
SE			1.74
p			0.17
CO6	VEGFR	Combined	% Change

CO1	Control	Combined VEGFR - PI3K inhibited	% Change
	36.66	38.57	5.20
	28.76	28.63	-0.44
	32.38	28.60	-11.66
Mean	32.60	31.93	-2.30
SE			4.95
p			0.73
CO3	Control	Combined VEGFR - PI3K inhibited	% Change
	37.60	28.07	-25.35
	53.18	49.50	-6.91
	45.59	33.80	-25.86
Mean	45.45	37.12	-19.37
SE			6.23
p			0.07
CO5	Control	Combined VEGFR - PI3K inhibited	% Change
	43.65	35.93	-17.70
	39.04	30.77	-21.19
	36.70	32.82	-10.57
Mean	39.80	33.17	-16.49
SE			3.13
p			0.04
CO6	Control	Combined	% Change

	inhibited	VEGFR - PI3K inhibited	
	26.93	26.96	0.10
	30.82	29.45	-4.45
	43.29	36.73	-15.15
Mean	33.68	31.04	-6.50
SE			4.52
p			0.32
SNO	VEGFR inhibited	Combined VEGFR - PI3K inhibited	% Change
	23.69	23.98	1.24
	26.43	26.09	-1.29
	41.01	47.83	16.63
Mean	30.38	32.63	5.53
SE			5.60
p			0.43
H1299	VEGFR inhibited	Combined VEGFR - PI3K inhibited	% Change
	37.24	34.54	-7.25
	34.76	31.46	-9.48
	40.95	41.37	1.03
Mean	37.65	35.79	-5.24
SE			3.20
p			0.25

		VEGFR - PI3K inhibited	
	44.35	26.96	-39.22
	36.84	29.45	-20.07
	44.34	36.73	-17.17
Mean	41.84	31.04	-25.48
SE			6.92
p			0.08
SNO	Control	Combined VEGFR - PI3K inhibited	% Change
	25.05	23.98	-4.26
	31.37	26.09	-16.85
	52.37	47.83	-8.66
Mean	36.26	32.63	-9.92
SE			3.69
p			0.11
H1299	Control	Combined VEGFR - PI3K inhibited	% Change
	44.01	34.54	-21.53
	40.90	31.46	-23.09
	45.13	41.37	-8.32
Mean	43.35	35.79	-17.65
SE			4.69
p			0.06

Data Table for Figure 24: Combined VEGFR and PI3K inhibition influences the abundance of pPKB, pGSK3βser9 and pFAK in HOSCC cell lines

pFAK:

CO1	VEGFR inhibited	Combined VEGFR - PI3K inhibited	% Change
	183.68	212.81	15.86
	76.09	96.98	27.45
	310.88	278.24	-10.50
Mean	190.22	196.01	10.94
SE			11.23
p			0.79

CO1	Control	Combined VEGFR - PI3K inhibited	% Change
	233.08	212.81	-8.70
	76.46	96.98	26.84
	261.14	278.24	6.55
Mean	190.23	196.01	8.23
SE			10.29
p			0.70

CO3	VEGFR inhibited	Combined VEGFR - PI3K inhibited	% Change
	19.14	49.83	160.42
	95.93	98.96	3.16
	102.61	77.91	-24.07
Mean	72.56	75.57	46.50
SE			57.50
p			0.87

CO3	Control	Combined VEGFR - PI3K inhibited	% Change
	10.75	49.83	363.38
	34.89	98.96	183.65
	114.05	77.91	-31.69
Mean	53.23	75.57	171.78
SE			114.20
p			0.54

CO5	VEGFR inhibited	Combined VEGFR - PI3K inhibited	% Change
	407.89	368.62	-9.63
	405.36	299.64	-26.08
	32.45	123.01	279.03
Mean	281.90	263.76	81.11
SE			99.08
p			0.78

CO5	Control	Combined VEGFR - PI3K inhibited	% Change
	439.56	368.62	-16.14
	183.29	299.64	63.48
	15.60	123.01	688.59
Mean	212.82	263.76	245.31
SE			222.83
p			0.49

CO6	VEGFR inhibited	Combined VEGFR - PI3K inhibited	% Change
	460.62	241.20	-47.64
	326.42	329.53	0.95
	337.63	392.60	16.28
Mean	374.89	321.11	-10.13
SE			19.27
p			0.59
SNO	VEGFR inhibited	Combined VEGFR - PI3K inhibited	% Change
	262.98	127.90	-51.36
	19.13	82.61	331.94
	229.08	244.35	6.67
Mean	170.40	151.62	95.75
SE			119.28
p			0.78
H1299	VEGFR inhibited	Combined VEGFR - PI3K inhibited	% Change
	454.29	162.54	-64.22
	247.27	-1.64	-100.67
Mean	350.78	80.45	-82.44
SE			18.22
p			0.05

CO6	Control	Combined VEGFR - PI3K inhibited	% Change
	429.27	241.20	-43.81
	388.60	329.53	-15.20
	353.34	392.60	11.11
Mean	390.40	321.11	-15.97
SE			15.86
p			0.40
SNO	Control	Combined VEGFR - PI3K inhibited	% Change
	255.01	127.90	-49.84
	203.23	244.35	20.23
Mean	229.12	186.13	-14.81
SE			35.04
p			0.70
H1299	Control	Combined VEGFR - PI3K inhibited	% Change
	543.54	164.87	-69.67
	308.01	162.54	-47.23
	512.94	-1.64	-100.32
	699.35	594.65	-14.97
Mean	515.96	230.10	-58.05
SE			18.02
p			0.06